# INNOVATIVE ADAPTIVE THRESHOLD-BASED BATTERY ENERGY STORAGE SYSTEM CONTROLLER USING DEEP LEARNING FORECAST FOR PEAK DEMAND REDUCTIONS

**MD MAHMUDUL HASAN**

**MASTER OF ENGINEERING SCIENCE**

**LEE KONG CHIAN FAULTY OF ENGINEERING AND SCIENCE**
**UNIVERSITI TUNKU ABDUL RAHMAN**
**September 2025**

**INNOVATIVE ADAPTIVE THRESHOLD-BASED BATTERY ENERGY STORAGE SYSTEM CONTROLLER USING DEEP LEARNING FORECAST FOR PEAK DEMAND REDUCTIONS**

By

**MD MAHMUDUL HASAN**

A dissertation submitted to the Department of Electrical and Electronic Engineering,
Lee Kong Chian Faculty of Engineering and Science,
Universiti Tunku Abdul Rahman,
In partial fulfilment of the requirements for the degree of Master of Engineering Science
September 2025

## ABSTRACT


**INNOVATIVE ADAPTIVE THRESHOLD-BASED BATTERY ENERGY STORAGE SYSTEM CONTROLLER USING DEEP LEARNING FORECAST FOR PEAK DEMAND REDUCTIONS**

**Md Mahmudul Hasan**

Battery-based energy storage system (BESS) can reduce daily peak demands when it is managed by an effective controller or a control strategy. However, most existing BESS controllers are implemented in simulation platforms, with limited experimental validations under real operating conditions. Even when implemented experimentally, they are often tested on limited case studies or evaluated without any evaluation metrics. Additionally, majority of the controllers are developed using paid proprietary platforms, and do not incorporate any advanced load forecasting model. Therefore, this research aims to address these gaps by developing an innovative adaptive threshold-based BESS controller using free, open-source platforms Node-RED and Python, integrating an advanced deep learning-based one-dimensional convolution neural network (1D-CNN) model for load forecasting. The proposed controller is initially evaluated through simulation using six-months of data, with its performance benchmarked against four different controllers using two different evaluation metrics: daily peak reduction factor ($K_{PDR}$), and monthly failure rate ($\eta_{failure}$). Subsequently, the controller is deployed on a 200 kW/200 kWh BESS setup at a university campus in Malaysia to evaluate its practical performance over 21 days under real operating conditions. In simulation, the proposed controller performs better than that of those benchmark controllers, achieving an

average $K_{PDR}$ of 41.62% and $\eta_{failure}$ of 16.55%. When tested on the actual BESS setup, the controller shows improved performance, with an average $K_{PDR}$ of 49.45% and $\eta_{failure}$ of just 4.76%. These findings highlight the potential of the proposed adaptive threshold-based controller enhanced with advanced load forecasting model for real-world grid applications and can provide significant benefits to both utilities and end customers.

**Keywords: Battery energy storage system (BESS), bess controller, peak demand reduction, load forecasting, deep learning, 1D-CNN**

## ACKNOWLEDGEMENTS

All praise is due to Allah (SWT), the Lord of the worlds, for granting me the strength, determination, and opportunity to complete this dissertation. Without His mercy and blessings, this journey would not have been possible.

I am sincerely grateful to my research supervisor, **Ir. Prof. Dr. Lim Yun Seng**, for his continuous support, valuable guidance, and insightful feedback throughout this journey. From the very beginning till the end, his invaluable guidance, continuous support, and insightful feedback have helped me to complete this research

My heartfelt thanks also go to my co-supervisor, **Asst. Prof. Dr. Hau Lee Cheun**, for his consistent support and helpful guidance, which deepened my understanding and improved the quality of my work.

I would like to thank my parents for their endless love, prayers, and support, which have been vital in completing this journey. I also appreciate my colleagues at the Smart Grid Lab, UTAR Sungai Long campus, for their collaboration and encouragement.

Lastly, I sincerely thank Petronas for sponsoring this project. Their financial support made this research possible.

## TABLE OF CONTENTS

Page

## LIST OF TABLES

## LIST OF FIGURES

## LIST OF ABBREVIATIONS

| | |
|---|---|
| ANN | Artificial neural network |
| BESS | Battery-based energy storage system |
| CNN | Convolution neural network |
| $CO_2$ | Carbon dioxide |
| C&I | Commercial and industrial |
| DAQs | Data acquisition system |
| DOD | Depth of discharge |
| DSM | Demand side management |
| DR | Demand response |
| ESS | Energy storage system |
| GRU | Gated recurrent unit |
| LSTM | Long-short term memory |
| MAE | Mean absolute error |
| RMSE | Root mean square error |
| $R^2$ | Coefficient of determination |
| SOC | State of charge |
| TNB | Tenaga Nasional Berhad |

# CHAPTER 1

# INTRODUCTION

## 1.1 Research Background

As developing countries experience rapid economic growth, maximum demand (MD) is likely to increase in coming years. Along with economic growth, factors like population growth, urbanization, increased use of electrical and electronic devices are also driving this surge in MD (Shabalov *et al.*, 2021). As an emerging economy in Southeast Asia, Malaysia has also experienced substantial increase of MD. Following a yearly growth rate of 2.3%, the MD in Malaysia climbed to 18,808 MW in 2020, as shown in Fig. 1.1 (Suruhanjaya Tenaga Malaysia, 2020). The projection also shows that the MD in Malaysia is expected to increase steadily, reaching 22,815 MW by 2030, with an estimated growth rate of 1.3% per year.

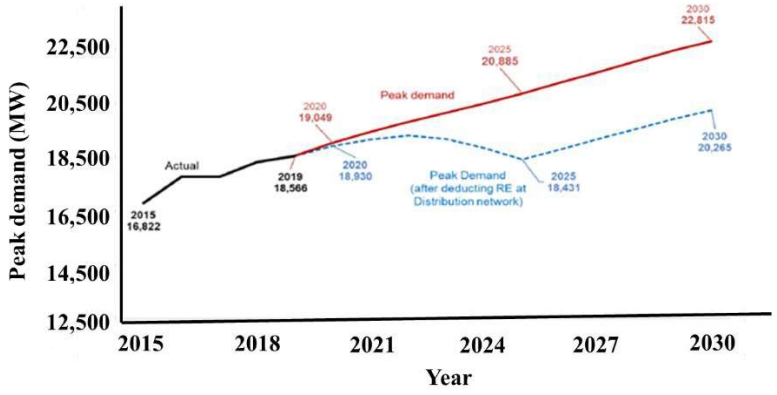


**Figure 1.1: Peak demand trend in Malaysia based on TNB's projection. (Suruhanjaya Tenaga Malaysia, 2020)**

To meet the rising MD, utility companies must take necessary initiatives including the investments on the expansion of their generation and network infrastructures. Investments on the peaking power plants, which are normally run for short durations to meet the high peak demands, are often required. However, such investments can be substantially costly due to their high operational and maintenance expenses (IRENA, 2019). These high expenses can be attributed to low efficiency, reliance on expensive fuels, frequent start-stop cycling, and high standby costs (GAO, 2024). Consequently, customers are subject to extra charges in addition to their regular electricity bills, as utility companies try to recoup their investments. (Borenstein, 2016). In Malaysia, utility companies impose additional demand charges specially on commercial and industrial customers, alongside their standard electricity bills (Tenaga Nasional Berhad, no date). For some customers, these added demand charges may comprise up to 70% of their total monthly electricity bill, placing a significant financial burden for them (Dieziger, 2000; Zhang and Augenbroe, 2018a) .

Beyond its financial burden, MD also poses substantial environmental challenges. Addressing high MD often requires utility companies to activate additional generation capacity, most of which rely on fossil fuels due to their fast ramp-up capabilities and consistent availability. This intensified operation causes a notable rise in greenhouse gas emissions, along with other air pollutants (Di Gianfrancesco, 2017a). In Malaysia, the energy sector accounts almost 80% of their total greenhouse gas emission (Latif *et al.*, 2021). Therefore, lowering

MD is crucial, as it can bring both cost savings and positive environmental impacts.

Customers can focus on reducing their daily peak demands throughout a billing cycle to reduce their overall monthly MD. Among the many methods introduced for peak demand reduction, Demand Side Management (DSM) is being widely implemented approaches across different sectors. (Williams *et al.*, 2023). This approach includes a range of actions, which lead to change the consumers' electricity consumption patterns (Panda *et al.*, 2022a). Another popular approach for peak demand reduction is Demand Response (DR), which is mainly a specific method within the broader DSM framework (Darwazeh *et al.*, 2022). This method aims to motivate consumers to adjust their electricity consumption patterns instantly, often triggered by incentives or signals offered by utilities (Jordehi, 2019).

Both DSM and DR approaches are implemented through different programs with the participation of the customers. The key difference between these two approaches is that DSM focuses on promoting long-term energy-efficient habits, whereas DR targets immediate, short-term shifts in consumptions in response to fluctuating prices or grid demands (Panda *et al.*, 2022b). Both approaches significantly rely on the active participation of the customers to effectively reduce peak demands (Iqbal *et al.*, 2021a). However, motivating consumers to adjust their energy usage habits can be a challenging task in practice. A major obstacle is the fear of discomfort, especially when consumers are asked to shift

their energy consumptions to less convenient times. For example, reducing electricity usage during peak hours, such as turning off air conditioning on hot afternoons, can be uncomfortable for many. In addition, the success of DSM programs in reducing peak demands relies on collaboration among various parties such as utility companies, regulatory agencies, and technology providers, which often leads to potential complexities in policy and governance (Nebey, 2024a).

To address high peak demands without sacrificing users' comforts, Battery-based Energy Storage System (BESS) provide a reliable and effective solution compared to the other alternatives (Martinez-Bolanos *et al.*, 2020; Sahoo and Timmann, 2023). A BESS unit, placed downstream of the utility meter, as shown in Fig. 1.2., can help to reduce peak demands without changing customers' regular energy usage patterns.

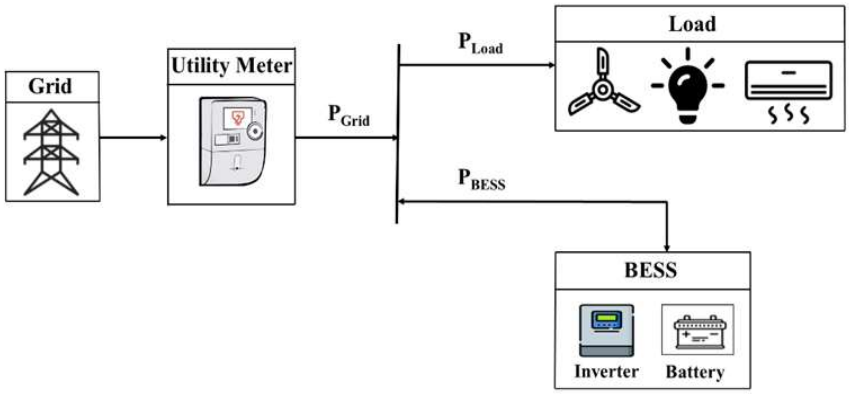


**Figure 1.2: Strategic placement of BESS after the utility meter for peak demand reductions.**

During off-peak hours, when system loads are comparatively low, BESS operates in charging mood, absorbing energy from the grid. As load increases during peak hours, BESS switches to its discharging mode, supplying stored energy to reduce peak demands and maintain grid power to a certain level during peak hours, as presented in Fig. 1.3.

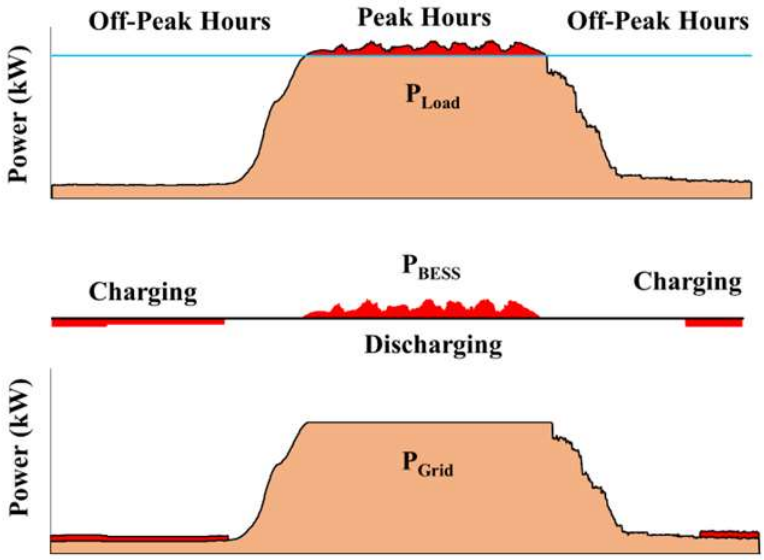


**Figure 1.3: BESS functionality illustrating energy storage during off-peak hours and discharge during peak periods to reduce demand**

BESS offers a promising solution for peak demand reductions; however, its full potential can only be achieved with an effective control strategy or controller. The performance of the BESS is significantly influenced by the ability of the controller to set an effective threshold level, discharging the batteries to meet demand when it surpasses this level, and recharging them when demand drops below the threshold level (Yang *et al.*, 2023).

The best threshold, often referred to as the optimal threshold, is defined as the lowest point on the load profile such that the energy above this level equals the total energy the BESS can deliver (Ng *et al.*, 2022a). For any specific load profile, this threshold marks the highest level to which the BESS can effectively limit the load, based on its available energy capacity. However, identifying this optimal threshold requires full knowledge of the entire load profile in advance.

Since no load forecasting method can provide 100% accuracy in load predictions, identifying the optimal threshold is a major challenge for controllers in real operating conditions (Ng *et al.*, 2022a). Setting the threshold too low may cause the BESS to discharge energy too early or too often, depleting its capacity before the peak demand is met, potentially resulting in no reduction at all. In contrast, a threshold set too high can cause the BESS to discharge less energy than required, causing the system to underperform during peak demand periods. Therefore, it is crucial to have a controller that can effectively set the thresholds and guide the BESS to charge and discharge at the appropriate time for maximum peak demand reductions.

A number of BESS controllers have therefore been introduced to effectively charge and discharge the batteries, aiming to reduce peak demands. The fundamental strategies of the controllers include predicting load demands in advance using various load forecasting techniques, defining a threshold, and controlling the charge-discharge operations of the batteries in line with the threshold. Existing literature provides numerous examples of these approaches

(Zheng et al., 2015; Pholboon et al., 2016; Barchi et al., 2019), where fixed thresholds are used without any real-time threshold adjustments to guide battery charge-discharge actions to achieve peak demand reductions. However, if the peak demand is unexpectedly high or lasts longer than expected, the controllers that rely on fixed thresholds may struggle to manage it effectively (Chua et al., 2017). Therefore, advanced controllers that can optimize battery usage dynamically are essential to effectively prevent peak reduction failures and enhance overall peak demand reductions.

The existing literature also features several state-of-the-art controllers with different optimization techniques for maximum peak demand reductions. For example, Oudalov et al. introduced an advanced BESS controller that applies dynamic programming to effectively manage battery operations, targeting peak demand reduction for end users (Oudalov et al., 2008). In addition, Mishra et al. proposed another advanced BESS controller that uses a linear programming method for optimizing the power dispatch of the batteries to achieve maximum peak demand reductions (Mishra *et al.*, 2012). Apart from the dynamic and linear programming techniques, a particle swarm optimisation (PSO) is also introduced in a BESS controller to optimize the power output of the batteries for peak demand reductions (Mquqwana and Krishnamurthy, 2024).

Though numerous BESS controllers use optimization strategies to schedule BESS power output for peak load reductions, many of the controllers still rely on conventional load forecasting methods. Only in few of the BESS controllers,

advanced load forecasting techniques that involve machine learning or deep neural networks, are adopted. This shortcoming may often result in poor forecasting performance that limit the overall effectiveness of the BESS controller.

In addition, most of the existing controllers are developed on paid commercial platforms. These platforms may offer comprehensive toolsets and structured environments for rapid development; they also present several challenges. The commercial paid development platforms often come with substantial subscription fees, restrictive licensing policies, limited customization capabilities, and potential compatibility issues with other systems.

Moreover, many existing controllers assess their performance solely based on the observed reduction in peak demand, without employing standardized evaluation metrics. This practice limits the ability to comprehensively assess controller effectiveness or to conduct fair performance comparisons across different control strategies. For instance, a controller with a large BESS capacity can effectively reduce the peak demand in a load profile that has a sharp and short-duration peak. However, the same controller may struggle to effectively reduce the peak demands in cases where the peak is more prolonged or when the available storage capacity is comparatively limited. Hence, selecting suitable evaluation metrics is essential to effectively measure the performance of controllers under varying load profiles and operating conditions.

Apart from the aforementioned limitations, majority of the controllers are tested only in simulations with limited case studies, real-time testing at an actual experimental site under real operating conditions is yet to be explored. Performance evaluation based on a limited case studies may not adequately reflect the robustness of the controller. A controller that performs well in reducing peak demand on a specific day may fail under different load profiles encountered on subsequent days. Therefore, it is important to evaluate the performance of a controller to consistently reduce daily peak demands over an extended period, ensuring reliability across diverse and dynamic load conditions.

## 1.2 Problem Statement

Battery Energy Storage Systems (BESS) have gained significant attention as a potential solution for peak demand reductions. The existing literature presents both the conventional fixed threshold-based and state-of-the-art BESS controllers that can adjust the thresholds in real-time for peak demand reductions. Different load forecasting techniques are used in these controllers to predict the load demands. However, limited focus is placed on using advanced load forecasting techniques to accurately predict the load demands. Additionally, most of the controllers are developed on paid proprietary platforms that increase the overall controller development costs as well as limits the accessibility, customization, and system compatibility. Moreover, many studies evaluate controller performance solely based on peak demand reduction and are often limited to a small number of case studies. The use of comprehensive evaluation

metrics and benchmarking against alternative control strategies remains insufficiently explored. Apart from these, the majority of existing controllers are tested exclusively through simulation, with experimental validation under real-world operating conditions still largely underexplored.

### 1.3 Research Objectives

The purpose of this research can be summarized in the following objectives:

1. To develop an innovative adaptive threshold-based BESS controller using free, open-source platforms Node RED and Python to achieve daily peak demand reductions, integrating an advanced deep learning-based one-dimensional convolutional neural network (1D-CNN) model for day-ahead load forecasting.
2. To assess the performance of the BESS controller using two distinct evaluation metrics, daily peak reduction factor ($K_{PDR}$) and monthly peak reduction failure rate ($\eta_{failure}$); and benchmark the results with four different controllers in an extensive simulation study conducted using six months of data.
3. To integrate the controller into an actual BESS setup within a university building to evaluate its practical performance over an extended period under real operating conditions.

## 1.4 Significance of the Research

This research introduces an innovative BESS controller using deep learning forecast to reduce daily peak demands for customers. The significances of this research are listed below.

1. A simple yet effective adaptive threshold-based BESS controller is developed for peak demand reduction using free, open-source platform Node-RED and Python. Node-RED is used to design the control algorithm of the BESS, while the Python is used to develop the load forecasting model that is integrated with the control algorithm. Using these free platforms substantially reduce the controller development expenses compared to using commercial platforms.
2. In comparison with other existing controllers that forecast the load demands without using any specialised load forecasting model, the proposed adaptive threshold-based controller forecasts the load demands in advance using an advanced deep learning-based 1D-CNN model for peak demand reductions.
3. In contrast to other existing controllers which are evaluated solely based on the actual peak demand reductions, the performance of the proposed adaptive threshold-based controller is evaluated through a daily peak demand reduction factor ($K_{PDR}$), along with a monthly peak reduction failure rate ($\eta_{failure}$). Through the evaluation metric $K_{PDR}$, one can assess the true peak demand reduction's ability of a controller. In addition, the evaluation metric $\eta_{failure}$ presents the

consistency of a controller in daily peak demand reduction within a billing cycle.

4. In comparison to the other existing controllers that are usually not benchmarked against other alternative solutions, the proposed adaptive threshold-based controller is benchmarked against four different controllers, namely the forecasted threshold-based controller, historical threshold-based controller, active controller, and fuzzy controller in simulation using six months of data collected from a university building in Malaysia.
5. Unlike other existing controllers that are only tested in simulations, the proposed adaptive threshold-based controller is integrated into an actual 200 kW/200 kWh BESS setup, and the performance of the controller is also evaluated over 21 working days under real operating conditions.

## 1.5 Research Process and Stages

This entire research is carried out in total six phases, which are outlined as follows:

1. Phase 1: In the early phase of this research, an extensive review of existing literature is undertaken to get familiarised with the fundamental concepts and latest developments related to the peak demand reductions. This step helps to identify the gaps in the existing research.

2. Phase 2: A data acquisition system (DAQs) is set up at the experimental site in this phase of the research. Data collected from the DAQs is used to train the load forecasting model as well as to conduct the simulation study.
3. Phase 3: A deep-learning-based 1D-CNN load forecasting model is developed in this phase of the research. An extensive literature on other load forecasting models is also carried out before developing the 1D-CNN model.
4. Phase 4: A fully operational 200 kW/200 kWh BESS setup is installed at the experimental site in this phase of the research. A set of lithium iron phosphate (LiFePO4) batteries, a bi-directional inverter, a battery monitoring system (BMS) and other essential components are set up following the standards and safety regulations. A communication network among the devices in BESS setup is also established in this phase of the research.
5. Phase 5: In the fifth phase of this research, the adaptive threshold-based controller is developed using Python programming language to evaluate its effectiveness in the simulation platform. As part of this phase of the research, the proposed controller's performance is compared with four other controllers implemented through the same simulation environment.
6. Phase 6: In the final phase of this study, the adaptive threshold-based controller is designed in Node-RED platform and deployed to the actual 200 kW/200 kWh BESS setup to evaluate its practical performance under real operating conditions.

## 1.6 Structure of the Dissertation

The structure of the dissertation is organised as follows:

1. Chapter 1: This chapter presents an in-depth overview of the research background, highlighting the challenges associated with high peak demands from different perspectives. The research aims are clearly outlined, and the relevance of the study is emphasized. Additionally, the chapter presents the research methodology, illustrating how the research is conducted.
2. Chapter 2: This chapter mainly focuses on the existing approaches for peak demand reductions. It starts with a clear definition of peak demand, followed by the importance of peak demand reductions both from commercial and environmental perspectives. The chapter then delves into various strategies employed to tackle this issue, offering a detailed analysis of the approaches. It further investigates various control strategies to manage the charging and discharging operations of the BESS for peak demand reductions.
3. Chapter 3: This chapter outlines the overall system architecture of the experimental site. It begins with a brief description of the hardware configuration of the data acquisition systems (DAQs) installed on-site, followed by details of the battery energy storage system (BESS) and the battery monitoring system (BMS). The chapter concludes by highlighting the communication network architecture connecting the devices involved in the experimental setup for peak demand reduction.

4. Chapter 4: This chapter mainly presents the BESS control algorithms for peak demand reductions. The control algorithm of the proposed adaptive threshold-based controller is explained at the beginning of the chapter. Following that the control algorithms of the other four controllers that are benchmarked against the proposed adaptive threshold-based controller is also explained. The implementation of the control algorithms both in simulation and experimental studies is then highlighted in this chapter. Lastly, the architecture of the proposed 1D-CNN load forecasting model that is used to perform day-ahead load forecasting is detailed.
5. Chapter 5: This chapter presents the finding of this research. At the beginning of this chapter, findings from the simulation study are outlined. The performance of the 1D-CNN model throughout the simulation period is first presented, followed by the performance comparison of the controllers is explained comprehensively. At the last part of this chapter, the experimental results of the proposed adaptive threshold-based controller are presented thoroughly.
6. Chapter 6: In the concluding chapter, the key findings of the research are summarized, along with recommendations for further studies.

## 1.7 List of Publications

Table 1.1 lists the peer-reviewed journal and international conferences where the results of this research have been published.

**Table 1.1: Publications overview**

| No | Title of the paper | Publication status | Details of the paper |
|---|---|---|---|
| 1 | An Innovative Adaptive Threshold-based BESS Controller utilizing Deep Learning Forecast for Peak Demand Reductions. | Published | Journal (Q1)<br>IEEE Access<br>Impact Factor: 3.4<br>Position: 1st Author |
| 2. | Short-Term Load Forecasting for Peak Demand Reduction with Limited Historical Data. | Published | Conference<br>ICSGCE 2023<br>Index: Scopus<br>Position: 1st Author |
| 3 | Power Quality Analysis on Peak Demand Reductions using Battery Energy Storage System | Accepted | Conference<br>PEPSC 2025<br>Index: Scopus<br>Position: 2nd Author |

# CHAPTER 2

# LITERATURE REVIEW

## 2.1 Introduction

This chapter outlines a detailed overview of the strategies currently implemented to address high peak demand. It initiates with introducing the concept of peak demand, outlining the challenges it presents. The importance of peak demand reductions is then highlighted, emphasizing its financial and environmental impacts. Following this, the chapter delves into an extensive review of established solutions for reducing peak demand, such as DSM, DR, and ESS. BESS, a specific form of ESS, is chosen as the primary focus of this research, considering its advantages compared to other existing solutions. Therefore, several BESS controllers, that aim to achieve peak demand reductions, are thoroughly examined in the latter section of this chapter.

## 2.2 Peak Demand

Peak demand is the highest level of electricity consumption recorded over a specific time frame, often measured in short intervals like 30 minutes within a 24-hour period. To maintain a stable and reliable power supply across the electrical network, it is essential that the generated power consistently matches the demand at all times (Benetti *et al.*, 2016). To achieve this, utility companies

must adjust their generation levels in real-time, responding to fluctuations in load demands. To ensure a stable match between power generation and consumption, utility providers generally rely on three types of power stations: baseload, intermediate-load, and peaking units (Leonard et al., 2018). The base-load power plants are usually designed to operate continuously at a constant output to meet the minimum power demand (Di Gianfrancesco, 2017b). In contrast, intermediate-load power plants are designed to cope with daily variations in power consumption (Diewvilai and Audomvongseree, 2024). These types of power plants usually adjust their power outputs according to the fluctuation of the load demands. Lastly, the peaking power plants, which are operate solely during peak hours to deliver the surplus power necessary for supporting grid reliability (Di Gianfrancesco, 2017b).

Since the peaking power plants are designed to operate during peak demand periods, their runtime is limited to short durations, resulting in a comparatively lower contribution to the overall energy supply than baseload or intermediate load power plants. However, the costs associated with these peaking power plants, are relatively high due to their lower efficiency, reliance on expensive fuels, frequent start-stop cycling, and higher standby costs (GAO, 2024b) . To recover the substantial investments and operational expenditures, the electricity they produce is often sold at high rates (Hu *et al.*, 2013). As a result, utility providers implement various billing structures to pass these costs on to the end customers.

Apart from standard electricity usage charges, commercial and industrial customers in Malaysia are also liable for MD charges, which can considerably elevate their total electricity bill (Tenaga Nasional Berhad (TNB), no date). The standard electricity usage charges are usually measured in kWh and are applied to all categories of consumers including residential, commercial, and industrial customers based on their energy usages. However, for commercial and industrial customers, additional MD charges are added to the electricity bills. These charges, measured in kW, are based on the peak electrical demand recorded during the billing cycle, usually within a 30-minute window. Typically, MD charges make up roughly 20% of a customer's monthly electricity bill, but this proportion can increase up to 70% for some customers (Dieziger, 2000; Zhang and Augenbroe, 2018b; Ayyappan et al., 2019).

Table 2.1 presents the various MD rates imposed under different tariff categories set by Tenaga Nasional Berhad (TNB) in Malaysia. Tariff categories B and D, which fall under low voltage, are exempt from MD charges. However, other tariff categories are subject to different MD rates. For instance, a customer under C2 tariff category who records MD of 200 kW in a given month will incur MD charges calculated at RM45.10 per kW. This results in a total MD charge of RM 9,020, calculated as follows:

$$\text{MD Charge} = \text{Maximum Demand} \times \text{Rate per kW}$$

$$= 200 \text{ kW} \times 45.10 \text{ RM}$$

$$= 9020 \text{ RM}$$

**Table 2.1: Maximum demand rates for different tariffs by TNB**

| Tariff Plan | Charge (RM/kW) |
|---|---|
| Low-voltage commercial tariff (Plan B) | - |
| Medium-voltage standard commercial tariff (Plan C1) | 30.30 |
| Medium-voltage peak/off-peak commercial tariff (Plan C2) | 45.10 |
| Low-voltage industrial tariff (Plan D) | - |
| Medium-voltage standard industrial tariff (Plan E1) | 29.60 |
| Medium-voltage peak/off peak industrial tariff (Plan E2) | 37.00 |
| High voltage peak/off peak industrial tariff (Plan E3) | 35.50 |

In addition to imposing a considerable financial burden on consumers, high peak demand also creates significant environmental issues. To address high peak demands, fossil fuel-powered peaking power plants are frequently required to function at their maximum capacity for extended periods. Unlike other power plants that run more efficiently, peaking power plants are less efficient and emit disproportionately higher levels of $CO_2$ and other harmful pollutants (Ang *et al.*, 2022). These emissions substantially pollute the environment and contribute to the acceleration of global warming. Moreover, the increased pollutions degrade the air quality, adversely affecting both public health and the natural environment (Perera, 2018).

## 2.3 Importance of Peak Demand Reductions

Peak demand reduction is important due to its significant economic and environmental benefits. From an economic perspective, reducing peak demand enables utility companies to avoid major capital expenditures associated with constructing new peaking power plants and reinforcing existing electrical infrastructure (Nebey, 2024b). By reducing peak demands, utility companies can ensure the best use of their existing infrastructure and can minimize the costly investments for network upgrades (Wallberg *et al.*, 2024). These allow them to offer electricity at significantly lower rates compared to when large sums were spent to accommodate high peak demands. Customers can also enjoy low electricity tariff rates from the utility companies. Moreover, reducing peak demands help customers to save on their MD charges, which would otherwise be significantly higher if the peak demand reductions are not carried out (Gohary et al., 2023).

Apart from the financial benefits, reducing peak demands also provide significant environmental benefits. Peaking power plants, which are activated for short durations to manage the peak demands, usually run on fossil fuels. The highest level of greenhouse gas emissions and the most severe impacts on ecosystems are caused by fossil fuels (Mubarak et al., 2024). Reducing peak demands can decrease the reliance on these non-environmentally friendly fossil fuel-based peaking power plants, leading to lower $CO_2$ emissions and improve air quality (Hoa et al., 2024).

In addition to the aforementioned benefits, reducing peak demands allow utilities to operate more efficiently by lowering the power supply during high peak demand periods (Kalkhambkar et al., 2016). It also helps to maintain the balance between supply and demand and improves overall power quality (Silva et al., 2020). For these reasons, peak demand reduction has become a key area of attention, and numerous strategies are actively being introduced to address this issue. The following section provides a comprehensive overview of the existing solutions for peak demand reductions.

## 2.4 Existing Strategies for Peak Demand Reductions

Numerous strategies for reducing peak demands are discussed in literature, with DSM, DR, and ESS being especially prominent and extensively implemented in different countries. Different ESS technologies are widely used to reduce peak demands, yet BESS offers a more adaptable and reliable option than other ESS types (Chatzigeorgiou *et al.*, 2024). The subsequent sections explain the DSM and DR strategies implemented for peak demand reductions, followed by their limitations. The various ESS technologies are also explained at the end of these sub-sections, along with an explanation of why BESS is the more suitable for peak demand reductions compared to the other alternatives.

### 2.4.1 Demand Side Management (DSM)

DSM is a long-term strategy focused on promoting lasting changes in customers' energy consumption patterns, especially during peak demand periods (Nebey, 2024b). It helps to reduce peak demands by encouraging customers to adopt energy-efficient devices or install dynamic load management tools at their locations to control and schedule their energy usage. Customers are encouraged to use different energy-efficient devices such as LED lighting, smart thermostats, high-efficiency appliances, and variable speed HVAC systems in DSM strategy (Iqbal *et al.*, 2021b). These energy-efficient devices allow the customers to lower their overall energy usage, helping to reduce demands during peak hours.

Along with implementing energy-saving equipment, DSM strategies utilize various real-time load management tools, including smart meters, controllable loads, and programmable switching devices at the user end (Panda *et al.*, 2022a). Smart meters allow both customers and utilities to monitor real-time data on energy consumption, thus helping to take necessary actions to reduce the loads during peak demand periods. Load controllers and programmable switches usually adjust or shift the energy use of the customers during peak demand periods, ensuring that power demand remains balanced and avoids overloading the grid (Iqbal *et al.*, 2021b). DSM strategy mainly involves different load management techniques, as illustrated in Fig. 2.1, for peak demand reductions (Panda *et al.*, 2022a). The overview of the load management techniques used in DSM strategy are outlines below-

1. Peak clipping: This technique reduces the peak demands by remotely controlling the customers' devices or offering incentives to customers.
2. Valley filling: This technique reduces the peak demands by encouraging the customers to increase their electricity usage during off-peak hours, helping to balance the overall load demands throughout the day.
3. Load shifting: This technique reduces the peak demands by shifting the load consumptions from peak demand periods to non-peak demand periods through incentives or smart scheduling of the appliances.
4. Strategic conservation: This technique strategically reduces the overall electricity consumption during peak demand periods through behavioural changes or energy-saving practices.
5. Flexible load shape: This technique reduces the peak demands by dynamically adjusting the electricity usage in real-time based on the grid conditions.
6. Strategic load growth: This technique strategically reduces the peak demands by adding new electricity use, such as EV charging, in a planned way, ensuring that the load growth happens during off-peak hours when overall load demands is lower. In this technique, adding new loads may increase overall load demands, but the new loads are added in a planned way, preventing them from contributing to increase the actual peak demand during peak hours.

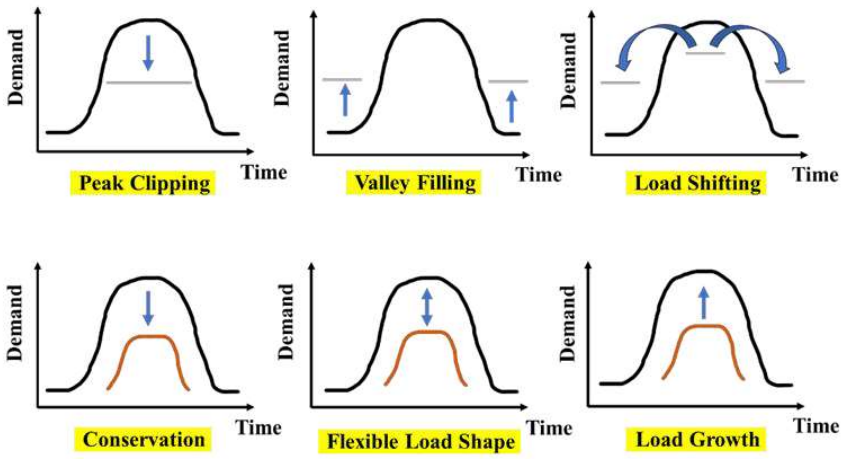


**Figure 2.1: Load management techniques in DSM for peak demand reductions.**

### 2.4.2 Demand Response (DR)

Unlike DSM, DR is a short-term strategy designed to enable consumers to adjust their electricity usage during peak demand periods in response to market conditions (Paterakis et al., 2017). The DR is usually implemented through various customer programs for peak demand reductions. These programs can be categorized into two main categories: incentive-based programs (IBP), and price-based programs (PBP) (Nebey, 2024b).

In IBP, utility companies encourage their customers to reduce or shift their electricity usage during peak demand periods to non-peak demand periods in exchange for financial incentives. Direct load control, curtailable load programs, capacity market programs, emergency DR programs, and demand bidding are the common examples of IBP for peak demand reductions (Albadi and El-Saadany, 2008). Utility companies directly control the loads of the customers

during peak demand periods in direct load control program, whereas in curtailable load programs, customers agree to reduce their consumption during peak demand periods in return for financial incentives for peak demand reductions. Additionally, customers are committed to reduce their consumptions during high peak demand periods in exchange for upfront payments in capacity market programs (Bogdanova et al., 2023a). In these programs, the commitments between the customers and utility companies are usually made in advance, and customers are expected to be available to curtail their loads when called upon. Moreover, customers are incentivised to reduce or shift their energy usage during critical periods, such as extreme weather events or grid emergencies in emergency demand response programs for peak demand reductions (Siano, 2014). These programs are only initiated during emergency conditions and typically involve immediate load reduction actions from the participants. Lastly, in demand bidding programs, customers typically submit bids specifying the amount of loads they are willing to reduce and the price at which they are willing to do so for peak demand reductions (Huang, Li and Zhang, 2025). These bids are then evaluated by the system operator, and accepted bids result in load reductions during specified periods.

On the other hand, In PBP, customers are incentivized to alter their regular energy usage patterns, particularly by shifting their consumptions from peak demand periods to off-peak demand periods, through the provision of adjusted electricity prices. Under PBP, various dynamic pricing mechanisms such as Time of Use (TOE), Real-time Pricing (RTP), Critical Peak Pricing (CPP), Extreme Day Pricing (EDP), and Variable Peak Pricing (VPP) are introduced to

motivate the customers to alter their regular energy usage patterns (Kanakadhurga and Prabaharan, 2022). The details of these pricing mechanisms are outlined below –

1. Time of use (TOU): A pricing mechanism where electricity rates vary depending on the time of day, with higher rates during peak demand periods and lower rates during off-peak periods.
2. Real-time pricing (RTP): A pricing mechanism where electricity rates fluctuate dynamically based on the actual wholesale market price of electricity in real time, typically changes on an hourly basis.
3. Critical peak pricing (CPP): A pricing mechanism where electricity rates are set significantly high during a particular period of extreme demands to encourage reduced consumption.
4. Extreme day pricing (EDP): Same as CPP structure but applied throughout the entire 24-hour period on days of extreme demand.
5. Variable peak pricing (VPP): A pricing mechanism where electricity rates vary during peak hours based on the level of electricity demand, with prices typically increasing as demand rises.

### 2.4.3 Limitations of DSM and DR Strategies

Both DSM and DR strategies are widely used for peak demand reductions. However, both strategies have limitations that affect their overall effectiveness in reducing peak demands for customers. The DSM strategy primarily focuses on the long-term results, and it takes more time to achieve the results compared

to the other short-term solutions (Panda *et al.*, 2022a). Therefore, DSM may not be the most effective solution in addressing immediate peak demand challenges. Additionally, the high upfront costs of energy-efficient technologies and potential consumer reluctance to adopt behaviour changes can limit the effectiveness of DSM in reducing peak demands (Strbac, 2008).

On the other hand, DR strategies offer more immediate solution for peak demand reductions compared to DSM strategies (Silva et al., 2020). However, implementing DR programs in real-world may face significant challenges. Designing and managing DR programs can be complicated and resource-intensive (Bogdanova et al., 2023a). Utilities must coordinate the delivery of incentives and ensure that all participants satisfy the eligibility criteria. Often, customers are unaware of the potential benefits associated with DR programs (Bogdanova et al., 2023). Hence, they are often not motivated to participate the programs for peak demand reductions. Even those who do understand the benefits of the programs, they may not adjust their routines and sacrifice comfort (Nolan and O'Malley, 2015). In addition to other issues, the collection and exchange of consumer energy data may lead to privacy and security risks, highlighting the importance of strong data protections to minimize threats and enhance trust in DR programs (Bogdanova et al., 2023a). Additionally, technology-based demand response solutions often demand technical skills and training for proper deployment and operation. This complexity can pose challenges for smaller utilities or consumers lacking sufficient technical expertise.

### 2.4.4 Energy Storage Systems (ESS)

Unlike DSM and DR strategies, Energy Storage Systems (ESS) offer fast, flexible and adaptable solutions for reducing peak demands without disrupting the daily activities of the customers (Hannan *et al.*, 2021; Lee *et al.*, 2023). Customers can enjoy the benefits of peak demand reductions while maintaining their comfort and convenience. Energy stored by the ESS from the grid in off-peak hours is released during peak hours to assist in reducing customer peak demand. Different ESS technologies have been broadly used to store energy in diverse forms such as thermal, potential, kinetic, electromagnetic, and electrochemical over time. (Amir *et al.*, 2023). Fig. 2.2 presents the general classification of the ESS technology in the form of thermal, mechanical, electrical, chemical, and electrochemical energy storage.

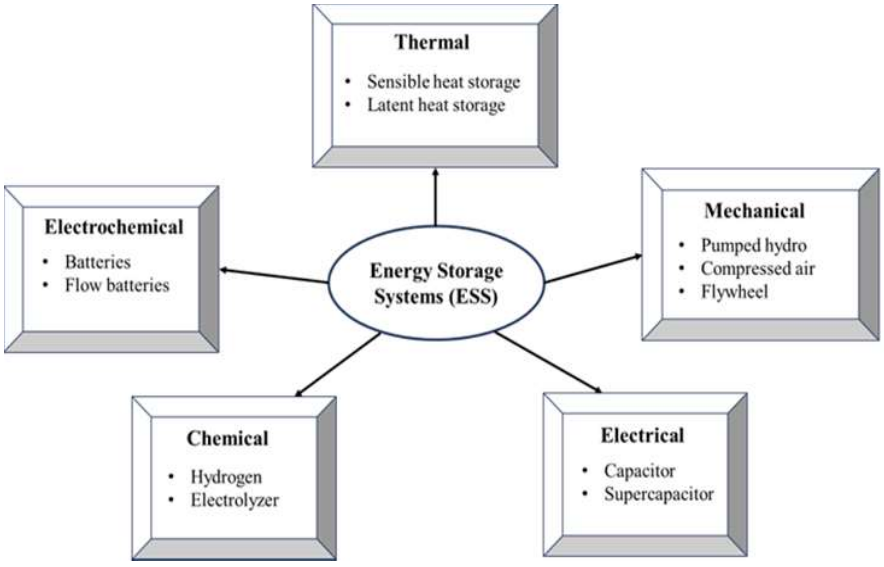


**Figure 2.2: Energy storage technologies for peak demand reductions.**

Each of the ESS technologies comes with its own advantages and disadvantages. Thermal ESS, which usually have slower response times compared to other storage systems, making them less effective to reduce the sudden spike of the load demands (Das *et al.*, 2018). In contrast, Mechanical ESS usually have higher response time compared to the thermal ESS, making them a better choice for peak demand reductions. However, one major drawback of the mechanical ESS is their geographical limitations (Chakraborty *et al.*, 2022). Mechanical ESS, such as pumped hydro systems, are heavily rely on specific geographical features, like the availability of natural water sources and elevation differences, which are essential to set up the systems. These special locations may not be accessible everywhere which limits the widespread implementation of such ESS technologies for peak demand reductions. In addition, both pumped hydro and flywheels storage system require substantial infrastructure and significant capital investments, making them less cost-effective solutions (Li and Palazzolo, 2022; Nikolaos et al., 2023). The space requirements for these storage systems, especially for large-scale flywheels and pumped hydro, can also be significant. Therefore, reducing peak demands using the mechanical ESS may not be the most effective solution.

Other types of ESS, such as electrical and chemical storage technologies, also face specific limitations when applied to peak demand reduction in practical, real-world scenarios. Electrical ESS such as capacitors and supercapacitors have low energy density (Naseri *et al.*, 2022). In addition, the energy discharge duration is also relatively short compared to the other ESS technologies, restricting them for effective peak demand reductions when the peak demands

occur for long duration. Similarly, chemical ESS technologies, including hydrogen storage and electrolysers, present challenges in real-world implementation. Complex infrastructure is essential for their storage and conversion purposes, which increases capital costs and maintenance requirements (Kandari et al., 2023). Additionally, the process of converting electricity into hydrogen through electrolysis and then using it to generate power when required is relatively slow (Hossain Bhuiyan and Siddique, 2025). Consequently, electrical ESS technologies are not ideal for managing sudden or prolonged peak demand events.

In contrast, electrochemical energy storage systems, especially BESS, is better suited for efficiently reducing peak demand than other ESS technologies (Hannan *et al.*, 2021). Unlike other ESS technologies, BESS offers faster response time and can discharge the stored energy almost instantly, which is ideal for handling sudden spikes in load demands. In addition, BESS provide high round-trip efficiency, typically around 90%, allowing them to utilize the stored energy effectively for peak demand reductions (Kwon *et al.*, 2024). Furthermore, BESS are scalable and compact in size, making them suitable to deploy in any location without requiring significant infrastructure or geographical constraints (Saldarini *et al.*, 2023). In contrast to mechanical or thermal storage systems, BESS are easier to operate and maintain, with less complex infrastructure and lower operational costs. These features ensure quick and reliable response to fluctuations in power demands, making them ideal for effective peak demand reductions.

In practice, BESS can reduce peak power needs for customers when installed after the meter, delivering energy during peak periods. A controller is however essential for BESS to reduce the peak demands efficiently. The controller mainly guides the BESS when to charge and discharge the batteries to achieve maximum peak reduction.

## 2.5 BESS Controllers for Peak Demand Reductions

Over the years, various BESS controllers have been developed to manage battery charging and discharging schedules, aiming to reduce customers' peak demand. These controllers generally fall into two categories, each with its own pros and cons. The first category is known as fixed threshold-based controllers. These controllers operate based on a predetermined threshold value, typically derived from a specific load forecasting technique (Ng *et al.*, 2022b). The BESS charging and discharging processes are managed by this fixed threshold. Throughout the day when peak reduction is targeted, the threshold does not change and regulates battery discharge to manage the actual peak of the day. The conventional fixed threshold-based controllers are usually simple in design, and comparatively easy to implement compared to more advanced controllers. Additionally, they tend to be more cost-effective, as they do not require frequent threshold adjustment using multiple operational parameters (Rowe *et al.*, 2014).

Conversely, the second category of the BESS controller is known as the adjusting threshold-based controller. These controllers set an initial threshold at

the beginning of the day of peak reductions, and then subsequently adjusts the threshold to optimize the battery operations for peak demand reductions (Ng *et al.*, 2022b). These advanced controllers are more complex in design because they consider several parameters when adjusting the threshold (Prakash *et al.*, 2022). However, they offer better peak demand reduction capabilities compared to the conventional fixed threshold-based controller by dynamically updating the threshold in response to real-time load conditions.

### 2.5.1 Literature on the Conventional Fixed Threshold-based BESS Controllers

Over the years, several fixed threshold-based controllers are developed and implemented to reduce the peak demands for customers. These controllers are relatively easy to design and require less computational resources to operate. Therefore, these controllers are widely adopted for peak demand reductions. Table 2.2 presents a comprehensive overview of the existing conventional fixed threshold-based controllers used for peak demand reductions.

**Table 2.2: Overview of the existing conventional fixed threshold-based BESS controllers for peak demand reductions.**

| Reference | Method of Evaluation | Control Strategy for Peak Demand Reduction | Performance of the Controller |
|---|---|---|---|
| (Salis et al., 2014) | Simulation | • In control strategy α, load demands are forecasted in | • Data from four distinct buildings, labelled A through |

| | | | |
|---|---|---|---|
| | | advance using historical data.<br>• On the day of peak reduction, a threshold-like control limit is set by adding a safety margin to the forecasted loads to guide the BESS power dispatch for peak demand reductions. | D, over 1 year are used for simulation studies.<br>• Each building uses a fixed but different-sized BESS, and the control strategy α reduces monthly peak demand by an average of 33.7%. |
| (Shin et al., 2016) | Simulation | • Load demands are forecasted in advance to schedule the power dispatch of the BESS.<br>• Exact method of load forecasting, however, is not disclosed. | • A single case study is presented.<br>• With a 300 kWh BESS, the controller effectively reduces the peak demand from 180.9 kW to 133 kW, achieving a peak reduction of 26.5%. |
| (Pholboon et al., 2016b) | Simulation | • Load demands are forecasted in advance using data from the same day of the previous week.<br>• Based on forecasted the loads and price rates, a threshold is established to manage how the BESS dispatches power. | • Simulation studies are carried out using 1 year of data.<br>• With a 350 kWh BESS and 114 kWp PV setup, the controller manages to reduce the average annual peak demands of 32%. |

| | | | |
|---|---|---|---|
| (Chua et al., 2017b) | Experimental | • Load demands are forecasted in advance using historical data rather than relying on any specialised models.<br>• Based on the forecasted load demands, two thresholds are defined on the day of peak reduction to dispatch the BESS power. | • Two case studies are presented.<br>• With a 15 kVA/64 kWh of BESS, the controller reduces peak demand from 78.4 kW to 70.9 kW, achieving a 9.57% reduction, the highest between the two case studies. |
| (Hau et al., 2017) | Experimental | • Load demands are forecasted in advance by calculating the mean of the envelope of the historical load demands.<br>• On the day of peak reduction, a threshold is set based on the forecasted load demands to dispatch the BESS power. | • The controller is tested experimentally over 31 days.<br>• With an 18 kW / 64 kWh BESS, the controller achieves a maximum reduction of kW 9.28 kW. |
| (Barchi et al., 2019b) | Simulation | • Load demands are predicted ahead of time using a persistence approach, assuming that the load profile for the upcoming day will be the same as the previous days.<br>• The power dispatch of the BESS is determined by a | • Simulation studies are carried out using 1 year of data.<br>• With a 500 kWh BESS coupled with 1000 kWp PV setup, the controller achieves an annual |

| | | | |
|---|---|---|---|
| | | threshold, which is calculated through a specialized optimization technique. | energy reduction of 1236 MWh. |
| (Bereczki et al., 2019) | Simulation | • Two thresholds are set based on the historical load demands.<br>• On the day of peak demand reduction, the power dispatch of the BESS is controlled by the thresholds. | • Simulation studies are carried out using 1 year of data.<br>• The BESS is not specified.<br>• The controller reduces the annual peak load from 48.49 kW to 41.59 kW, resulting a 14.23% reduction. |
| (Danish *et al.*, 2020) | Simulation | • Two thresholds are set in advance based on the generic daily load demand profiles.<br>• The BESS power output on the peak reduction day is regulated by the set thresholds and battery SOC. | • Two case studies are presented.<br>• With a 3.61 MWh BESS, the controller reduces peak demand from 10.13 MW to 9 MW, achieving a 11.15% reduction, the highest between the two case studies. |
| (Kim *et al.*, 2025) | Experimental | • Load demands are forecasted in advance using a multi-cluster LSTM model that integrates k-means | • The controller is tested experimentally over 5 days. |

| | | | |
|---|---|---|---|
| | | clustering with LSTM networks.<br>• During the peak reduction day, the BESS power dispatch is governed by a threshold determined from the forecasted load demands. | • With a 100 kW/ 150 kWh BESS, the controller achieves a 21.3% reduction in total energy usage. |

### 2.5.2 Literature on the State-of-the-art Adjusting Threshold-based BESS Controllers

Apart from the conventional fixed threshold-based controllers, several state-of-the-art adjusting threshold-based controllers are also introduced over the years for peak demand reductions. These types of controllers usually forecast the load demands in advance, set an initial threshold and dynamically adjusts the threshold throughout the day for peak demand reductions using different optimization techniques. The BESS charging and discharging schedules are managed based on these adjusted thresholds. Although the state-of-the-art adjusting threshold-based controllers are more complex in design due to the use of advanced optimization methods, these controllers offer clear advantages. Unlike fixed threshold-based controllers, they can adapt thresholds in real-time using forecasts or real-time data, allowing more precise and efficient responses to peak demand events (Ng *et al.*, 2022b). Table 2.3 presents an overview of the existing state-of-the-art BESS controllers for peak demand reductions.

**Table 2.3: Overview of the existing state-of-the-art adjusting threshold-based BESS controllers for peak demand reductions.**

| Reference | Method of Evaluation | Control Strategy for Peak Demand Reduction | Performance of the Controller |
|---|---|---|---|
| (Reihani *et al.*, 2016) | Simulation | • A complex value neural network (CVNN) is employed in a series-parallel forecasting model to estimate load demands in advance.<br>• Based on the forecasted load, an initial SOC profile for the BESS is established and later optimized with a simple control method.<br>• The power scheduling of the BESS on peak reduction days is directed by the optimized SOC trajectory. | • Simulation studies are carried out based on 108 days of data.<br>• With a 1 MW/ 1100 kWh BESS, the controller proves effective in reducing peak demands, though the specific amount of reduction remains unspecified. |
| (Yun *et al.*, 2016) | Experimental | • Load demands are forecasted in advance by averaging the historical load demands.<br>• Based on the forecasted load demands, an initial threshold is established and then fine-tuned using battery SOC and TOU | • A single case study is presented.<br>• With a 500 kWh of BESS, the controller successfully reduces the peak demand from 82.44 kW to 43.12 kW, achieving a reduction of 47.69%. |

| | | | |
|---|---|---|---|
| | | rates to manage the BESS's power dispatch during peak demand periods. | |
| (Yunusov *et al.*, 2017) | Simulation | • Load demands are forecasted in advance using five different forecasting models.<br>• On the day of peak reduction, a model predictive control (MPC) algorithm is used to optimize the power dispatch of the BESS for peak demand reductions. | • Simulation studies are carried out using 14 days of data.<br>• Size of the BESS is not disclosed.<br>• Using the Snt forecasting method, the MPC controller achieves up to 11.4% peak demand reduction over 14 days. |
| (Kim *et al.*, 2017) | Simulation | • Load demands are forecasted in advance using a double seasonal Holt-Winters method.<br>• On the day of peak reduction, the power dispatch of the BESS is optimized using a robust control algorithm. | • Simulation studies are carried out using 24 months of data.<br>• By using a 200 MW/ 400 MWh BESS setup, peak demand for the customer is reduced by 49.9%. |
| (Hau et al., 2017b) | Experimental | • Load demands are forecasted in advance by calculating the mean of the envelope of the historical load demands. | • The controller is experimentally tested over 31 days.<br>• With an 18 kW/64 kWh BESS, the controller |

| | | | |
|---|---|---|---|
| | | • On the day of peak reduction, an initial threshold is set based on the forecasted load demands, which is subsequently adjusted based on a meta-heuristic method to manage the power dispatch of the BESS. | achieves a highest reduction of 10.02 kW, lowering peak demand from 79.96 kW to 69.94 kW, a reduction of 12.53%. |
| (Chua et al., 2017) | Experimental | • Load demands are forecasted in advance based on historical data to set an initial threshold.<br>• On the day of peak reduction, the initial threshold is dynamically adjusted through a fuzzy control logic to manage the BESS power output. | • Five different case studies are presented in the study.<br>• With a 64 kWh of BESS, the controller achieves a maximum reduction of 12.04%, lowering peak demand from 100.5 kW to 88.4 kW. |
| (Agamah and Ekonomou, 2017) | Simulation | • An initial charge-discharge schedule of the BESS is determined based on a simple combinatorial optimization heuristic method.<br>• On the day of peak reduction, a genetic algorithm (GA) is used to | • A single case study is presented.<br>• With a 6 MW/ 10 MWh BESS, the GA optimized controller achieves a peak reduction of 15.69%. |

| | | | |
|---|---|---|---|
| | | optimize the charge-discharge scheduling. | |
| (Taylor *et al.*, 2019) | Experimental | • Load demands are forecasted in advance using an auto-regressive moving average model to set an initial charge-discharge scheduling of the BESS.<br>• On the day of peak reduction, a stochastic optimization method optimizes the charge-discharge scheduling of the BESS. | • 3 days of experimental results are provided.<br>• With a 200 kW/ 1 MWh BESS, the controller manages to achieve a maximum 97 kW of peak reduction. |
| (Lange *et al.*, 2020) | Simulation | • The controller operates without relying on the forecasting results.<br>• Instead, it uses a battery dimensioning method to manage the BESS charge-discharge operations for peak demand reduction. | • Four case studies are presented.<br>• With a 66 kW/ 60 kWh BESS, the controller achieves a maximum peak reduction of 8.13%, lowering peak demands from 619 kW to 568.7 kW. |
| (Engels *et al.*, 2020) | Simulation | • A novel control framework is introduced to manage the BESS power dispatch to jointly | • A single case study is presented.<br>• With a 1 MW/ 1 MWh BESS, the controller manages to reduce the |

| | | | |
|---|---|---|---|
| | | perform peak reduction and frequency regulation.<br>• On the day of peak reduction, a stochastic optimization technique is used to optimize the BESS power dispatch. | peak demand from 1.91 MW to 1.35 MW, achieving a reduction of 29.32%. |
| (Efkarpidis *et al.*, 2023) | Simulation | • Load demands are forecasted in advance using a hybrid GRU-RNN model to set an initial threshold for managing BESS power output.<br>• A rule-based optimization technique optimizes the BESS power output on the day of peak reduction. | • Simulation studies are carried out using 4 years of data.<br>• With a 1.25 MW/ 1.35 MWh BESS, the controller manages to reduce significant monthly peak demands. |
| (Ebrahimi and Hamzeiyan, 2023) | Simulation | • Load demands are forecasted in advance using an artificial neural network (ANN) model to set an initial threshold to control the power dispatch of the BESS.<br>• On the day of peak reduction, the power dispatch of the BESS is optimized through a complex control algorithm. | • Simulation studies are carried out using four different load profiles.<br>• The size of the BESS is not specified.<br>• The controller achieves a maximum reduction of 28.12% among the four load profiles. |

| | | | |
|---|---|---|---|
| (Ghafoori et al., 2023) | Simulation | • Load demands are forecasted in advance using LSTM model.<br>• On the day of peak reduction, a demand management optimization model based on linear programming is used to optimally charge and discharge the EVs for peak demand reductions. | • Simulation results for a three-month period are provided.<br>• With a 10 kW/82 kWh BESS, two electric vehicles (EV) each having 15 kW/62 kWh, and a 40-kW photovoltaic (PV) setup, the controller reduces peak demand by up to 36%. |
| (Rafayal et al., 2024) | Simulation | • Load demands are forecasted in advance using a probabilistic time-series forecasting method.<br>• On the day of peak reduction, the charge-discharge schedule of the BESS is controlled by a two-stage stochastic programming model. | • Simulation studies are carried out using 30 days of data.<br>• With a 15 kW/60 kWh BESS, the controller reduces the daily energy peaks by up to 26%. |
| (Mary and Dessaint, 2025) | Experimental | • Load demands are forecasted in advance using a two-stage neural network-based forecasting model to set a threshold-like setpoint to control the charge- | • Two case studies are presented.<br>• With a 500 kW/2200 kWh BESS, the controller successfully reduces peak demands in both case studies, with the |

| | | | |
|---|---|---|---|
| | | discharge scheduling of the BESS.<br>• On the day of peak reduction, a robust model predictive control (MPC) strategy optimizes the charge-discharge scheduling of the BESS. | reduction being 60 kW less than the optimal in the first case and 3.5 kW less than the optimal in the second. |

### 2.5.3 Research Gaps in the Existing Conventional and State-of-the-art BESS Controllers

The current literature highlights various conventional fixed threshold-based and state-of-the-art adjusting threshold-based controllers for peak demand reductions. Some of the controllers forecast the load demands using either the previous day's load profile or the profile from the same weekday of the previous week (Pholboon et al., 2016b; Barchi et al, 2019b). In addition, many of the controllers forecast their load demands by averaging the historical data rather than using any specific load forecasting models (Salis et al., 2014; Yun et al., 2016; Hau et al., 2017a; Chua et al., 2017). These forecasting approaches are easy to implement and rely on the assumption that load patterns stay consistent over time. However, in real-world scenarios, load demands vary from day to day, and this variability is especially pronounced in commercial sites where fluctuations are often significant and do not follow a clear trend. Using a

specialized load forecasting model can provide greater accuracy than simpler methods such as relying on the previous day's data, the same day from the previous week, or averaging historical load profiles.

Many of the existing BESS controllers are developed on paid commercial platforms like MATLAB and LABVIEW (De Salis et al., 2014; Pholboon, Sumner and Kounnos, 2016b; Reihani et al., 2016; Hau et al., 2017b, 2017a; Chua et al., 2017; Efkarpidis et al., 2023). Dependency on proprietary paid platforms can lead to considerable challenges. One major concern is the high licensing cost, which can significantly increase the overall expense of controller development. In addition, these commercial platforms often have restricted flexibility in terms of customization and integration with other systems, potentially limiting the ability to adapt solutions to specific requirements. Furthermore, reliance on such platforms can create vendor lock-in, where users are tied to a specific provider for future updates or support, limiting long-term scalability.

Moreover, most of the existing BESS controllers assess their performance based on the actual peak demand reduction, rather than using any evaluation metric (Yun et al., 2016; Yunusov et al., 2017; Taylor et al., 2019; Engels et al., 2020; Lange et al., 2020; Ghafoori et al., 2023). Assessing a controller’s performance using appropriate metrics is important to gain a comprehensive understanding of its effectiveness under varying operational conditions. An appropriate metric not only evaluates how effectively a controller reduces peak

demands but also facilitate fair, consistent benchmarking against alternative control approaches. For example, a controller with a larger BESS capacity may perform exceptionally well in scenarios where the load profile features sharp, short-duration peaks, as it can respond quickly and discharge sufficient energy to reduce those peaks. However, the same BESS controller may underperform in situations where the daily peak is more prolonged or where the BESS has limited storage or power capacity. Therefore, it is crucial to assess a controller's performance through appropriate evaluation metrics.

Apart from these, majority of the controllers are tested only in simulations with limited case studies (Shin et al., 2016; Agamah and Ekonomou, 2017; Yunusov et al., 2017; Danish et al., 2020; Engels et al., 2020; Lange et al., 2020; Ebrahimi and Hamzeiyan, 2023). Testing a controller's performance only in simulation under a controlled environment may not fully represent the complexities and uncertainties present in real-world environments. Real-time validation at an actual experimental site, under dynamic and unpredictable operating conditions, is yet to be explored. Additionally, assessing a controller's performance on limited case studies may not fully capture its effectiveness and consistency. For instance, a controller may appear effective in reducing peak demand on a particular day, yet it could underperform the very next day if the load profile changes significantly. Therefore, assessing a controller's ability to consistently reducing daily peak demands over an extended period is crucial.

## 2.6 Summary

In summary, this chapter provides a thorough review of the relevant literature that forms the foundation of this study. It begins by introducing the concept of peak electricity demand and the various challenges associated with high peak demand. The significance of reducing peak demand is subsequently emphasized. Following that, existing strategies for reducing peak demand are discussed, including DSM, DR, and ESS. Among these, BESS is selected as the focus of this research due to its flexibility, scalability, and ability to respond rapidly to demand fluctuations. Several conventional fixed threshold-based and state-of-the-art adjusting threshold-based BESS controllers are also extensively reviewed in this chapter. Each type of controller is critically analysed to understand its strengths, limitations. Finally, the chapter highlights significant research gaps within the existing conventional and state-of-the-art BESS controllers for peak demand reductions. These identified gaps serve as the foundation for defining the research objectives and emphasize the necessity for developing a new innovative BESS controller using deep learning forecast for peak demand reductions.

# CHAPTER 3

# SYSTEM ARCHITECTURE

## 3.1 Introduction

This chapter presents the overall system architecture implemented for the experimental study aimed at reducing peak demands. The experimental study is carried out at UTAR KA block, an academic building of Universiti Tunku Abdul Rahman (UTAR), Sungai Long, Malaysia campus, as shown in Fig. 3.1. The chapter begins with the hardware setup of the data acquisition system (DAQs), which primarily includes the setup of two digital power meters, labelled MSB1 and MSB2, along with a utility grid meter referred to as the TNB meter, all used to measure key electrical parameters at the experimental site. Following the DAQs, the chapter proceeds with a detailed description of the hardware setup for the entire BESS including its key components and operational configuration. Finally, the chapter outlines the communication network architecture that facilitates seamless data exchange among the hardware components, enabling efficient control and monitoring throughout the experimental study.


**Figure 3.1: UTAR KA block, the experimental site for this study.**

## 3.2 Hardware Architecture of the Data Acquisition System (DAQs)

A real-time DAQs is installed at the UTAR KA block to collect and monitor the load demand data at the experimental site. Two power meters, MSB1 and MSB2, are positioned downstream of the site's electrical busbar to capture instantaneous load demand data at one-minute intervals. This real-time data is compiled into a comprehensive dataset, which serves both for training the load forecasting model and for carrying out the simulation study. Additionally, the real-time load demands help to set the BESS power output in real-time for peak demand reductions. Apart from the MSB1 and MSB2 power meters, a grid power meter, labelled as the TNB meter, is installed upstream of the busbar to record the total energy drawn from the grid. Data from this meter is essential for

assessing the peak demand reductions achieved by the controller through the operation of the BESS.

### 3.2.1 Hardware Setup of the MSB1 and MSB2 Power Meters

Two units of SPM33 digital power meters, labelled MSB1 and MSB2 as shown in Fig. 3.2, are installed at the site to measure the instantaneous load demands of the entire UTAR KA block. This block is mainly a multi storied academic building which consists of several classrooms, laboratories, faculty office rooms as well as cafeteria. The multifunctional MSB1 and MSB2 power meters measure various electrical parameters of the building including voltage (V), current (A), active power (kW), reactive power (kVAR), apparent power (kVA), power factor (PF), frequency (Hz), and active energy (kWh). These parameters are shown in real-time on the LCD screen positioned on the meters' front panels, enabling on-site personnel to quickly verify the readings. Technical specifications of the MSB1 and MSB2 power meters are outlined in Table 3.1.


**Figure 3.2: SPM33 digital power meters (MSB1 and MSB2) installed at UTAR KA Block for load monitoring.**

**Table 3.1:Specification of the SPM33 digital power meters.**

| Parameters | Ratings |
|---|---|
| Rated power supply | AC 85 ~ 265 V, DC 100 ~ 300 V |
| Rated input voltage | 220/380 V, 35 Hz ~ 65 Hz |
| Rated input current | 5A or 1A |
| Power loss | < 5VA |
| Power frequency withstand voltage | 2000 VAC |
| Insulation resistance | ≥ 100 MΩ |
| Impulse voltage | 6000 V |
| Standards | IEC 62053-21, IEC 62053-23 |

### 3.2.2 Hardware Setup of the TNB Meter

With support from TNB Malaysia, the country's main utility provider, an SL7000 grid meter by Itron labelled as the TNB meter, shown in Fig. 3.3, is installed at the point of common coupling at the experimental site. This meter is installed at the point of common coupling, which serves as the interface between the building's electrical system and the utility grid. Accurate measurement of the total power drawn from the grid can be easily achieved from this meter. Unlike MSB1 and MSB2 power meters that provide instantaneous load demands data with 1-minute intervals, the TNB meter provides total energy consumptions in kWh at 30-minute intervals. Technical specifications of the SL7000 TNB meter is outlined in Table 3.2.

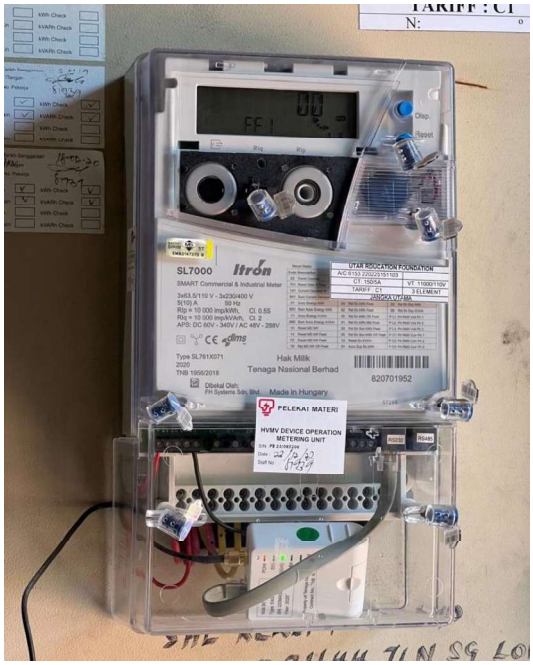


**Figure 3.3: SL7000 TNB meter installed at UTAR KA block.**

**Table 3.2: Technical specifications of Sl7000 TNB power meter.**

| Parameters | Ratings |
|---|---|
| Rated power supply | AC 48 V ~ 288 V, DC 60 ~ 340 V |
| Rated input voltage | 3*63.5/110V ~ 3*230/400V, 50 Hz |
| CT connection | 150/5A |
| VT connection | 11,000/110 V |
| Active energy pulse output rate | 10,000 imp/kWh, Cl. 0.5S |
| Reactive energy pulse output rate | 10,000 imp/kVArh, Cl 2 |
| Standards | IEC 62052, IEC 62053 |

### 3.3 Hardware Architecture of the 200 kW/200 kWh Battery-based Energy Storage System (BESS)

A three-phase BESS is installed in a cabin, as shown in Fig. 3.4, located near the UTAR KA block. The system comprises 223 lithium iron phosphate (LiFePO4) batteries, each operating within a voltage range of 2.8V to 3.6V. LiFePO4 batteries are selected for this study because of their superior safety, longer lifespan, excellent thermal stability, and enhanced efficiency.

**Figure 3.4: Cabin at UTAR campus to set the BESS setup.**

Fig. 3.5 presents the overall BESS setup at the experimental site. A 200 kW/200 kWh BESS is connected to the main electrical busbar of the UTAR KA block. The electrical busbar serves as the main distribution point for supplying electrical power to various loads within the building, such as lighting, HVAC systems, air conditioners, laboratory equipment, and other electrical devices. In charging mode, the BESS sources its power supply from the grid through busbar. The grid supplies electricity to the busbar, and then the BESS draws power from there with the help of a bi-directional inverter to charge its batteries. On the other hand, when the BESS switches to its discharging mode, it delivers power back

into the busbar, supporting the building loads to reduce the peak demand of the building. A battery monitoring system (BMS) is installed on-site to continuously observe and record battery data. The control algorithm responsible for managing the BESS charging and discharging processes aimed at peak demand reduction is implemented within a central control unit. This unit comprises a computing device linked to the entire BESS infrastructure, ensuring efficient coordination and execution of control functions.

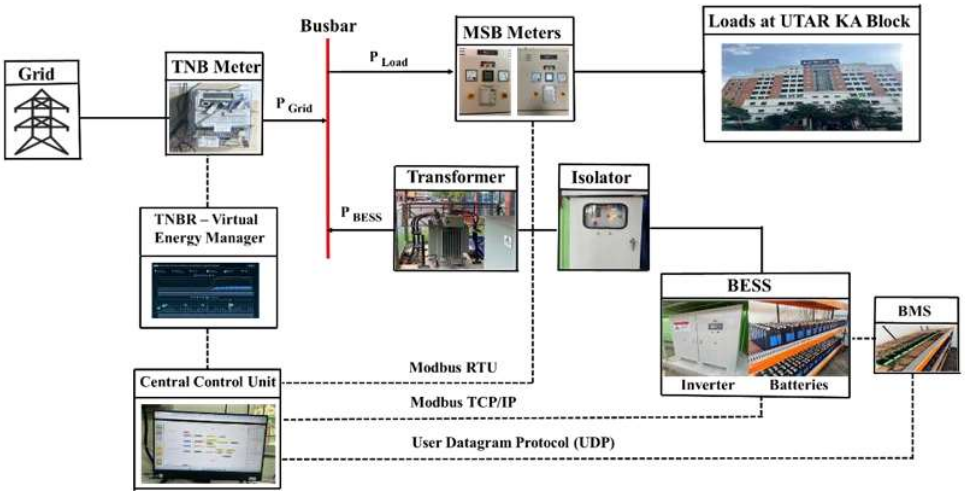


**Figure 3.5: Experimental setup of 200kW/200 kWh of BESS at UTAR campus for peak demand reduction.**

The installed battery bank has a total rated energy capacity of 200 kWh, which defines the maximum amount of energy the system can theoretically store and deliver. However, using the entire BESS capacity in practical applications is not recommended. Overusing the battery through frequent deep discharges can lead to faster battery degradation and shorten its life cycle. Therefore, consistent with

industry standards and manufacturer recommendations, the depth of discharge (DOD) is limited to around 60–70% to maintain a balance between maximizing usable energy and ensuring battery durability. In this study, the SOC range is restricted to 20% to 80%, resulting in a DOD of 60%.

Additionally, the bi-directional inverter is rated to deliver a maximum discharge power of 200 kW. However, empirical analysis of historical load demands data indicates that reducing peak demand at this specific site seldom requires discharge levels greater than 100 kW. Based on this observation, the maximum usable power output of the inverter is conservatively limited to 100 kW for this study. This helps to minimize the operational stress on the inverter and supports the longevity of the equipment. Further technical specifications of the installed BESS are detailed in Table 3.3.

**Table 3.3: Technical Specifications of the installed BESS at UTAR campus.**

| ESS Specification | Rating |
|---|---|
| Battery Type | LiFePO4 |
| Battery cell capacity | 280Ah |
| Voltage range per battery cell | 2.8V- 3.6V |
| Total capacity of the battery bank | 200 kWh |
| Useable Energy | 120 kWh |
| Depth-of-discharge (DOD) | 60% |
| Size of the bi-directional inverter (Rated) | 200 kW |
| Useable power rating of the inverter | 100 kW |

### 3.4 Hardware Architecture of the Battery Monitoring System (BMS)

An advanced battery monitoring system (BMS) by Batrium is installed at the experimental site to monitor battery performance and ensure safety. The BMS plays a crucial role in optimizing the performance and lifespan of the batteries by continuously tracking the key parameters such as SoC, battery cell voltage, shunt voltage, shunt current, and temperature. Monitoring battery SoC helps to prevent overcharging and deep discharging, both of which can harm the battery cells and reduce their overall lifespan. Additionally, monitoring cell voltage helps identify imbalances or faults in individual cells, ensuring consistent performance throughout the battery pack and triggering balancing processes when necessary. The shunt voltage and current measurements are also essential for calculating real-time power flow into and out of the battery, enabling precise energy tracking. Moreover, continuous temperature tracking across the battery cells is crucial as it ensures that the cells operate within safe thermal limit.

Fig. 3.6 presents the hardware setup of the installed BMS at the experimental site. The BMS is connected to the LiFePO4 battery bank through individual CellMate-K9 module. The CellMate-K9 module is mainly an advanced cell monitoring unit designed to connect with 3 to 16 individual cells arranged in series. A total of 14 CellMate-K9 modules are installed at the site, each connected to 16 individual LiFePO4 cells, enabling the monitoring of all 223 cells in the BESS. Each unit of CellMate-K9 module collects the data from the individual cells and transmits it to the WatchMon Core, which acts as the central supervisory unit in the overall BMS setup.

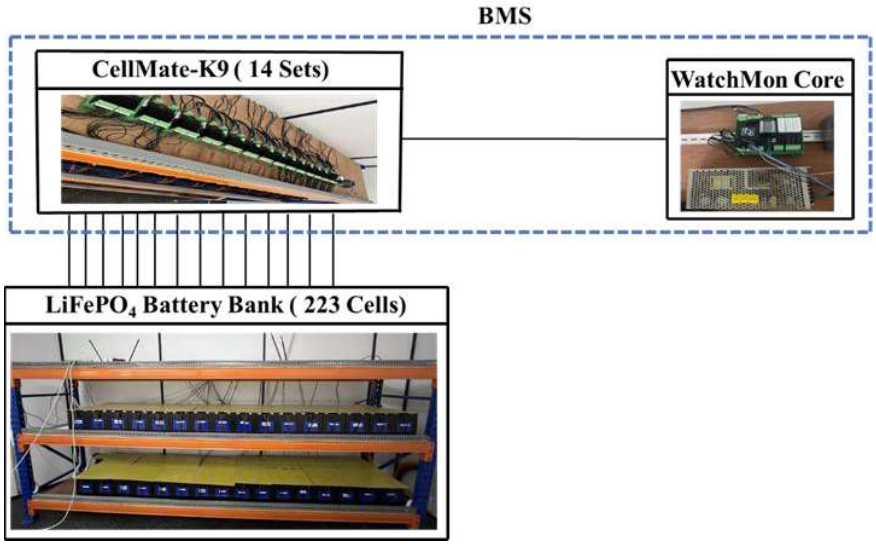


**Figure 3.6: Battery monitoring system (BMS) setup at the experimental site.**

### 3.5 Communication Network Architecture

This section outlines a comprehensive overview of the communication network architecture implemented at the experimental site. A central control unit (PC) acts as the main communication hub of the entire experimental setup and it is strategically installed in a cabin room located near the UTAR KA block. The central control unit also hosts the BESS control algorithm developed for peak demand reductions, thereby it plays a dual role in both coordination and real-time decision-making. The communication network is structured into two primary layers: communication with the data acquisition system (DAQs) and communication with the bi-directional inverter and BMS. The following sub-sections provide a detailed explanation of each of these communication layers.

### 3.5.1 Communication with the Data Acquisition System (DAQs)

Fig. 3.7 illustrates the communication configuration of the overall DAQs deployed at the experimental site. In this setup, the MSB1 and MSB2 power meters, dedicated to capturing instantaneous load demands at 1-minute intervals, are connected to the central control unit using the Modbus RTU communication protocol. An RS-485 to USB converter, which functions as the physical interface for enabling serial data transmission between the meters and the central control unit, is installed to facilitate reliable communication and ensure seamless data acquisition from the power meters.

On the other hand, an energy monitoring toolkit is installed with the assistance from TNB to capture the data from the TNB meter. As the meter is owned and protected by TNB, unauthorized access could breach security, regulatory, and legal standards. Therefore, with TNB's authorization, an optical pulse sensor is attached to the meter to detect its LCD pulse signals. Each pulse signal represents a certain amount of energy used and by counting these pulses, the total energy usage in kWh is accurately calculated. The calculated energy data is transmitted to TNB's dedicated portal via the energy monitoring toolkit designed for this meter. The portal provides secure access to monitor energy consumption data recorded at half-hour intervals.

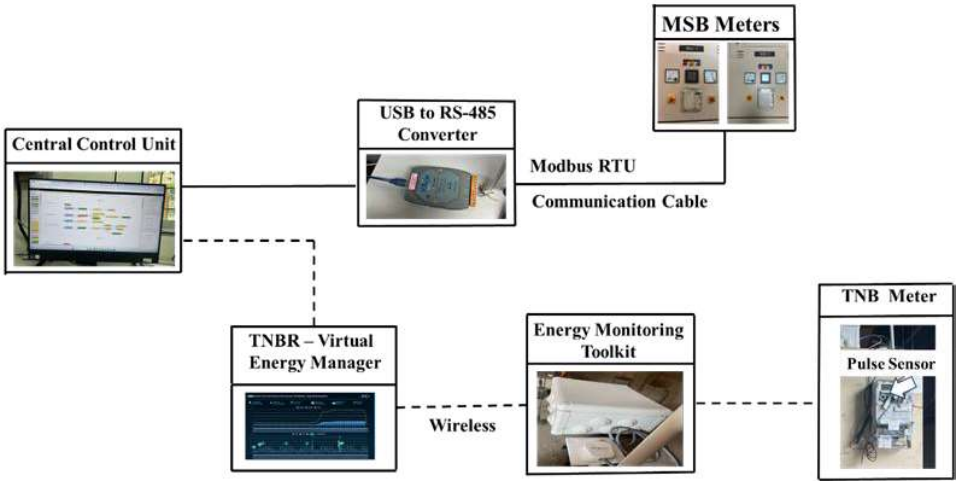


**Figure 3.7: Communication setup with the data acquisition system (DAQs) at the experimental site.**

A free, open-source platform "Node-RED" is used to interface the central control unit with the MSB1 and MSB2 power meters. Node-RED is a development environment built by IBM that uses a flow-based approach to connect hardware, APIs, and cloud services with ease. It is widely used in various DAQs due to its simplicity, reliability and flexibility in handling multiple communication protocols. Apart from these, Node-RED platform offers its own dashboard feature that allows the users to monitor and visualize real-time data without relying on additional dashboard platforms.

Once the power meters are installed at the site, a communication cable is used to physically connect them to the central control unit. An RS-485 converter is used to establish serial communication between the power meters and the central control unit, with data transmission managed by the Modbus RTU protocol. Both the MSB1 and MSB2 power meters act as slave devices, while the central control unit serves as the master, continuously polling the meters for real-time data.

Table 3.4 outlines the Modbus RTU communication settings for the MSB1 and MSB2 power meters at the experimental site.

**Table 3.4: Modbus RTU settings in Node-RED for MSB meters.**

| Parameter | Value |
|---|---|
| Device ID (MSB1) | 1 |
| Device ID (MSB2) | 2 |
| Data bit | 8 bits |
| Baud Rate | 19200 bps |
| Parity bit | none |
| Stop bit | 1 bit |
| Timeout | 1000 ms |

MSB1 and MSB2 power meters store the measurement data in predefined registers, each assigned to a specific parameter. These registers serve as fixed memory locations that hold either instantaneous readings or cumulative values. The Node-RED flow sends a read request via the Modbus Getter node to access the data at specific register addresses. The meters, functioning as slave devices, respond to the master device with the requested data. Once received, the data is processed through function nodes within the Node-RED platform, saved as CSV files on the central unit, and displayed on dashboard for real-time monitoring and visualization. Fig. 3.8 presents the Node-RED flow designed in the Node-RED platform to collect and monitor the data from the meters. Additionally, Fig. 3.9 and 3.10 present the dashboard interfaces developed within the same Node-

RED platform for visualizing data from MSB1 and MSB2 power meters, respectively.

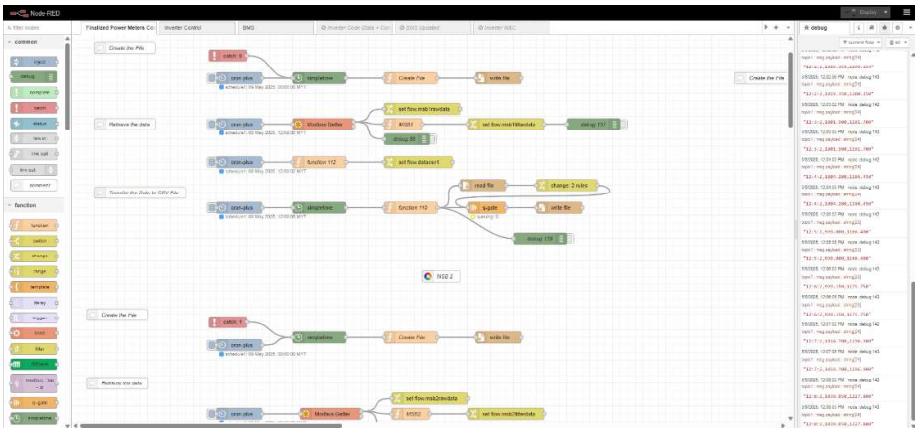

**Figure 3.8: Node-RED flow to collect and monitor data from the MSB1 and MSB2 power meters.**


**Figure 3.9: Real-time monitoring dashboard for MSB1 power meter.**


**Figure 3.10: Real-time monitoring dashboard for MSB2 power meter.**

### 3.5.2 Communication with the Bi-directional Inverter and Battery Monitoring System (BMS)

Fig. 3.11 shows the communication setup of the bi-directional inverter and the battery monitoring syestem (BMS) at the experimental site. The bi-directional inverter is electrically linked to the LiFePO4 battery bank and the grid to facilitate two-way power flow, allowing the batteries to be charged from the grid or to discharge energy back to the grid when required. Hence, maintaining a stable communication link with the bi-directional inverter is essential. The inverter is connected to the central control unit via a LAN cable. The BMS, on the other hand, is wirelessly connected to the central control unit via a Wi-Fi network.

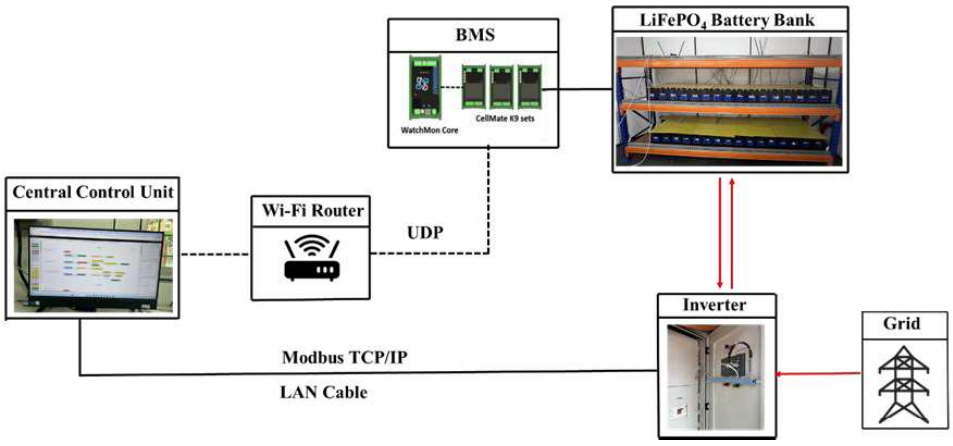


**Figure 3.11: Communication setup with the bi-directional inverter and the BMS at the experimental site.**

As shown in Fig. 3.12, a dedicated Node-RED flow is developed to interface the bi-directional inverter with the central control unit. Modbus TCP/IP communication protocol is used to transfer the data between the inverter and the control unit. A Modbus Getter node in Node-RED platform initiates requests to

the inverter by specifying the appropriate register addresses and data types. The inverter responds by sending the requested data back through the TCP/IP protocol. Additionally, a Modbus Write node is used to control the inverter for charging and discharging operations of the batteries. The Write node sends a request to specific registers within the inverter and the inverter executes the charging or discharging commands based on the Node-RED's request. The dashboard to monitor and control the inverter is shown in Fig. 3.13.

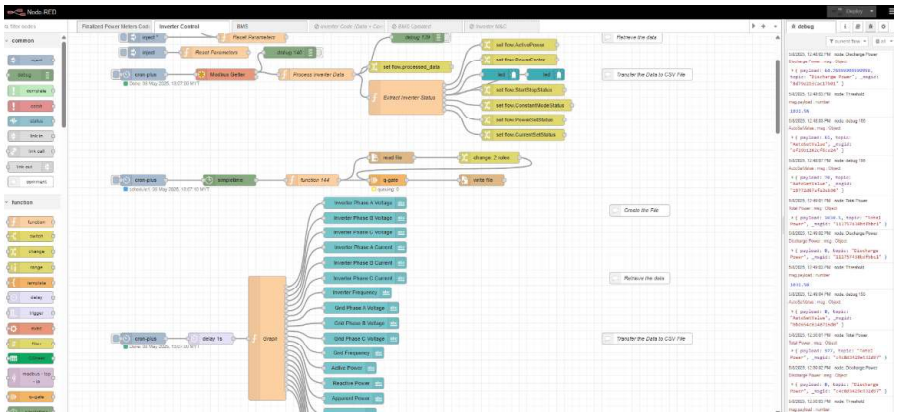

**Figure 3.12: Node-RED flow for monitoring and controlling the bi-directional inverter.**


**Figure 3.13: Real-time monitoring and controlling dashboard for the bi-directional inverter.**

The communication between the BMS and the central control unit is also established using the same free, open-source Node-RED platform. A dedicated Node-RED flow, as presented in Fig. 3.14, is developed to interface the BMS with the central control unit. User Datagram Protocol (UDP) is used to retrieve the data from the BMS. Unlike Modbus RTU and TCP/IP communication protocols, which follow a request-response model where a master polls specific registers from a slave device, UDP functions as a one-way communication protocol, transmitting data without the need for prior coordination from the receiver. The dashboard for monitoring the real-time BMS data is illustrated in Fig. 3.15.

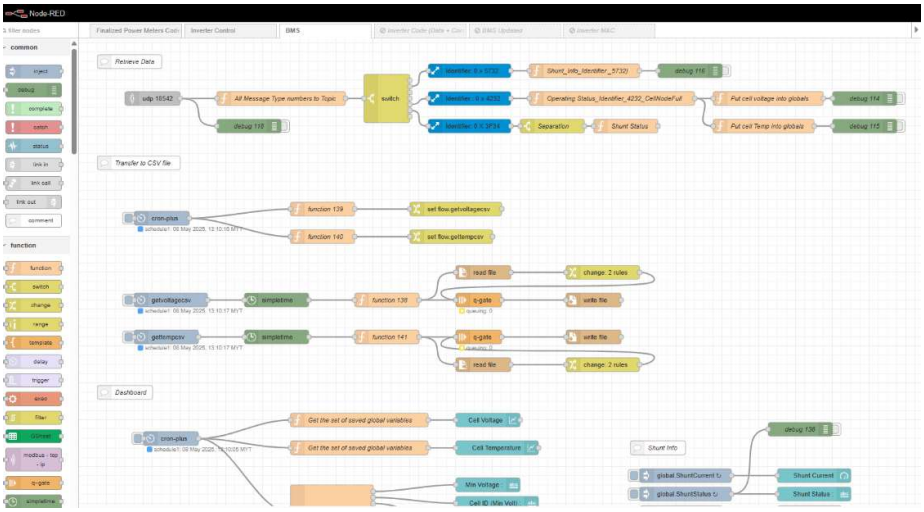


**Figure 3.14: Node-RED flow to retrieve the data from the BMS.**


**Figure 3.15: Real-time monitoring dashboard for the BMS.**

## 3.6 Summary

This chapter outlines the overall system architecture of the experimental site at the UTAR campus. It presents the hardware configuration of the Data Acquisition Systems (DAQs), including the placement of power meters for real-time load monitoring. The 200 kW/200 kWh Battery Energy Storage System (BESS), which serves as the core of the study, is described along with its operational role within the system. The Battery Monitoring System (BMS) is also covered in this chapter, highlighting its function in ensuring safe and efficient battery operation. In addition to the hardware setup, the communication network architecture among the hardware setup at the experimental site is detailed, describing the flow of data between key system components to support coordinated control and monitoring.

# CHAPTER 4

# DESIGN AND IMPLEMENTATION OF BESS CONTROL ALGORITHMS FOR PEAK DEMAND REDUCTIONS

## 4.1 Introduction

The proposed adaptive threshold-based BESS controller is initially implemented within a simulation environment using Python programming language. To evaluate and compare its performance, two conventional fixed threshold-based and two state-of-the-art adjusting threshold-based controllers, are also implemented in simulation. The two conventional controllers that operate using fixed thresholds are identified as the forecasted threshold-based controller and the historical threshold-based controller. These two controllers are not directly adopted from existing literature but instead developed based on the fundamental principles of fixed threshold control. In contrast, two advanced controllers capable of adjusting thresholds in real-time, are referred to as the active controller and fuzzy logic controller. These controllers are developed based on the methodologies presented in references ( Hau, Lim and Chua, 2017b) and (Kein Huat Chua, Lim and Morris, 2017). Following the simulation study, the proposed adaptive threshold-based controller is deployed at the experimental site at UTAR campus to assess its practical effectiveness under real-world operating conditions.

This chapter begins by presenting the control strategies of the proposed adaptive threshold-based controller designed for peak demand reductions. It also includes comprehensive overview of the additional control strategies used to benchmark the performances. An advanced deep learning-based load forecasting model is used in the proposed adaptive threshold-based controller as well as the two fixed threshold-based controllers. As a results, the chapter also provides a detailed explanation of the architecture of the load forecasting model.

## 4.2 Design of the proposed Adaptive Threshold-based BESS Controller

### 4.2.1 Control Strategy Overview

An innovative adaptive threshold-based BESS controller is implemented in both simulation and experimental setups to effectively reduce peak demands. The controller incorporates an advanced deep learning-based 1D-CNN model to forecast the load demands in advance. An initial threshold is determined using the forecasted load demands and is subsequently adjusted in real-time based on three different parameters – actual load demands, forecasted load demands, and observed grid demands.

The proposed adaptive threshold-based BESS controller operates in three distinct modes: charging, discharging, and idle. However, in the simulation environment, it is assumed that the BESS begins each day fully charged to its usable capacity. As a result, the simulation study primarily focuses on the

discharging mode of the controller to demonstrate its capability to manage and lower peak demands using the available BESS energy. In contrast, during practical implementation at the experimental site, the charging, discharging and idle modes are actively managed.

### 4.2.2 Algorithm Design

Fig. 4.1 shows the operational flow chart of the proposed adaptive threshold-based controller designed to reduce peak demands. The process starts with a day-ahead load forecasting task. At 00:00, a deep learning-based 1D-CNN model forecasts the load demands in advance for the upcoming day. Based on the forecasted load demands, the controller sets an initial threshold ($P_{th\_initial}$), which serves as a reference to set the final thresholds ($P_{th\_final}$) that are used to schedule the power dispatch of the BESS throughput the day of peak reduction. The subsequent steps after determining $P_{th\_initial}$ are outlined in Fig. 4.1 under Block A and Block B. The processes in Block A mainly illustrate how the $P_{th\_initial}$ is updated to $P_{th\_final}$ in every 15-minute intervals. On the other hand, the processes in Block B demonstrate how the BESS power is being supplied to the load in every 1-minute intervals based on the $P_{th\_final}$ achieved from the steps in Block A.

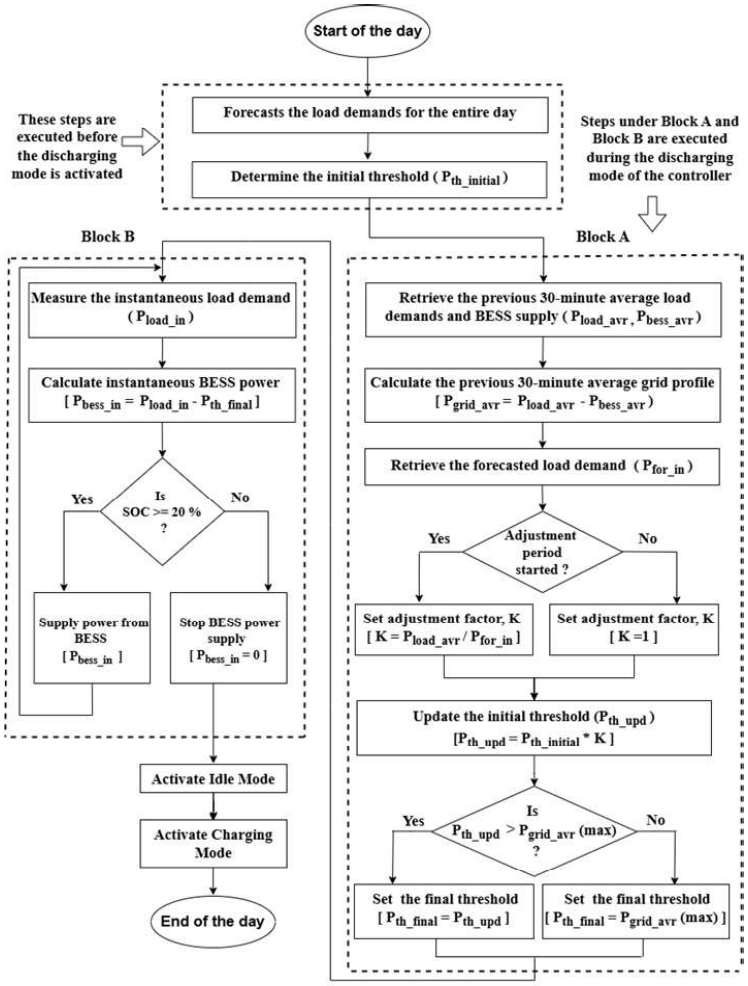


**Figure 4.1: Control algorithm flow chart of the proposed adaptive threshold-based BESS controller to achieve daily peak reduction.**

The discharging phase of the controller begins at 8:00, aligning with the classes and official activities of the university building at the experimental site. As classes and other official activities commence, electricity consumption begins to rise. Consequently, this period is set as the starting point for the discharging phase. At 8:00, the adaptive threshold-based controller retrieves the average real-time load demands ($P_{load\_avr}$) and the average power output of the BESS ($P_{bess\_avr}$) over the preceding 30-minute period. Since the discharging phase

begins precisely at 08:00, no power is supplied by the BESS during this prior interval, resulting in a $P_{bess\_avr}$ of 0 at this time. However, in subsequent intervals, $P_{bess\_avr}$ may increase depending on BESS discharge activity. The average grid profile ($P_{grid\_avr}$) at 8:00 is then calculated as follows:

$$P_{grid\_avr} = P_{load\_avr} - P_{bess\_avr} \tag{3.1}$$

Afterward, the adaptive threshold-based controller retrieves the forecasted load demand ($P_{for\_in}$) at 8:00 and sets the threshold adjustment factor (k) using Equation (3.2). To ensure a balanced adjustment, both real-time and forecasted load demands are considered.

$$K = \begin{cases} \frac{P_{load\_avr}}{P_{for\_in}} & 09{:}00 \leq t \leq 18{:}00 \\ 1 & \text{otherwise} \end{cases} \tag{3.2}$$

After determining k, the adaptive threshold-based controller computed the updated threshold ($P_{th\_upd}$) using Equation (3.3). $P_{th\_upd}$ is used to determine the final threshold ($P_{th\_final}$), which primarily manages the power dispatch of the batteries.

$$P_{th\_upd} = P_{th\_initial} \times K \tag{3.3}$$

Once the $P_{th\_upd}$ is determined, the controller sets the final threshold ($P_{th\_final}$) based on Equation (3.4). To determine $P_{th\_final}$, the controller compares $P_{th\_upd}$

with the preceding peak of the grid profile ($P_{grid\_avr}(max)$) up to that time. If $P_{th\_upd}$ is higher than ($P_{grid\_avr}(max)$), $P_{th\_upd}$ is set as $P_{th\_final}$ and the power dispatch of the batteries are managed based on the latest $P_{th\_final}$. Otherwise, ($P_{grid\_avr}(max)$) is set to $P_{th\_final}$ and discharge the batteries accordingly. The ($P_{grid\_avr}(max)$) acts as a lower bound, ensuring the threshold does not drop excessively during periods of declining real-time load demands.

$$P_{th\_final} = \begin{cases} P_{th\_upt} & P_{th\_upd} \geq (P_{grid_{avr}}(max)) \\ P_{grid\_avr}(max) & \text{otherwise} \end{cases} \quad (3.4)$$

After setting $P_{th\_final}$, the controller measures the instantaneous load demands at 8:00 and calculates the required BESS power $P_{bess\_in}$ to be supplied to the load at that moment, according to Equation (3.5).

$$P_{bess\_in} = P_{load\_in} - P_{th\_final} \quad (3.5)$$

If the battery SOC is above 20%, indicating adequate available battery energy, the controller enables the BESS to supply power to the load as described. The BESS continues to deliver $P_{bess\_in}$ in every minute by following the steps outlined in Block B of Fig. 4.1 until the SOC drops to 20%.

At the end of the discharging phase, the proposed adaptive threshold-based controller enters idle mode, during which the BESS neither supplies power to the load nor draws energy from the grid. At the UTAR KA Block, electricity demand significantly drops after 18:00, as the classes and other official activities

typically conclude by that time. Therefore, the discharging phase is scheduled to end at 18:00. The system remains idle until 22:00, when the charging phase begins, taking advantage of low nighttime demand. Once the BESS is fully charged, the controller returns to idle mode and stays in that state until the next discharging cycle starts.

## 4.3 Design of the Fixed Threshold-based BESS Controllers

Two conventional fixed threshold-based controllers are implemented in this simulation study. The first controller is identified as the forecasted threshold-based controller, whereas the second one is referred to as the historical threshold-based controller. In simulation, both of the controllers are implemented using Python programming language. The 1D-CNN model that is integrated with the proposed adaptive threshold-based controller, is also incorporated with these two controllers. The following subsections outlines the overview of these conventional fixed threshold-based controllers.

### 4.3.1 Control Algorithm of the Forecasted Threshold-based Controller

The forecasted threshold-based BESS controller mainly functions in 5 different steps for peak demand reductions. The detailed step-by-step processes of this controller are explained below –

**Step 1:** Forecast the load demands in advance using the 1D-CNN load forecasting model.

**Step 2:** Determine a forecast-based threshold ($P_{th\_for}$) based on the forecasted load demands and available BESS capacity. $P_{th\_for}$ represents the target peak demand limit for the entire forecasted profile, where the area above the threshold corresponds to the total energy expected to be supplied by the BESS.

**Step 3:** Starting from 8:00, the controller retrieves the instantaneous load demands $P_{load\_in}$ and delivers BESS power $P_{bess\_in}$ at 1-minute intervals according to $P_{th\_for}$, continuing this process until the maximum usable BESS capacity is depleted.

$$P_{bess\_in} = \begin{cases} P_{load\_in} - P_{th\_for} & P_{load\_in} > P_{th\_for} \\ 0 & \text{otherwise} \end{cases} \quad (3.6)$$

**Step 4:** At the end of the day, compute the instantaneous grid profile based on the $P_{load\_in}$ and $P_{bess\_in}$.

$$P_{grid\_in} = P_{load\_in} - P_{bess\_in} \quad (3.7)$$

**Step 5:** Measure the effective reduction in peak demand $(PDR_a)$ for the given day by subtracting the maximum average grid demand, $\text{Max}\left(P_{grid\_avr}\right)$ over a 30-minute period from the maximum average load demand, $\text{Max}\,(P_{load\_avr})$ within any 30-minute interval of the day.

$$PDR_a = Max\,(P_{load\_avr}) - Max\,(P_{grid\_avr}) \quad (3.8)$$

### 4.3.2 Control Algorithm of the Historical Threshold-based Controller

The other conventional historical threshold-based controller is also implemented using Python programming language. The control strategies of this controller closely resemble that of the forecasted threshold-based controller, with the primary difference lying in step 2 as outlined in Section 4.3.1. Therefore, the steps explained in section 4.3.1 is also applicable for this controller except the process of determining the threshold that manages the power dispatch of the BESS.

Unlike forecasted threshold-based controller that directly use the forecasted threshold ($P_{th\_for}$) to manage the power dispatch of the BESS, the historical threshold-based controller incorporates an additional reference threshold ($P_{th\_ref}$) derived from the historical data before it sets the operational threshold ($P_{th\_op}$) that manages the power dispatch of the BESS in historical threshold-based controller for peak demand reductions.

The $P_{th\_op}$ in historical threshold-based controller is determined through 2 steps, which are explained below -

**Step 1:** Compute the reference threshold ($P_{th\_ref}$) based on the optimal threshold ($P_{th\_optimal}$) achieved from the actual historical load demands as follows -

$$P_{th\_ref}(d) = \begin{cases} 1000 & d = 1 \\ \frac{1}{d-1}\sum_{i=1}^{d=1} P_{th\_optimal}(i) & \text{otherwise} \end{cases} \quad (3.9)$$

Here,

$P_{th\_ref}(d)$ = Reference threshold on day d

$P_{th\_optimal}(i)$ = Optimal threshold on day i, calculated from actual historical data.

d = Day index within the month

**Step 2:** Determine the operational threshold ($P_{th\_op}$) by comparing the $P_{th\_ref}$ and $P_{th\_for}$ as presented in Equation (3.10). This process selects the higher value between $P_{th\_for}$ and $P_{th\_ref}$ to set $P_{th\_op}$, allowing the controller to maintain the threshold at the highest possible level and thus prevent peak reduction failures caused byunder-forecasting.

$$P_{th\_op}(d) = \begin{cases} P_{th\_ref} & P_{th\_ref} > P_{th\_for} \\ P_{th\_for} & \text{otherwise} \end{cases} \quad (3.10)$$

Once the $P_{th\_op}$ is determined, the historical threshold-based controller supplied power to the load according to $P_{th\_op}$ for peak demand reductions. Therefore, steps 3,4 and 5 described in 4.3.1 remain unchanged for this

controller, except that this controller uses $P_{th\_op}$ instead of $P_{th\_for}$ to manage the power dispatch of the BESS.

## 4.4 Design of the State-of-the-art Adjusting Threshold-based BESS Controllers

Two state-of-the-art adjusting threshold-based BESS controllers are implemented in this simulation study. The first controller is known as active controller, whereas the second controller is known as the fuzzy logic controller. The control algorithms for both controllers are designed using Python programming language. The details of the control algorithms are explained in the following subsections-

### 4.4.1 Control Algorithm of the Active Controller

The operational flow chart of the active controller is presented in Fig 4.2. The process begins with a load demand forecasting step, where the controller uses historical load consumption data to predict future demand patterns. Once the forecasted load demands are determined, a threshold ($P_{Th}$) is established by evaluating the remaining energy capacity of the BESS alongside its power rating. The calculated $P_{Th}$ is subsequently updated throughout the day of peak reduction, considering the differences between the actual real-time load and the forecasted load demands. A more comprehensive description of the active controller, along with all relevant equations is presented in the literature (Hau Lee Cheun, 2017).

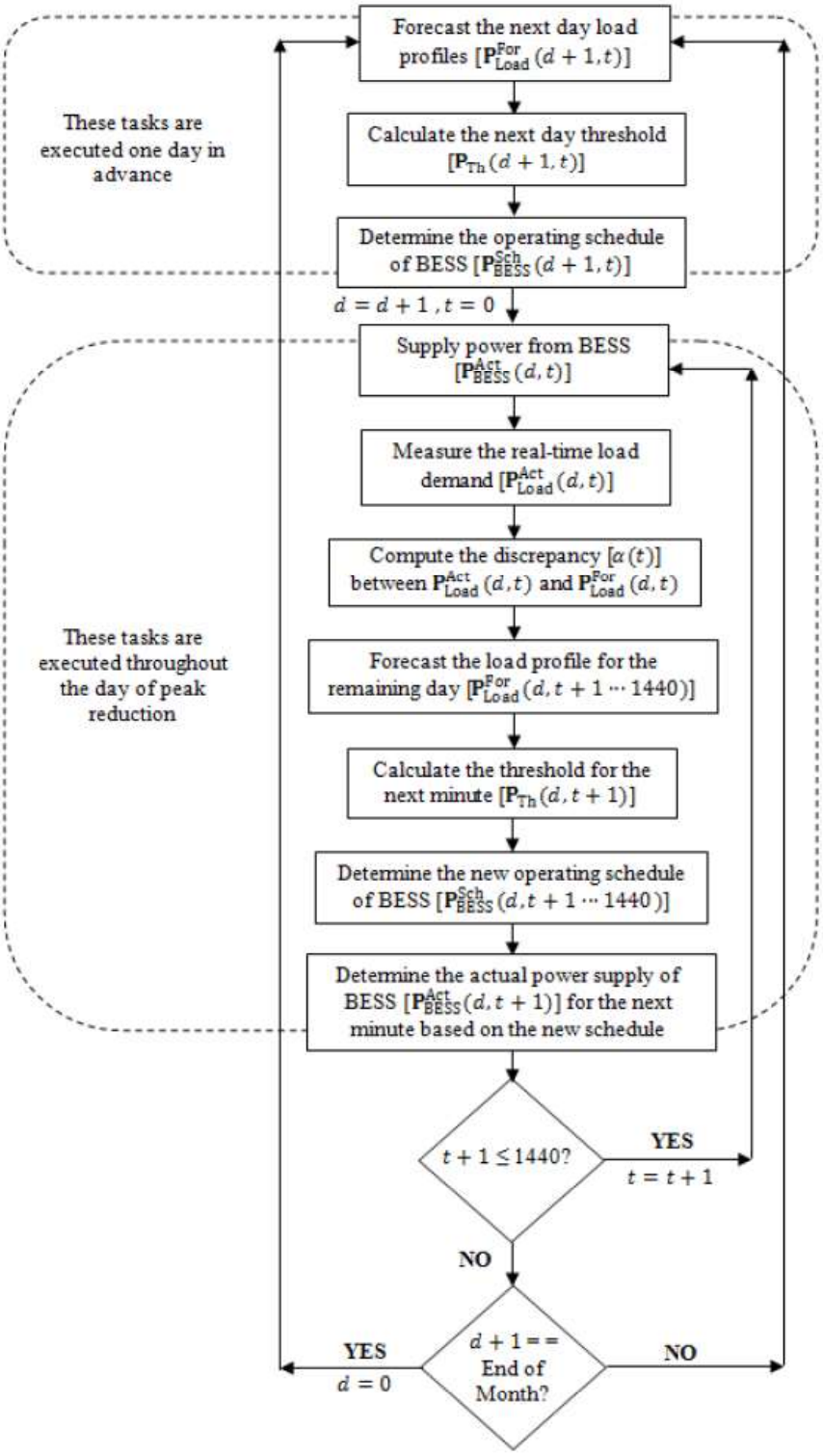


**Figure 4.2: Operational flow chart of the active BESS controller to achieve daily peak demand reductions.**

### 4.4.2 Control Algorithm of the Fuzzy Logic Controller

The operational flow chart of the fuzzy logic controller to achieve daily peak demand reduction is presented in Fig. 4.3. The controller forecasts the future load demands by utilizing the average of historical load data. During the peak reduction period, an upper threshold ($P_{UTh}$) is set to guide the discharging activity of the BESS. At the beginning of the day, $P_{UTh}$ is set to the maximum demand of the forecasted load ($P_{load\_max}$). Simultaneously, the initial battery SOC ($SOC_{Ini}$) is set to its maximum value of 95%. The power output of the BESS ($P_{ES}$) is set to as follows-

$$P_{ES} = P_{load\_max} - P_{UTh} \tag{3.11}$$

Initially, $P_{ES}$ is set to zero because the $P_{UTh}$ is equal to $P_{load\_max}$. As time progresses, the fuzzy controller continuously monitors the battery SOC and, if it remains above 50%, it incrementally lowers the $P_{UTh}$ by 0.1 kW. This iterative process continues and the $P_{ES}$ is updated until the SOC drops to 50% or below. A detailed overview of the fuzzy control algorithm for peak demand reduction can be found in the literature (Chua Kein Huat, 2016) .

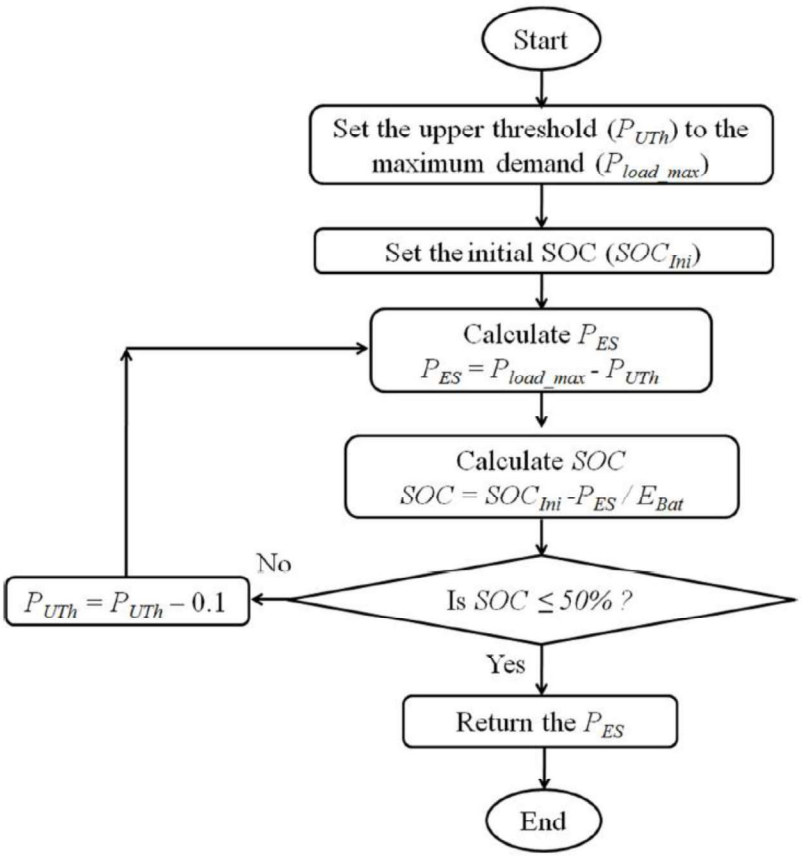


**Figure 4.3: Detailed flow chart of the fuzzy logic BESS controller for peak demand reductions.**

### 4.5 Design of the Load Forecasting Model

The proposed adaptive threshold-based controller, along with the two fixed threshold-based controllers used for benchmarking in the simulation study, all employ a deep learning-based one-dimensional convolution neural network (1D-CNN) for day-ahead load forecasting aimed at reducing peak demands. The following subsection first presents the justification for selecting the 1D-CNN model, followed by a description of the dataset used for model training. Finally,

the architecture of the 1D-CNN model used in this study and the associated training parameters are presented in detail.

### 4.5.1 Overview of the Load Forecasting Approach

Convolution neural networks (CNNs), first introduced in 1960s, have emerged as a powerful architecture in deep learning (Purwono *et al.*, 2022). They are widely used across various domains including image processing, video processing, speech recognition, natural language processing, and time-series forecasting. There are different types of CNNs architectures available, each designed to handle different types of data based on its shape and structure. For instance, 1D-CNNs are usually well suited for time-series or sequential data, where the input data is arranged in a single dimensional array over time (Ige and Sibiya, 2024). 2D-CNNs, on the other hand, are commonly used for image data that has both the height and weight dimensions(Syed M. Hur Rizvi, 2022). For more complex data such as videos or volumetric medical images, 3D-CNNs are used because they can capture patterns across width, height, and depth (Zhao *et al.*, 2024).

Load consumption data is one-dimensional (1D), as it consists of values recorded sequentially over time. Consequently, 1D-CNNs are well-suited for forecasting such data. One major benefit of the 1D-CNNs is that they can automatically detect the useful features from the data and extract them for further processing (Syed M. Hur Rizvi, 2022). This special capability makes the 1D-

CNNs well suited for load demand forecasting. In comparison with the other powerful forecasting models such as GRU, LSTM, and Transformer, which are heavily focused on long-term dependencies in time-series sequential data, the 1D-CNNs are highly effective at identifying local patterns and short-term dependencies through their convolutional filters (Su *et al.*, 2023; Wang, Liu and Bai, 2024).

Additionally, the 1D-CNNs offer greater computational efficiency compared to the other state-of-the-art forecasting models especially when dealing with time-series sequential data (Saif-Ul-Allah *et al.*, 2022; Wibawa *et al.*, 2022). This is largely because of their parallel processing capabilities and simpler architecture. Moreover, the 1D-CNNs require significantly less training time compared to the other complex deep learning-based models such as RNN, GRU and LSTM (Wibawa *et al.*, 2022). Apart from the aforementioned advantages, the 1D-CNNs demonstrate strong forecasting performance even with limited data, which makes them a reliable and efficient choice for applications where large volumes of historical data are not available (Cordeiro *et al.*, 2021). Considering the size of the dataset used in this study along with the advantages of 1D-CNN model over other load forecasting techniques, the 1D-CNN model is selected to forecast the load demands in the BESS control algorithms for peak demand reductions.

### 4.5.2 Dataset Preparation

The DAQs installed at the experimental site recorded a full year of load consumption data from Mar 2023 to Mar 2024. The load forecasting model is trained using data from the first seven months, while the data from the subsequent months is set aside for the simulation study. The raw dataset directly collected from the DAQs exhibited several quality issues such as non-numeric entries, missing values, and duplicate entries, as presented in Fig 4.4. It is essential to address all these issues before using the dataset to train the load forecasting model, as they can significantly impact the performance of the load forecasting model.

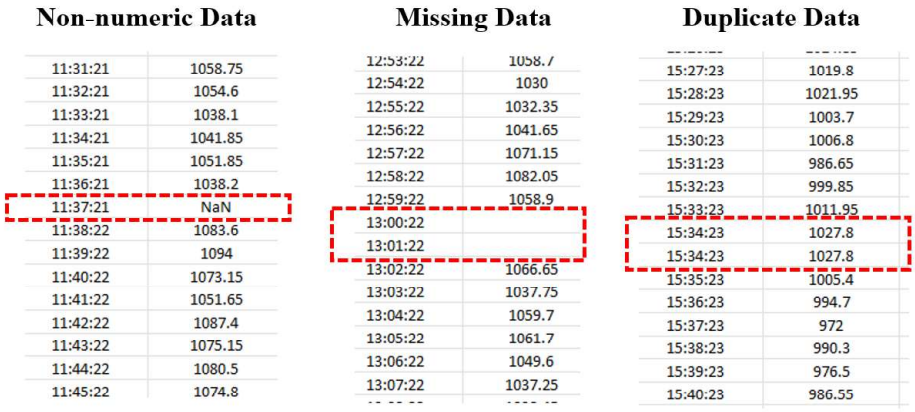


**Figure 4.4: Sample of data anomalies detected in the raw dataset, including non-numeric, missing and duplicate entries.**

A python script is developed to pre-process the raw dataset before it is used for training the load forecasting model. The Python script first identifies and

categorizes these anomalies, applying targeted correction strategies to each. For instance, the non-numeric entries are replaced with the data from the preceding minute to maintain the continuity of the dataset. A similar strategy is used for the missing entries, where the data from the preceding minute serves as the replacement. However, in situations involving extensive data loss, for example when the DAQs was offline and a full day's records are unavailable, the Python script replaces the missing entries using data from the same time on the same weekday from the previous week. These steps ensure the dataset remained accurate, continuous, and reflective of the building's natural weekly load patterns. Fig. 4.5 presents the pre-processed dataset that is used to train the load forecasting model in this study.

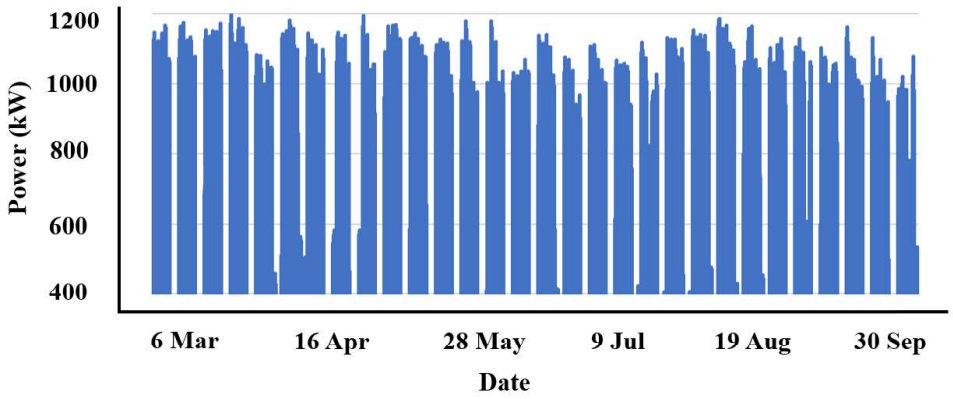


**Figure 4.5: Pre-processed dataset used to train the load forecasting model.**

### 4.5.3 Model Architecture of the proposed 1D-CNN model

Fig. 4.6 presents the architecture of the proposed 1D-CNN model used for load forecasting in this study. The model has two input layers, each dedicated to process different types of input data independently. The first input layer is specifically designed to process the sequential time-series data. The input of the first input layer comprises a continuous sequence of 5 days of load consumption data recorded at the experimental site. Although the load consumption data at the site is recorded at 1-minute intervals, the data is resembled to 15-minute intervals prior to being fed into the model to reduce the computational complexity as well as to capture broader temporal trends of the data. With 15-minute sampling, each day contributes 96 data points, and thus, a 5-day sequence yields a total of 480-time steps. Consequently, the final input shape of the first input layer is defined as (480,1), where 480 represents the time dimension and 1 denotes the number of features per time step. The load consumption values measured in kW is used as the feature of the input data.

On the other hand, the second input layer of the proposed 1D-CNN model is designed to process categorical data derived from the academic calendar of the experimental site. Since the experiments are carried out an in an academic building at the UTAR campus, load consumption varies depending on the type of the day. For instance, weekdays generally have higher load consumptions compared to weekends, while public holidays often see a significant drop in usage. To capture these variations, categorical input indicating whether a day is a weekday, weekend, or public holiday is provided in the form of a 24-hour

sequence in the second input layer. Consequently, the input to this layer is structured with a shape of (24,1).

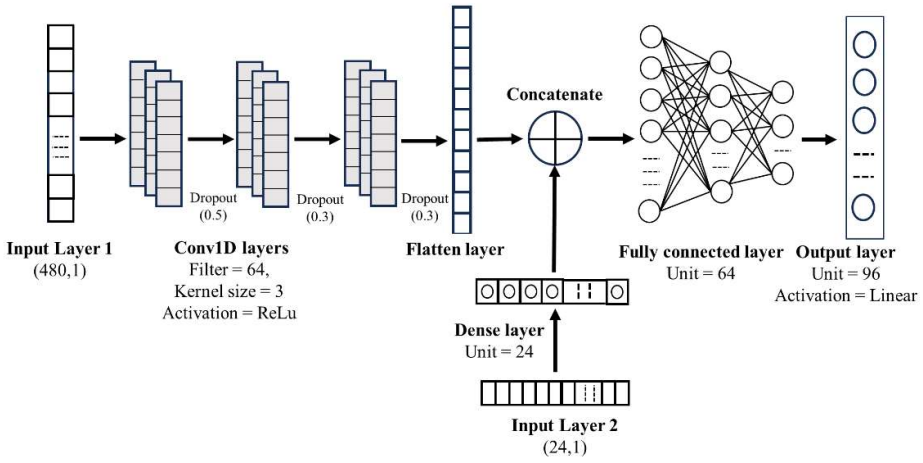


**Figure 4.6: Architecture of the proposed 1D-CNN model for load forecasting.**

After the sequential load consumption data is fed into the first input layer of the 1D-CNN model, it passes through three Conv1D layers with 64 filters, kernel size 3, and ReLU activation. These Conv1D layers help to extract meaningful patterns from the sequential time-series load consumption data. Different dropout rates of 0.5, 0.3, and 0.3 are used in between the Convo1D layers, as presented in Fig. 4.6., to prevent the overfitting during the training process. The output from these Convo1D layers is reshaped into a one-dimensional vector, allowing it to be used by the subsequent layers. Additionally, the output from the input layer 2 is fed into a dense layer with 24 neurons and ReLU activation, allowing the model to better capture the relationship between the type of day and load consumptions.

The sequential load consumption data, which is passed through Convo1D and flatten layers, and the categorical day-type data, which is processed through a dense layer, are concatenated into a single vector. This resulting feature vector is then passed through a fully connected layer with 64 units, allowing the 1D-CNN model to learn the temporal patterns of the load data with the day-type information to generate the forecast for the following day. Finally, the output layer, consisting of 96 units and using a linear activation function, provides the final load forecast for the entire day.

### 4.5.4 Training Configurations of the proposed 1D-CNN model

The proposed 1D-CNN load forecasting model is developed using Python and the Keras framework, with TensorFlow serving as the backend. Libraries like Pandas, NumPy, and Matplotlib, are used for data handling, numerical computations, and data visualization throughout the design and training phase of the model. The proposed 1D-CNN model is trained on a computer running the Windows operating system, equipped with an Intel Iris X integrated GPU, a 12th Gen Intel Core i5-12500H CPU, and 16 GB of RAM. The training process takes about two hours using the selected dataset collected from the experimental site. In this study, the 1D-CNN model is trained for 200 epochs with a batch size of 16, a learning rate of 0.001, and the AdamW optimizer. These parameters are fine-tuned through several rounds of trials to maximize the model performance.

After training, the 1D-CNN load forecasting model is saved for use in both simulation and experimental studies. During the simulation study, the saved model is stored in a specific location on the computer, where it accesses load demand profiles from another directory on the same system to generate forecasts for peak demand reduction. In the experimental study, the saved model is integrated into the system for inference, where it processes new load demand profiles collected by the on-site DAQ system to generate daily forecasts. In both the simulation and experimental studies, the trained 1D-CNN model forecasts load demands in less than a minute, using the aforementioned computer setup. This demonstrates its computational efficiency and suitability for real-time deployment, even on a machine with average processing power, memory, and storage compared to more advanced systems.

## 4.6 Implementation of the BESS Controllers in Simulation and Experimental Studies

Before proceeding to the experimental deployment, it is essential to validate the performance of the controller in a controlled simulation environment. The simulation phase allows a comprehensive performance evaluation of the BESS control algorithms under various operating conditions, without posing any risk to physical hardware setup. Therefore, the proposed adaptive threshold-based controller is first implemented in simulation environment using the Python programming language. For comparative benchmarking, the other two conventional fixed threshold-based controllers, the forecasted and historical threshold-based controllers, along with the two state-of-the-art adjusting

threshold-based controllers, active and fuzzy controllers are also implemented in Python-based simulation study.

Python version 3.10 is used for implementing the BESS control algorithms, with Jupyter Notebook serving as the primary development platform. Python version 3.10 is selected due to its broader compatibility with numerous advanced libraries, which facilitates a smoother and more efficient design process. developed separately to ensure modularity and ease of testing. Fig. 4.7 presents a segment of the implementation code for the adaptive threshold-based BESS controller, developed in Jupyter Notebook using the Python programming language. Similarly, the other benchmarking controllers are also implemented separately on the same platform to ensure consistency in the development process.

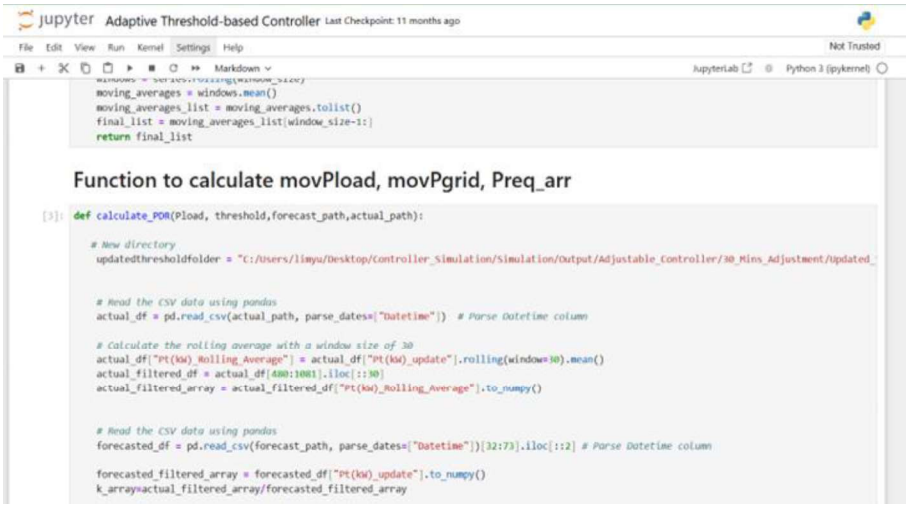


**Figure 4.7: Segment of Python code illustrating the adaptive threshold-based BESS controller, implemented in Jupyter Notebook.**

The proposed adaptive threshold-based controller, on the other hand, is implemented in the actual experimental site using the free, open-source platforms Node-RED and Python. A Python script is developed to run the 1D-CNN load forecasting model, which forecasts the load demands for peak demand reduction. Figure 4.8 displays a segment of the Python script that generates daily load forecasts throughout the experimental period and saves them to a specified location within the control unit installed at the experimental site.

main_script.py 2 | inference.py 4

C: > Users > limyu > Desktop > Adjustable_Controller > inference.py > ...

```
holidays = [datetime.strptime(date_str, '%m/%d/%Y').date() for date_str in holidays]

def preprocess_data():
    max_val, min_val = 1205, 0
    input_data = df['Pt(kW)_update'][cfg.INPUT_CSV_INDEX:cfg.INPUT_CSV_INDEX+7200]
    input_data = input_data.reset_index(drop=True)
    input_data = input_data / (max_val - min_val)

    model_input = []
    for k in range(0, len(input_data), cfg.MINUTE_GAP):
        data = [j for j in input_data[k:k+cfg.MINUTE_GAP]]
        if cfg.DATA_MODE == 'avg':
            model_input.append(sum(data) / cfg.MINUTE_GAP)
        elif cfg.DATA_MODE == 'exact':
            model_input.append(data[0])

    model_input = np.array(model_input)
    model_input = model_input.reshape(1, len(model_input), 1)
    current_date = date.today()

    weekday = current_date.weekday()
    if weekday in [5, 6]:  # Saturday, Sunday
        day = np.full(24, 1)
    elif current_date in holidays:
        day = np.full(24, 2 / 3)
    else:
        day = np.full(24, 1 / 3)
    day = day.reshape(1, len(day), 1)
    return model_input, day

def get_prediction(model_input, day):
    model = load_model(cfg.MODEL_PATH)
    y = model.predict([model_input, day])[0]
```

**Figure 4.8: Segment of Python script performing inference with the 1D-CNN model to generate daily load forecasts.**

Once the Python script generates the load forecast, a separate Python script, shown in Figure 4.9, is used to retrieve the daily forecast and determine the initial threshold for the corresponding day.

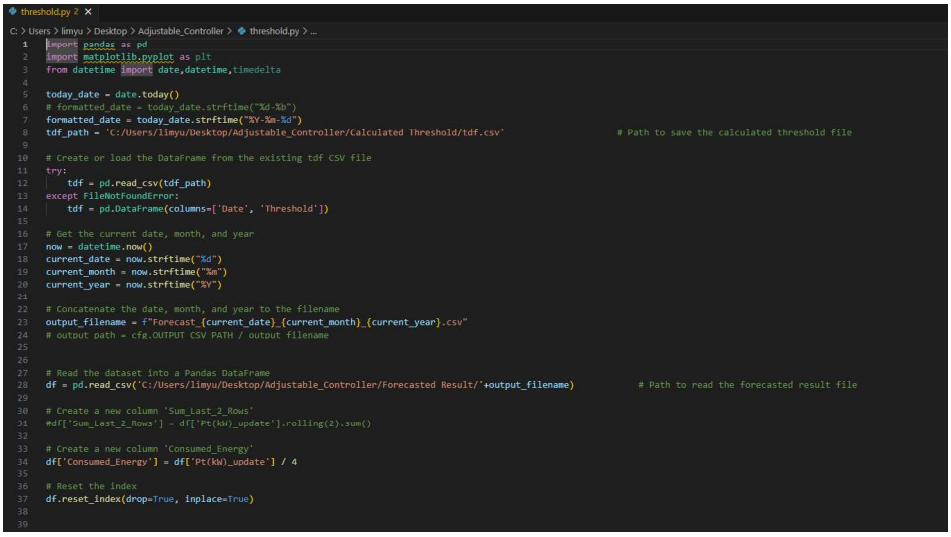


**Figure 4.9: Segment of Python script used to determine the initial threshold based on the forecasted load demands.**

The initial threshold, determined by the Python script, is retrieved by the Node-RED platform, which is also deployed on the same central control unit at the experimental site. The real-time load demand, together with the forecasted load profiles, is retrieved through the central control unit using the Node-RED platform. Both sets of data are employed to dynamically adjusts the initial threshold in real time during the entire peak demand reduction period.

The control of the bi-directional inverter for battery charging and discharging is also executed through the Node-RED platform. Dedicated nodes within Node-RED platform are employed to carry out specific control tasks. For instance, a Modbus Getter node, as illustrated in Fig. 4.10, is used to establish communication with the inverter, enabling the platform to transmit charge and discharge commands. Moreover, a custom Function Node is used to implement

the conditional logic for updating the initial threshold and managing other control tasks. Fig. 4.11 presents a segment of the Node-RED graphical programming interface developed for implementing the adaptive threshold-based BESS controller for peak demand reduction at the experimental site.

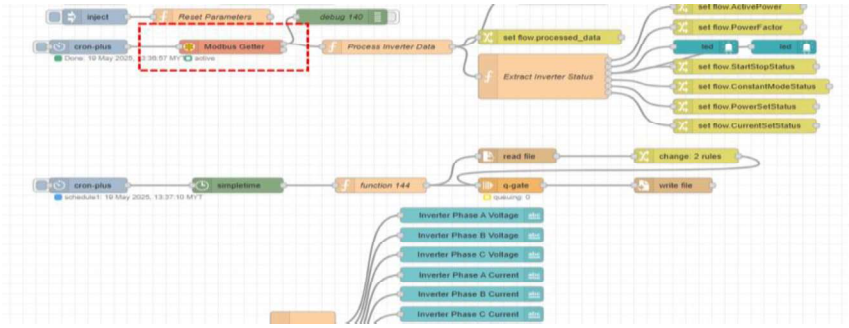


**Figure 4.10: Node-RED interface segment showing communication with the inverter using the Modbus Getter node.**

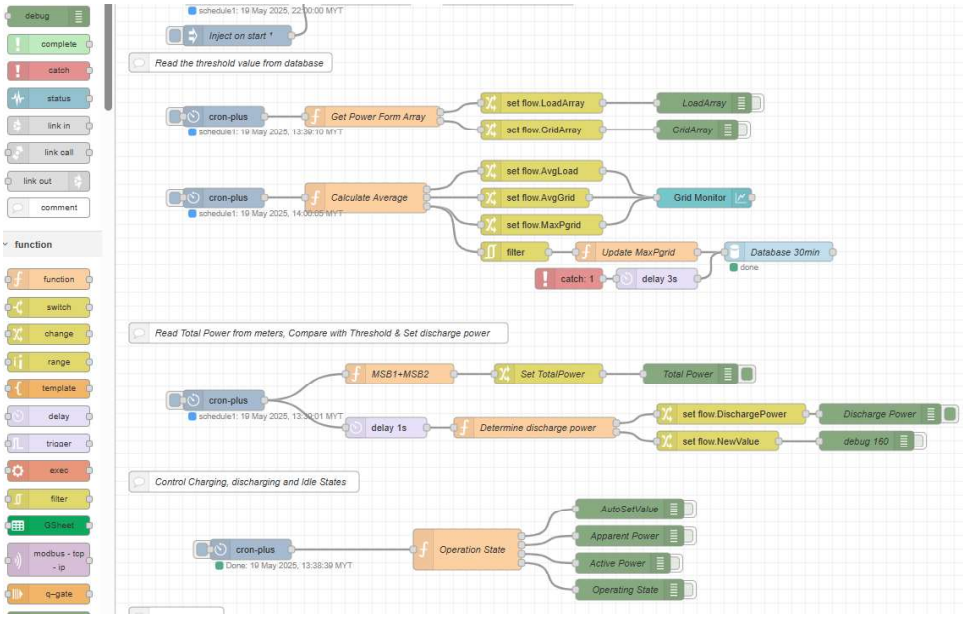


**Figure 4.11: Node-RED interface segment showing the adaptive threshold-based BESS controller for peak demand reductions.**

## 4.7 Summary

In summary, this chapter presents a comprehensive overview of the proposed adaptive threshold-based controller for peak demand reductions. Other controllers that are also implemented in simulation studies for benchmarking the results are also explained in detail. The proposed 1D-CNN load forecasting model, including its detailed architecture and training settings, which is integrated into the control algorithms of the adaptive threshold-based controller, is also explained in this chapter. Lastly, the implementation of the adaptive threshold-based controller both in simulation and experimental setup using the free, open-source platform Node-RED and Python highlighted at the end of this chapter.

# CHAPTER 5

# RESULTS AND DISCUSSIONS

## 5.1 Introduction

This chapter presents the results and in-depth discussions based on the findings of this research. It begins by describing the performance evaluation metrics used in the study, with distinct sections covering the evaluation of the 1D-CNN load forecasting model and the effectiveness of the proposed adaptive threshold-based BESS controller in managing daily peak demands. The chapter then thoroughly details the findings of the simulation study, highlighting the daily peak demand reductions achieved by the proposed controller, alongside results from other benchmark controllers. Finally, the chapter ends with an analysis of the experimental study, in which the proposed controller is evaluated over a 21-day period under real-world operating conditions to assess its effectiveness in reducing peak demands.

## 5.2 Performance evaluation metrics

In this study, five different metrics are employed. Three of them are used to assess the accuracy of the proposed 1D-CNN load forecasting model, while the remaining two evaluate how effectively the controller reduces daily peak demands. The following subsections provide further details on each metric.

### 5.2.1 Evaluation metrics for load forecasting accuracy

The forecasting performance of the 1D-CNN model is evaluated using three distinct quantitative evaluation metrics: the mean absolute error (MAE), root mean squared error (RMSE), coefficient of determination ($R^2$). Among these, MAE reflects the average prediction errors by computing the mean of absolute differences between the actual and forecasted load demands, as shown in Equation (5.1). RMSE, on the other hand, evaluates the forecasting performance by calculating the square root of the mean of squared errors, as presented in Equation (5.2). Lastly, $R^2$ reflects the degree to which the forecasting model captures variance in the actual data and is calculated using Equation (5.3). For both MAE and RMSE, lower values indicate greater forecasting accuracy. In contrast, $R^2$ scores closer to 1 represent stronger alignment between the forecasted and actual load demands.

$$\mathrm{MAE} = \frac{1}{n}\sum_{i=1}^{n}|y_i - x_i| \tag{5.1}$$

$$\mathrm{RMSE} = \sqrt{\frac{1}{n}\sum_{i=1}^{n}(y_i - x_i)^2} \tag{5.2}$$

$$R^2 = 1 - \frac{\sum_{i=1}^{n}(y_i - x_i)^2}{\sum_{i=1}^{n}(y_i - \mathrm{mean}(y_i))^2} \tag{5.3}$$

Here, $y_i$ denotes the actual load demand in kW at time step $i$,

$x_i$ denotes the forecasted load demand at time step $i$, and

$n$ denotes the total number of time steps.

### 5.2.2 Evaluation metrics for assessing the performance of the proposed controller

The performance of the proposed adaptive threshold-based controller is assessed using two different metrics, namely the daily peak reduction factor ($K_{PDR}$), and the monthly peak reduction failure rate ($\eta_{failure}$). From the literature, it is found that the performance of the most BESS controllers is assessed solely based on their actual reductions in kW. Such approach may not fully capture the true capability of a controller in reducing peak demands because it does not consider the other essential factors including the size of the BESS and shape of the load profiles (Hau and Lim, 2022). For instance, a controller with a fixed BESS capacity may achieve significant peak reduction in cases where the load profile is narrow and exhibits a single sharp peak. However, the same controller with the same BESS size may fail to achieve any peak reduction if the load profile is broader and contains multiple peaks, as compared to the earlier scenario.

Therefore, a daily peak reduction factor, $K_{PDR}$ is used in this study to assess the performance of the controllers in reducing daily peak demands. $K_{PDR}$ is calculated by comparing the actual peak reduction achieved by the controller in each day ($PDR_a$) to the ideal reduction that would be possible if the full load profile were known in advance on that day ($PDR_k$), as defined in Equation (5.4) (XC Miow *et al.*, 2025). $K_{PDR}$ allows a fairer comparison across controllers by evaluating their performance in relation to their ideal potential. A higher $K_{PDR}$ indicates better performance of a controller in reducing daily peak demands.

$$K_{pdr} = \frac{PDR_a}{PDR_k} \times 100\ \% \tag{5.4}$$

Additionally, it is essential not only to assess how well a controller reduces peak demand in a given day but also how consistently it reduces daily peak demands within a billing cycle. A BESS controller can achieve significant peak reduction on a given day but may fail to achieve any reductions on subsequent days. A controller that can consistently reduce the daily peak demands within the billing cycle is more reliable than those of that evaluated solely on individual days.

Consequently, this study uses a metric called monthly peak reduction failure rate ($\eta_{failure}$) to assess the consistency of a BESS controller in reducing daily peak demands throughout the billing cycle. For a particular month, $\eta_{failure}$ is computed by dividing the number of individual days with no peak reduction at all ($N_{failure}$) by the total number of working days in that month ($N_{total}$), with the result presented as a percentage, as defined in Equation (5.5). A lower $\eta_{failure}$ indicates that the controller performs more consistently in reducing daily peak demands throughout a billing cycle.

$$\eta_{failure} = \frac{N_{failure}}{N_{total}} \times 100\ \% \tag{5.5}$$

### 5.3 Performance evaluation in simulation study

A comprehensive simulation study is carried out using six months of data, collected from the experimental site during the period between Oct 23 to Mar 24, to assess the performance of the proposed adaptive threshold-based controller. The simulation study also includes the implementation of two conventional fixed threshold-based controllers, which are the forecasted threshold controller and the historical threshold controller, as well as two advanced adaptive controllers known as the active controller and the fuzzy logic controller. They are implemented to benchmark the proposed controller. The following subsections present the outcomes of the simulation study. Initially, the accuracy of the 1D-CNN load forecasting model is reviewed, and then the effectiveness of each controller in reducing peak demand is examined using two specific performance metrics, $K_{PDR}$ and $\eta_{failure}$.

#### 5.3.1 Performance assessment of the 1D-CNN load forecasting model

Fig. 5.1 presents an example of the forecasting performance of the proposed 1D-CNN model on 4$^{th}$ working day in Dec 23, as observed in the simulation study. The blue line represents the actual power in kW, whereas the brown line indicates the forecasted power in kW. As seen in the figure, the forecasted power closely matches the pattern of the actual power, except for minor discrepancies. This clearly indicates that the model can capture the patterns and trends of the load profile. On this day, the 1D-CNN model successfully forecasts the load demands with an MAE of 17.01 kW, RMSE of 22.31 kW, and $R^2$ value of 0.996.

Not only on this particular day, the 1D-CNN model maintains strong and consistent performance throughout in Dec 23, showing its reliability and consistency over a billing cycle. The performance of the proposed 1D-CNN load forecasting model within the billing cycle of Dec 23 is presented in Fig 5.2. Except for a few days, the 1D-CNN model successfully forecasts the load demands that closely align with the actual values. On this month, the model achieves an average MAE of 26.674 kW, RMSE of 35.337 kW, and $R^2$ of 0.988.

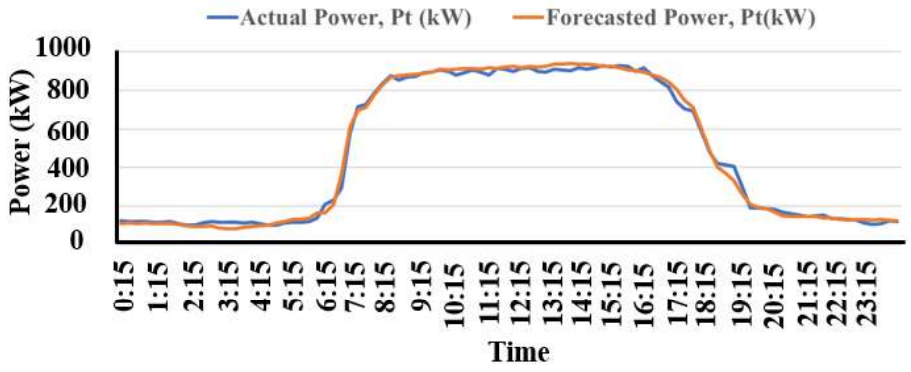


**Figure 5.1: Forecast accuracy of the 1D-CNN model on the 4th working day in Dec 23.**

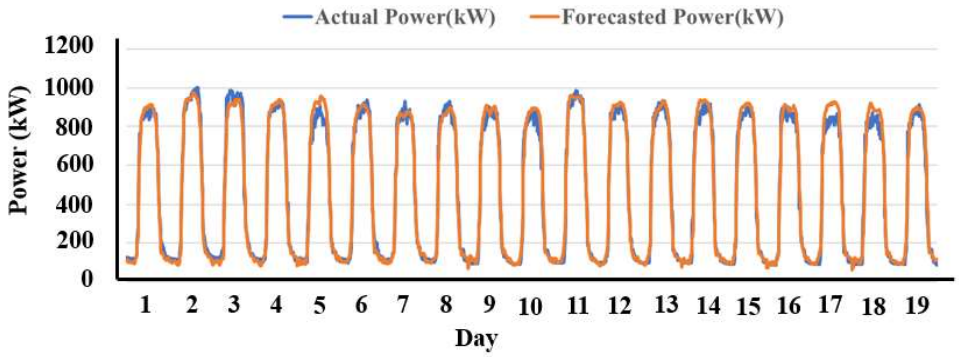


**Figure 5.2: Forecast accuracy of the 1D-CNN model in Dec 23.**

In other months of the simulation study, the proposed 1D-CNN model forecasts the load demands with differing levels of accuracy. Table 5.1 outlines the average of the evaluation metrics achieved by the 1D-CNN model in each month of the simulation study. The performance of the forecasting model fluctuates monthly, with the evaluation metrics differing accordingly. In Oct 23, the model achieves its lowest accuracy with the monthly average MAE of 62.751 kW, RMSE of 82.213 kW, and $R^2$ of 0.920. Although these average metrics indicate significant errors, the model relatively performs well throughout the month, aside from a few specific days with exceptionally high errors. These anomalous days significantly impact the overall monthly metrics, making Oct 23 the month with the least accurate forecasting performance.

On the other hand, the 1D-CNN model achieves its highest accuracy in Dec 23, yielding a monthly average MAE of 26.674 kW, RMSE of 35.337 kW, and $R^2$ of 0.988. In other months of the simulation study, the 1D-CNN model performs moderately well compared to Oct 23, as indicated by the evaluation metrics in Table 5.1. In Nov 23, the model achieves a monthly average MAE of 40.795 kW, RMSE of 53.720 kW, and $R^2$ of 0.968. In Jan 24, the model shows slightly lower accuracy compared to Nov 23, with the evaluation metrics showing a monthly average MAE of 48.824 kW, RMSE of 60.217 kW, and $R^2$ of 0.965. In the subsequent month, the model achieves results comparable to those of Jan 24, with a monthly average MAE of 49.621 kW, RMSE of 64.817 kW, and $R^2$ of 0.971. In Mar 24, the last month of the simulation study, 1D-CNN model

achieves better performance compared to the previous month, with a monthly average MAE of 42.906 kW, RMSE of 56.843 kW, and $R^2$ of 0.979.

**Table 5.1: Forecasting accuracy in simulation study.**

| Months | Evaluation Metrics | | |
|---|---|---|---|
| | MAE (kW) | RMSE (kW) | $R^2$ |
| Oct 2023 | 62.751 | 82.213 | 0.920 |
| Nov 2023 | 40.795 | 53.720 | 0.968 |
| Dec 2023 | 26.674 | 35.337 | 0.988 |
| Jan 2024 | 48.824 | 60.217 | 0.965 |
| Feb 2024 | 49.621 | 64.817 | 0.971 |
| Mar 2024 | 42.906 | 56.843 | 0.979 |

The aforementioned sections detail the monthly average error metrics achieved in each month of the simulation study. However, these monthly averages might not completely capture the actual capability of the 1D-CNN model in assisting the controllers to reduce daily peak demands. For instance, In Oct 23, the 1D-CNN model records the highest average monthly error metrics across the simulation study. However, the model forecasts the load demands with better accuracies in most of the days in this month. Fig. 5.3 shows the error metrics achieved by the 1D-CNN model in each individual days of Oct 23. The model performs well with relatively low errors across the month, except on individual days like $16^{th}$, $17^{th}$,$18^{th}$, and $19^{th}$, where substantial over-forecasting occurs. The high forecasting errors on these specific days inflate the overall monthly average

values, which could have been considerably lower if those specific individual days had less severe errors.

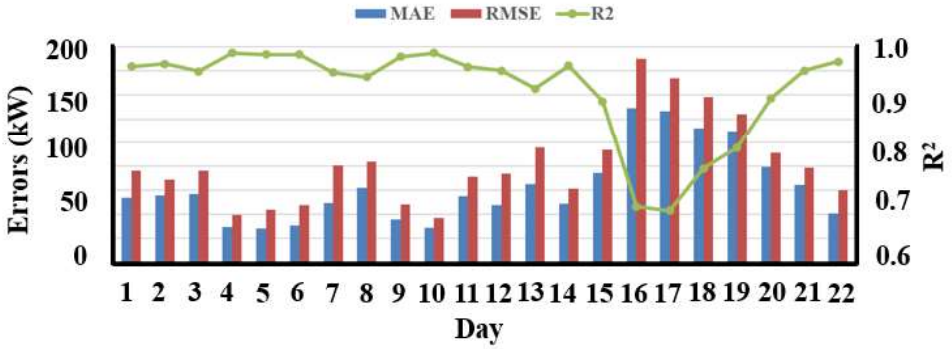


**Figure 5.3: Forecasting error metrics across individual days in Oct 23.**

From the analysis, it is clearly seen that the monthly average error metrics provide a general overview of the forecasting model's performance across different months. However, they may not adequately reflect the performance of the model on individual days. Consequently, it is crucial to assess the forecasting errors on individual days to achieve a more detailed performance evaluation of the proposed 1D-CNN load forecasting model. Fig 5.4 to Fig. 5.8 outlines the forecasting errors on individual days for the remaining month of the simulation study to better assess the performance of the 1D-CNN model.

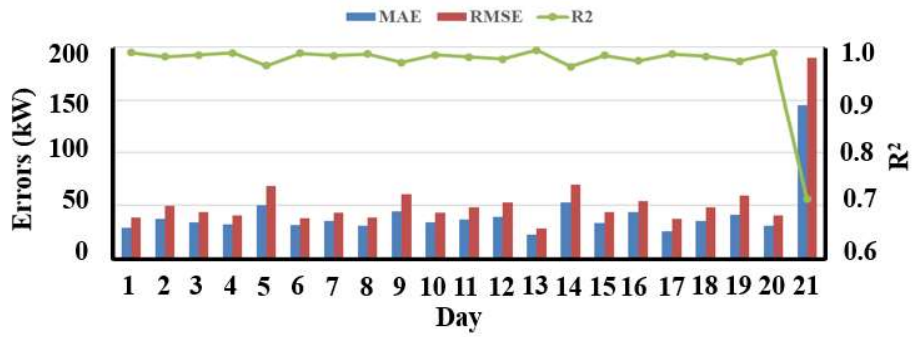


**Figure 5.4: Forecasting error metrics across individual days in Nov 23.**

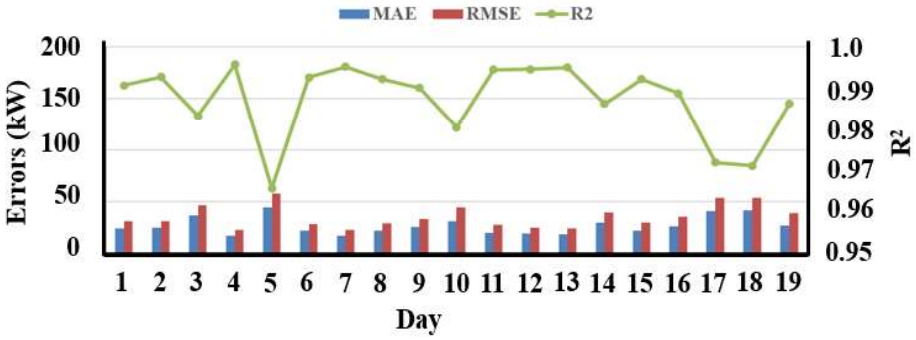


**Figure 5.5: Forecasting error metrics across individual days in Dec 23.**

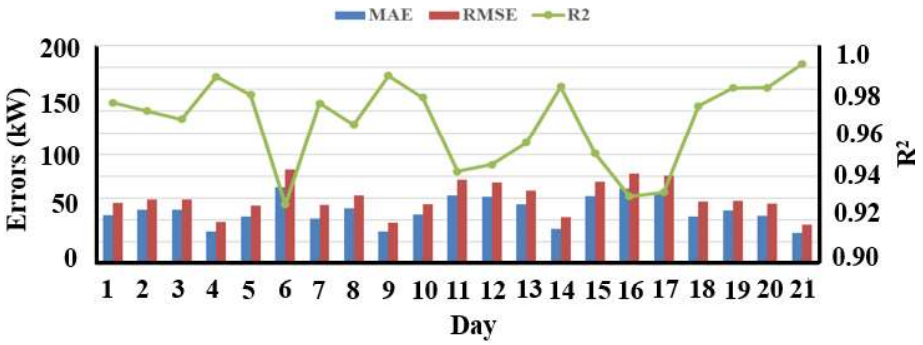


**Figure 5.6: Forecasting error metrics across individual days in Jan 24.**

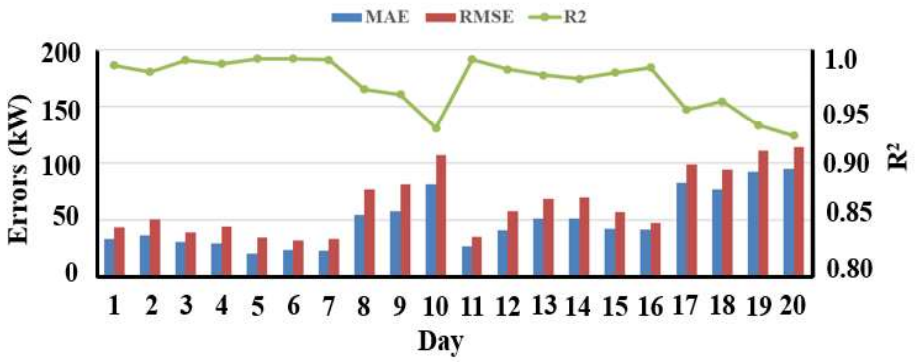


**Figure 5.7: Forecasting error metrics across individual days in Feb 24.**

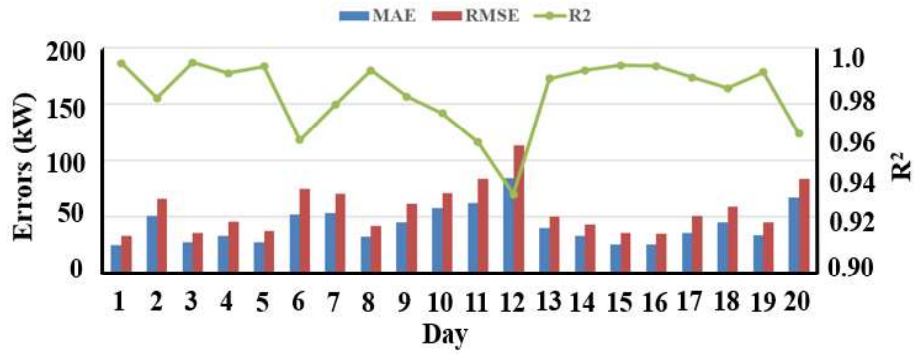


**Figure 5.8: Forecasting error metrics across individual days in Mar 24.**

### 5.3.2 Performance assessment of the proposed adaptive threshold-based controller using daily peak reduction factor, $K_{PDR}$

The operational results of the proposed adaptive threshold-based controller, achieved on the 8$^{th}$ working day of Oct 23, is presented in Fig. 5.9. On this particular day, the actual peak demand of 922.92 kW is recorded during the period between 15:00 to 15:30. To successfully reduce the actual peak of the day, the controller must guide the BESS to deliver its power to the load during this interval. First, a load demand profile for the entire day is forecasted in advance by the proposed 1D-CNN model. The load demand profile, consisting

of 96 data points at 15-minutes interval, is stored on a dedicated computing unit where the simulation study is conducted. Based on the forecasted load demands along with the available BESS capacity, an initial threshold ($P_{th\_initial}$) of 977.21 kW is determined for the day to guide the power dispatch of the BESS for peak demand reduction.

Starting at 8:00, the adaptive threshold-based controller determines the threshold adjustment factor (k) on every 15-minute interval, considering both the real-time and forecasted load demands. This factor helps set up the updated threshold ($P_{th\_upd}$), and the final threshold ($P_{th\_final}$) that mainly controls the power dispatch of the BESS throughout the day of peak reduction. The preceding peak of the grid ($P_{grid\_avr}(max)$) is also considered when $P_{th\_final}$ is set to guide the BESS power output for peak demand reduction.

The controller retrieves the instantaneous load demands ($P_{load\_in}$) at every 1-minute interval starting from 8:00. Whenever $P_{load\_in}$ exceeds the $P_{th\_final}$, the controller commands the BESS to discharge its power ($P_{bess\_in}$) equal to the difference between $P_{load\_in}$ and $P_{th\_final}$ of that moment to reduce the peak of the day. $P_{th\_final}$ is dynamically adjusted throughout the day, and $P_{bess\_in}$ is set based on the latest $P_{load\_in}$ and $P_{th\_final}$ to reduce the actual peak of the day. On this day, the controller successfully set $P_{th\_final}$ to reserve BESS to discharge during the period between 15:00 to 15:30, reducing the actual peak of the day.

On this day, the adaptive threshold-based controller manages to reduce the actual peak demand from 922.92 kW to 894.95 kW, achieving a daily actual peak reduction ($PDR_a$) of 27.97 kW. At the end of the day, the ideal reduction for that load profile ($PDR_k$) is calculated to be 30.97 kW. As a result, the controller achieves a $K_{PDR}$ of 90.31% for this day.

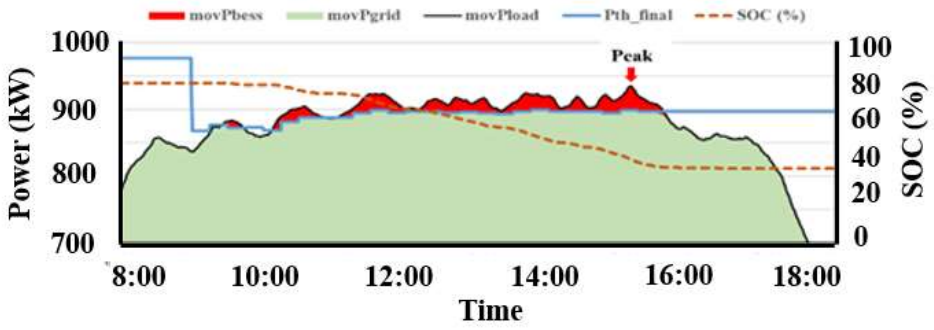


**Figure 5.9: Daily peak demand reduction achieved by the adaptive threshold-based controller on the 8th operational day in Oct 23.**

$K_{PDR}$ achieved by the proposed adaptive threshold-based controller for each individual day in Oct 23 is shown in Fig. 5.10. The controller manages to reduce peak demands on every single day of the month, without any failures. Although the 1D-CNN load forecasting model records the highest average monthly errors in this month, the controller manages to reduce all the daily peak demands of this month. As discussed earlier, the high average monthly errors occur in this month due to the factor that some days exhibits very high over-forecasting results. On other remaining days, the forecasting performances are relatively well. On those specific over-forecasted days, the controller effectively reduces the thresholds using the actual real-time load demands. Although $K_{PDR}$ values achieved on those specific over-forecasted days are lower compared to days with

more accurate forecasts, the proposed adaptive threshold-based controller manages to reduce the peak demands and achieve $K_{PDR}$ to some extent. The adaptive threshold-based controller records an average monthly $K_{PDR}$ of 51.18% in Oct 23, demonstrating its effectiveness and reliability in reducing daily peak demands within a billing cycle.

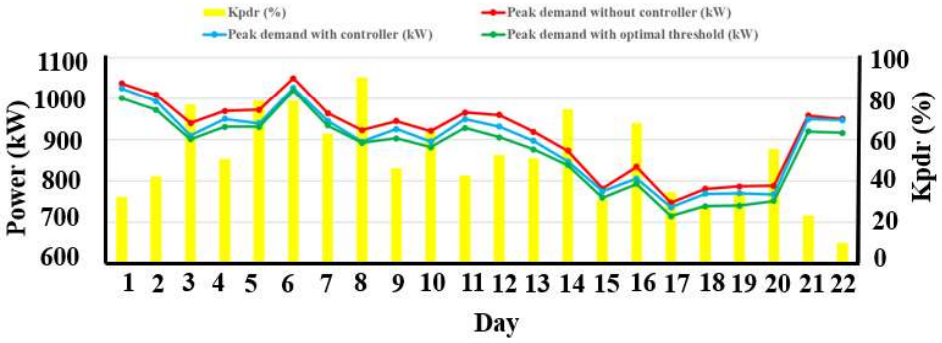


**Figure 5.10: Daily peak demand reduction achieved by the adaptive threshold-based controller in Oct 23.**

Conversely, the two fixed threshold-based controllers face difficulties in reducing daily peak demands in Oct 23. The forecasted threshold-based controller, as shown in Fig. 5.11, only manages to reduce peak demands on certain individual days. On days when the load demands are under-forecasted, the BESS often runs out of energy before the actual daily peak occurs, as the controller lacks the ability to adjust thresholds in real time. This leads to the controller being unsuccessful in reducing daily peak demands on most days, with no $K_{PDR}$ recorded on those days. The controller records a monthly average $K_{PDR}$ of just 16.52% on Oct 23.

Like forecasted threshold-based controller, the historical threshold-based controller also faces challenges in reducing daily peak demands on many occasions throughout Oct 23, as shown in Fig. 5.12. Although this controller sets the threshold differently to avoid peak reduction failures due to under-forecasting issues, the lack of real-time threshold adjustment limits its ability to deliver significant improved performance in reducing daily peak demands throughout this month. This controller records an average monthly $K_{PDR}$ of just 13.86% in Oct 23.

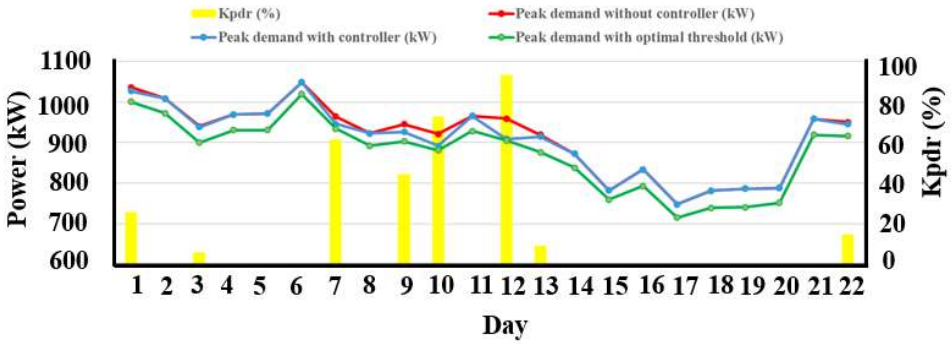


**Figure 5.11: Daily peak demand reduction achieved by the forecasted threshold-based controller in Oct 23.**

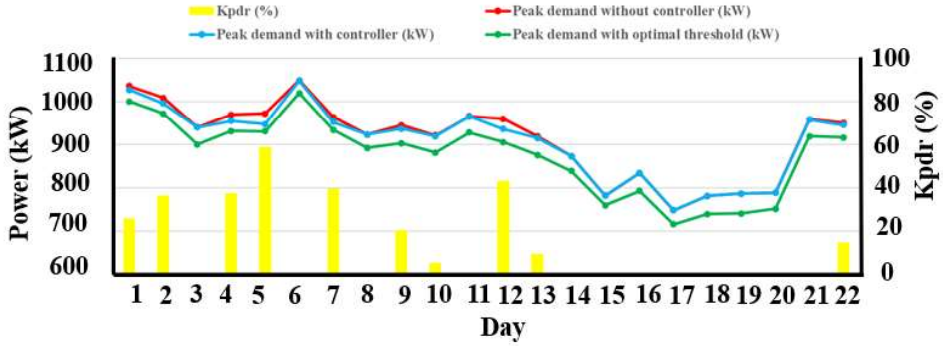


**Figure 5.12: Daily peak demand reduction achieved by the historical threshold-based controller in Oct 23.**

In comparison to the fixed threshold-based controllers, the state-of-the-art adjusting threshold-based active and fuzzy logic controllers perform comparatively well in Oct 23. The active controller adjusts the threshold throughout the day and manages to effectively reduce daily peak demands on several days in this month. As presented in Fig. 5.13, the active controller achieves high $K_{PDR}$ in many individual days in this month. However, on multiple days, the controller cannot reduce peak demands and does not record any $K_{PDR}$. On these days, the thresholds are set comparatively low, therefore the BESS runs out of its stored energy even before the actual peak occurs. In Oct 23, the state-of-the-art active controller records an average monthly $K_{PDR}$ of 18.03%, slightly better than those of the fixed threshold-based controllers.

On the other hand, the other state-of-the-art fuzzy logic controller shows strong performance on Oct 23. This controller sets the threshold and manages the power dispatch of the BESS more effectively than the active controller this month. As shown in Fig. 5.14, the fuzzy logic controller effectively reduces daily peak demands in most individual days of the month and achieves very high $K_{PDR}$ compared to the active controller. In Oct 23, the fuzzy controller records an average monthly $K_{PDR}$ of 36.60%, which is higher than that of active controller. However, it still underperforms compared to the proposed adaptive threshold-based controller, which achieves an average monthly $K_{PDR}$ of 51.18% in this month.

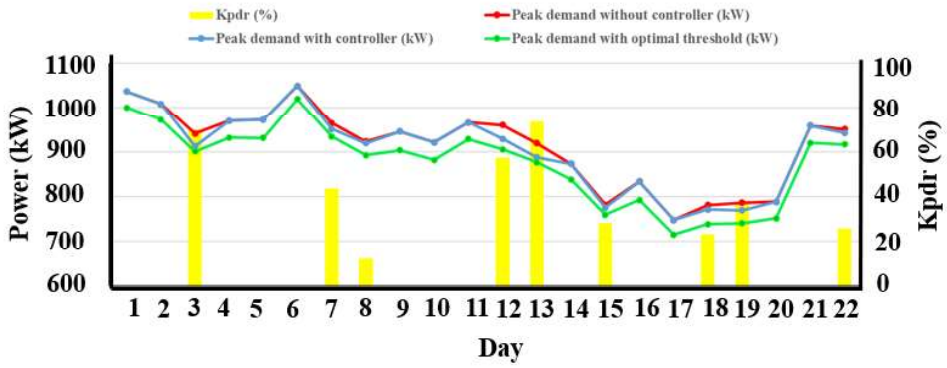


**Figure 5.13: Daily peak demand reduction achieved by the active controller in Oct 23.**

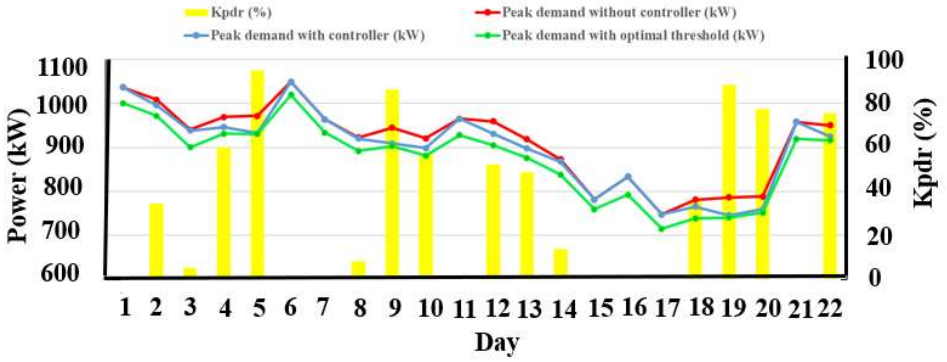


**Figure 5.14: Daily peak demand reduction achieved by the fuzzy logic controller in Oct 23.**

The average monthly $K_{PDR}$ achieved by the proposed adaptive threshold-based controller, along with the other benchmark controllers in simulation study, are summarized in Table 5.2. In Dec 23, the proposed adaptive threshold-based controller records its best result, with an average monthly $K_{PDR}$ of 58.71%. The 1D-CNN forecasting model forecasts the load demands more accurately in Dec 23 compared to the other months. Consequently, it helps the proposed adaptive threshold-based controller to set the thresholds that facilitate effective BESS power dispatch for peak demand reductions. Both fixed threshold-based controllers perform well in this month, as their performance heavily relies on the

forecasting performance of the 1D-CNN model. The forecasted threshold-based controller achieves an average monthly $K_{PDR}$ of 45.44% in Dec 23, whereas the historical threshold-based controller records an average monthly $K_{PDR}$ of 36.07%. In comparison, the state-of-the-art active controller comparatively performs less effectively this month compared to the other controllers. The thresholds are poorly set on most of the days of this month in this controller. Consequently, the controller experiences peak reduction failures on several individual days in this month and achieves an average monthly $K_{PDR}$ of 24.21%. Conversely, the fuzzy logic controller performs significantly well compared to the active controller this month. It records an average monthly $K_{PDR}$ of 41.27%, yet it does not surpass the performance of the proposed adaptive threshold-based controller.

The proposed adaptive threshold-based controller shows strong performance in reducing daily peak demands with high average monthly $K_{PDR}$ in the simulation study, outperforming other benchmark controllers in all months except Feb 24 and Mar 24. The performance of the adaptive threshold-based controller declines in these months due to high forecasting errors achieved from the 1D-CNN load forecasting model. On most of the days in these months, the demands are under-forecasted. Consequently, the thresholds are set relatively low, leading the BESS to deplete its energy prematurely before the actual peak occurs. Although the controller makes efforts to adjust the thresholds to overcome the forecasting errors, it faces challenges in reducing the actual peak on days when the peak occurs toward the end of the day.

Over the six-month simulation study, the proposed adaptive threshold-based controller consistently performs well in reducing daily peak demands. On average, the proposed controller records an average monthly $K_{PDR}$ of 41.62% in the simulation study. In comparison, the other two fixed threshold-based controllers show significantly lower performance. On average, the forecasted threshold-based controller achieves an average monthly $K_{PDR}$ of 20.21% in this simulation study, whereas the historical threshold-based controller records an average monthly $K_{PDR}$ of 24.43%.

Meanwhile, the state-of-the-art adjusting threshold-based controllers show strong capability in minimizing daily peak demand in the simulation study. The state-of-the-art active controller achieves an average monthly $K_{PDR}$ of 21.65% over the six-month simulation study, whereas the other state-of-the-art fuzzy logic controller records an average monthly $K_{PDR}$ of 38.47%. Among the four benchmark controllers, the fuzzy logic controller shows performance comparatively close to the proposed adaptive threshold-based controller. However, the proposed adaptive threshold-based controller demonstrates superior effectiveness, attaining the highest average monthly $K_{PDR}$ for daily peak demand reductions in this simulation study.

**Table 5.2: Performance of the proposed and benchmark controllers in the simulation study based on average monthly $K_{PDR}$.**

| Month | Average $K_{PDR}$ (%) | | | | |
|---|---|---|---|---|---|
| | Forecasted threshold-based controller | Historical threshold-based controller | Active controller | Fuzzy logic controller | Adaptive threshold-based controller |
| Oct 23 | 16.52 | 13.86 | 18.03 | 36.60 | 51.18 |
| Nov 23 | 28.40 | 42.63 | 23.46 | 45.99 | 50.06 |
| Dec 23 | 45.44 | 36.07 | 24.21 | 41.27 | 58.71 |
| Jan 24 | 12.84 | 9.20 | 13.42 | 41.00 | 45.11 |
| Feb 24 | 6.28 | 16.43 | 24.57 | 29.75 | 16.46 |
| Mar 24 | 11.75 | 28.37 | 26.19 | 36.19 | 28.19 |
| **Average** | **20.21** | **24.43** | **21.65** | **38.47** | **41.62** |

### 5.3.3 Performance assessment of the proposed adaptive threshold-based controller using monthly failure rate, $\eta_{failure}$

The monthly peak reduction failure rate ($\eta_{failure}$) achieved by the proposed adaptive threshold-based controller and the other benchmark controllers in the simulation study is presented in Fig. 5.15. Over the six-month simulation study, the proposed adaptive threshold-based controller achieves its best result in Oct 23. In this particular month, the controller effectively manages the power dispatch of the BESS and successfully reduces all the daily peak demands of the billing cycle. With no failures across the 22 working days in this month, the proposed controller records the lowest $\eta_{failure}$ of 0% in this month.

In comparison, both the fixed threshold-based controllers achieve high $\eta_{\text{failure}}$ in Oct 23. The forecasted threshold-based controller fails to achieve any peak reduction in 14 working days in this month. Consequently, it records an $\eta_{\text{failure}}$ of 63.64% in Oct 23. Likewise, the historical threshold-based controller does not manage to reduce daily peak demands on 12 working days during this month. Therefore, it records an $\eta_{\text{failure}}$ of 54.55% in Oct 23.

The state-of-the-art active controller also shows relatively low performance in terms of $\eta_{\text{failure}}$ in Oct 23. Out of 22 working days, the active controller manages to reduce daily peak demands on only 9 days, failing on the remaining 13. As a result, it records an $\eta_{\text{failure}}$ of 59.09% in this month. The other state-of-the-art fuzzy logic controller shows better consistency compared to the active controller in Oct 23. It manages to reduce peak demand on 14 days, with failures occurring on the remaining 8 days. Therefore, it achieves an $\eta_{\text{failure}}$ of 36.36% in Oct 23.

Over the six-month simulation study, the proposed adaptive threshold-based controller consistently reduces daily peak demands and maintains a lower $\eta_{\text{failure}}$ than the other benchmark controllers, with the exception of Feb 24. In this particular month, the controller experiences high $\eta_{\text{failure}}$, mainly due to the forecasting accuracies. On most days of this month, the 1D-CNN load forecasting model forecasts the load demands with under-forecast tendency. Although the average monthly forecasting errors in Feb 24 are not the highest observed in the study, the consistent under-forecasting performance of the 1D-CNN model significantly contributes to peak reduction failures, even when the

absolute error values are relatively low. In Feb 24, the adaptive threshold-based controller does not achieve any peak demand reductions on 10 working days, leading to achieve an $\eta_{\text{failure}}$ of 50% in this month. Similarly, the fixed threshold controllers struggle in Feb 24 because the under-forecasting performance by the 1D-CNN model severely impairs their effectiveness in lowering daily peak demands. The forecasted threshold and historical threshold-based controller fails to reduce daily peak demands on 17 and 14 working days respectively in Feb 24, resulting in an $\eta_{\text{failure}}$ of 85% and 70%. In Feb 24, both the state-of-the-art controllers comparatively perform well and achieve lower $\eta_{\text{failure}}$ compared to the other controllers. The active and fuzzy logic controllers each fail to reduce peak demand on only 6 working days during the month, resulting in an $\eta_{\text{failure}}$ of 30% for both controllers.

Over the six-month simulation study, the proposed adaptive threshold-based controller demonstrates the most reliable performance, achieving the lowest average $\eta_{\text{failure}}$ of just 16.55%. This clearly indicates its consistency in reducing daily peak demands over an extended period. In contrast, both the fixed threshold-based controllers exhibit poor and inconsistent performance, with the forecasted threshold and historical threshold-based controllers achieving high average $\eta_{\text{failure}}$ of 58.24% and 46.97%, respectively. Meanwhile, the state-of-the-art BESS controllers show comparatively better consistency compared to the fixed threshold-based controllers in the simulation study. The active controller achieves an average $\eta_{\text{failure}}$ of 43.70% in the simulation study, while the fuzzy logic controller performs more favourably with an average $\eta_{\text{failure}}$ of 28.30%. Although both controllers show improved consistency in reducing daily peak

demands compared to the fixed threshold-based controllers, their performance still falls short of the proposed adaptive threshold-based controller in this simulation study.

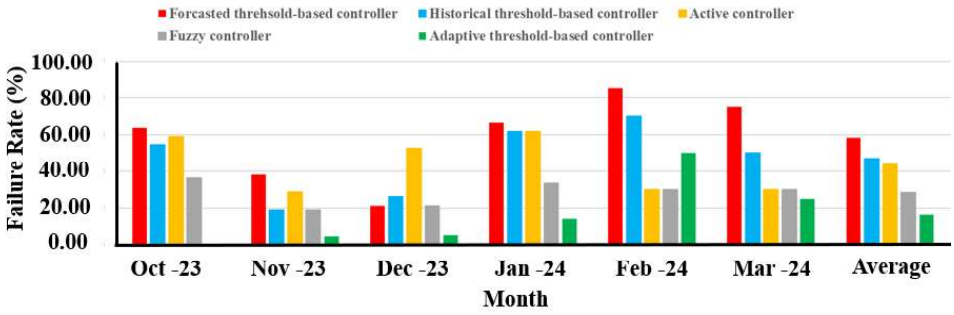


**Figure 5.15: Failure rates achieved by the BESS controllers across the simulation study.**

## 5.4 Performance evaluation in experimental study

After conducting the simulation study, the proposed adaptive threshold-based BESS controller is implemented to BESS at UTAR campus to assess its practical effectiveness under real operating conditions. The controller is deployed and tested at the site over a period of 21 working days, during which the performance of the controller is closely assessed using the two different metrics $K_{PDR}$ and $\eta_{failure}$. The following subsection presents a comprehensive analysis of experimental results achieved by the proposed adaptive threshold-based controller. Before that, the performance of the 1D-CNN load forecasting model during the experimental period is first presented to provide essential context for evaluating the controller's peak demand reduction capabilities.

### 5.4.1 Performance assessment of the 1D-CNN load forecasting model

Fig. 5.16 illustrates an example of the forecasting performance of the proposed 1D-CNN model on 17$^{th}$ working day in the experimental study. As presented in the figure, the forecasted load demands closely align with the pattern of the actual power demands, demonstrating the ability of the 1D-CNN model to capture the patterns and trends in the data. Although there are some minor discrepancies between the forecasted and actual load demands, especially outside peak demand periods, they do not significantly impact the controller's overall performance. On this experimental day, the 1D-CNN load forecasting model forecasts the load demands with an MAE of 32.72 kW, RMSE of 41.78 kW, and $R^2$ value of 0.99.

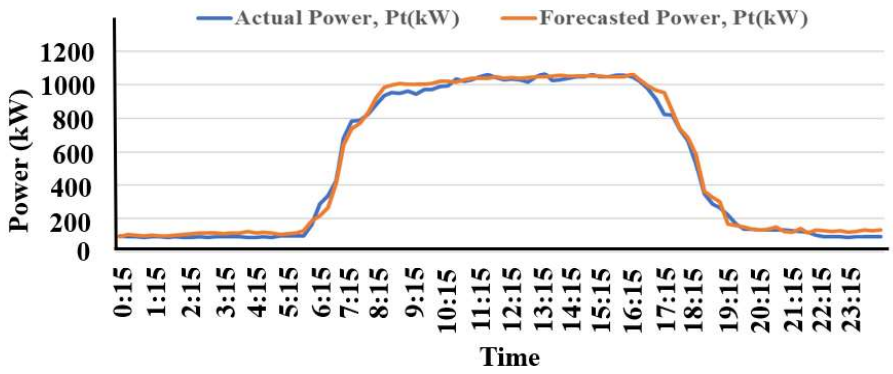


**Figure 5.16: Forecast accuracy of the 1D-CNN model on the 17th working day in the experimental study.**

The performance of the proposed 1D-CNN load forecasting model within the 21 days of experimental study is presented in Fig 5.17. The model performs relatively well except for a few days. During this experimental period, the 1D-CNN load forecasting model records an average MAE of 35.496 kW, RMSE of

48.621 kW, and $R^2$ of 0.986. To better analyse the performance of the model, the errors metrics achieved by the 1D-CNN model in each day of the experimental study is provided in Fig. 5.18.

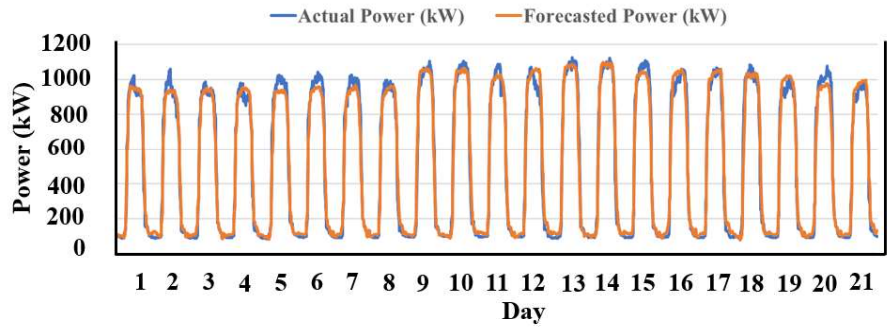


**Figure 5.17: Forecast accuracy of the 1D-CNN model during the experimental study.**

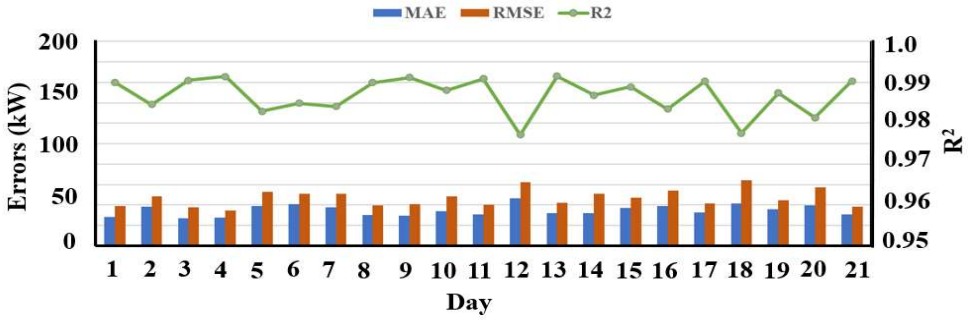


**Figure 5.18: Forecasting error metrics across individual days in the experimental study.**

### 5.4.2 Performance assessment of the proposed adaptive threshold-based controller using daily peak reduction factor, $K_{PDR}$ and monthly failure rate, $\eta_{failure}$

Fig. 5.16 shows the experimental results of the proposed adaptive threshold-based controller on the 17th working day of the study. On this particular

experimental day, the actual peak demand hits to 1081.90 kW, and it occurs during the period between 15:30 to 16:00. The controllers need to supply power during this period to reduce the actual peak of the day. During the nighttime charging phase, the BESS absorbs energy from the grid through the bi-directional inverter at the experimental site. Once the battery SOC reaches to 80%, the controller stops its charging operation and activates idle mode until the discharging mode is initiated.

Before the discharging mode initiates at 8:00, the 1D-CNN forecasts the load demands for the entire day and an initial threshold ($P_{th\_initial}$) of 1023.429 kW is set based on the forecasted load demands. Once the discharging mode is activated at 8:00, the adaptive threshold threshold-based controller starts calculating the adjusting threshold factor (k), that helps to set the final threshold ($P_{th\_final}$) to manage power dispatch of the BESS throughout the day. The controller continuously monitors the instantaneous load demands ($P_{load\_in}$) and dynamically adjusts $P_{th\_final}$ based on the forecasted and actual load demands along with the preceding peak of the grid profile. The power dispatch of the BESS in every 1-minute is managed based on the latest $P_{th\_final}$ and $P_{load\_in}$. Once $P_{load\_in}$ exceeds $P_{th\_final}$, the controller starts supplying BESS power $P_{bess\_in}$ to the load. As shown in Fig. 5.16, the controller dynamically adjusts the $P_{th\_final}$ and supplies $P_{bess\_in}$ whenever required. On this day, the controller successfully sets the $P_{th\_final}$ in such way that $P_{bess\_in}$ is effectively supplied to the load during the period between 15:30 to 16:00.

The adaptive threshold-based controller manages to reduce the actual peak of the day to 1051.20 kW, achieving an actual peak reduction $PDR_a$ of 30.70 kW for this day. The ideal peak reduction ($PDR_k$) of this day is calculated to be 32.02 kW. Therefore, the proposed adaptive threshold-based controller records a $K_{PDR}$ of 95.88% in this specific experimental day.

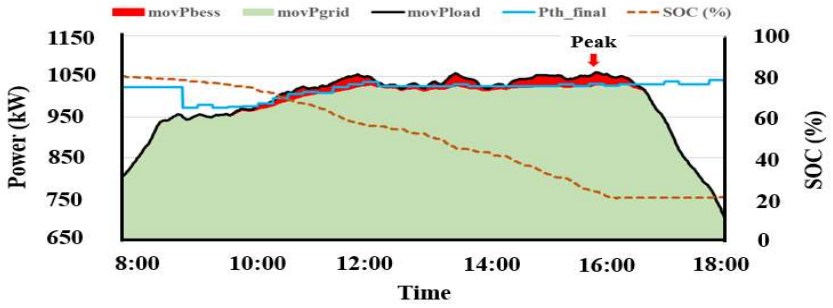


**Figure 5.19: Daily peak demand reduction achieved by the adaptive threshold-based controller on the 17th operational day in experimental study.**

Not only on this specific experimental day, but throughout the entire experimental period, the proposed adaptive threshold-based controller consistently shows its effectiveness in reducing daily peak demands. The performance of the proposed controller, evaluated in terms of $K_{PDR}$, is presented in Fig. 5.20. As shown in the figure, the controller manages to reduce daily peak demands and achieve notable $K_{PDR}$ in most of the experimental days. An exception is observed on the 15th working day, when the proposed controller cannot achieve any $K_{PDR}$. On this particular day, the peak occurs at the very last moment of the discharging phase, and the BESS runs out its energy just before the peak occurs. Apart from this single day of failure, the proposed adaptive threshold-based controller significantly shows its effectiveness in reducing daily peak demands under the real operating conditions at the experimental site.

Since the controller is unable to lower daily peak demands on only one day out of 21 working days in this experimental study, the proposed adaptive threshold-based controller records a significant low $\eta_{failure}$ of just 4.76%. This clearly demonstrates its strong consistency in reducing daily peak demands even under real operating conditions.

Overall, the proposed adaptive threshold-based BESS controller records an average $K_{PDR}$ of 49.45%, highlighting its strong effectiveness in reducing daily peak demands. These experimental results confirm the real-world effectiveness of the developed controller in lowering daily peak loads under actual operating conditions.

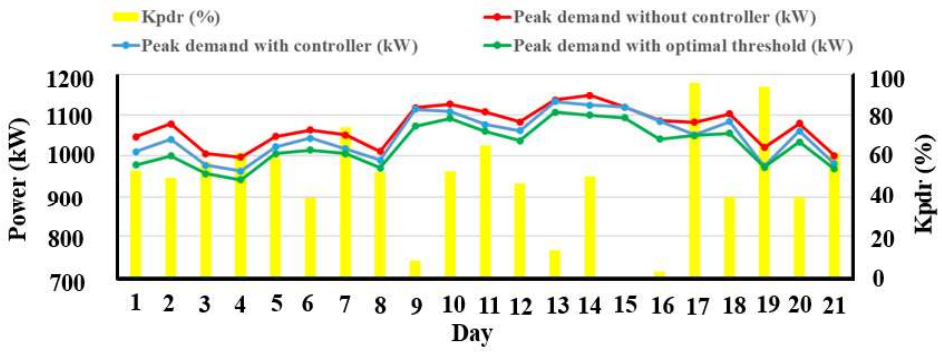


**Figure 5.20: Daily peak demand reduction achieved by the adaptive threshold-based controller during experimental study.**

## 5.5 Summary

The findings of this research are comprehensively presented in this chapter. Both the simulation and experimental results are presented in detail. The proposed adaptive threshold-based BESS controller outperforms the other benchmark controllers in simulation study, achieving an average $K_{PDR}$ of 41.62% and $\eta_{failure}$ of 16.55%. Not only in simulation, but the proposed controller also maintains a strong performance in reducing daily peak demands in the real experimental setup. Over 21 days of experimental study, the controller records an average $K_{PDR}$ of 49.45% and $\eta_{failure}$ of 4.76%, demonstrating even better performance than in the simulation results.

# CHAPTER 6

# CONCLUSIONS AND FUTURE WORKS

## 6.1 Conclusion

Peak demand reduction is important as it can yield significant financial savings by minimizing additional maximum demand charges. Additionally, it can also bring substantial environmental benefits by avoiding the fossil fuel-based peaking power plants. Several approaches are widely used to reduce the peak demands for end customers. However, Battery-based energy storage system (BESS) has gained more popularity due to its fast response capability, high efficiency, and ability to store excess energy for use during peak demand periods. BESS is charged during the periods when the consumptions are comparatively low, and discharged its stored energy when consumptions are relatively high. To achieve peak demand reduction using BESS, a controller is required that can effectively charge and discharge the batteries at the appropriate time.

Various BESS controllers exist in the literature aimed to achieve peak demand reductions. Most of them are tested only in simulation, experimental testing under real operating conditions is yet to be fully explored. Although some of the controllers are tested experimentally, many of them are tested only on limited case studies without using any evaluation metrics. Additionally, most of the existing controllers are developed using paid commercial platforms, which typically increases the overall controller development costs. Apart from these,

advanced load forecasting techniques are not incorporated in most of the existing controllers, which significantly impacts the performance of the controllers.

To address these gaps, this study proposed an innovative adaptive threshold-based controller for BESS using an advanced deep learning-based 1D-CNN load forecasting model to reduce the daily peak demands for end customers. The proposed controller employs a 1D-CNN model to forecast load demands ahead of time and establishes an initial threshold that is dynamically adjusted during the peak reduction day using both forecasted and actual load demands, as well as the previous peak in the grid profile, to optimize BESS power scheduling for peak reductions. The controller is first implemented in simulation using Python programming and benchmarked against four different controllers through two different evaluation metrics, $K_{PDR}$ and $\eta_{failure}$, based on six months on-site data. Following the simulation study, the proposed controller is deployed on a real 200 kW/200 kWh BESS setup installed in a university building in Malaysia, using the open-source Node-RED platform to assess its practical performance under real operating conditions.

In the simulation study, the proposed adaptive threshold-based controllers performs better than that of other four benchmark controllers, with an average $K_{PDR}$ of 41.62% and $\eta_{failure}$ of 16.55%. Compared to the proposed controller, two fixed threshold-based controllers, the forecasted threshold and historical threshold-based controllers, demonstrates significantly lower effectiveness. The average $K_{PDR}$ achieved by the forecasted and historical threshold-based

controllers in the simulation study is 20.21% and 24.43%, respectively, whereas their corresponding average $\eta_{failure}$ values are 58.24% and 46.97%. The performance of the other two state-of-the-art benchmark controllers, namely the active and fuzzy logic controllers also fall short compared to the proposed adaptive threshold-based controller. In this simulation study, the active controller achieves an average $K_{PDR}$ of 21.65% and $\eta_{failure}$ of 43.70%, whereas the fuzzy logic controller records a higher average $K_{PDR}$ of 38.47% and a lower $\eta_{failure}$ of 28.30%. The proposed adaptive threshold-based controller also shows its strong effectiveness in 21 days of experimental study under real operating conditions, achieving an average $K_{PDR}$ of 49.45% and $\eta_{failure}$ of just 4.76%.

The implications of this study are significant. By leveraging an open-source Node-RED platform and integrating advanced deep learning-based 1D- CNN load forecasting model, the proposed controller offers a cost-effective, scalable, and efficient solution for peak demand reductions. This makes it highly suitable for commercial, institutional, and industrial facilities, especially those with budget constraints or limited access to proprietary software. Moreover, its success in both simulation and real-world deployment validates its practical viability and positions it as a promising tool in the development of smart grid systems. This work also contributes to broader energy sustainability goals by supporting more intelligent energy use, reducing peak grid loads, and lowering dependence on fossil-fuel-based peaking plants. It provides a practical pathway for utilities, energy managers, and policymakers to enhance demand-side management and transition towards cleaner and more efficient energy infrastructures.

## 6.2 Limitations and future works

The proposed innovative adaptive threshold-based controller is primarily designed to reduce the daily peak demands by effectively managing the charge-discharge schedule of the $LiFePO_4$ batteries. This controller along with the existing experimental setup is able to successfully reduce the peak demands at an academic building of UTAR, Sungai Long campus. However, there is a potential to enhance the overall benefits of the system by integrating renewable energy sources, such as solar PV panels. By incorporating the solar PV with the existing setup, the system can generate renewable energy that can be used to further reduce the peak demands. Therefore, as a future recommendation, integrating a solar PV system with the existing setup is suggested to further enhance the peak demand reduction performance of the proposed controller.

## LIST OF REFERENCES


Agamah, S.U. and Ekonomou, L. (2017) 'Energy storage system scheduling for peak demand reduction using evolutionary combinatorial optimisation', *Sustainable Energy Technologies and Assessments*, 23, pp. 73–82. Available at: https://doi.org/10.1016/j.seta.2017.08.003.

Albadi, M.H. and El-Saadany, E.F. (2008) 'A summary of demand response in electricity markets', *Electric Power Systems Research*, pp. 1989–1996. Available at: https://doi.org/10.1016/j.epsr.2008.04.002.

Amir, M. *et al.* (2023) 'Energy storage technologies: An integrated survey of developments, global economical/environmental effects, optimal scheduling model, and sustainable adaption policies', *Journal of Energy Storage*. Elsevier Ltd. Available at: https://doi.org/10.1016/j.est.2023.108694.

Ang, T.Z. *et al.* (2022) 'A comprehensive study of renewable energy sources: Classifications, challenges and suggestions', *Energy Strategy Reviews*. Elsevier Ltd. Available at: https://doi.org/10.1016/j.esr.2022.100939.

Ayyappan, P., Kumar, J. and Kumar Venkiteswaran, V. (2019) 'Maximum Demand Management: An overlooked energy saving opportunity in industries', in *IOP Conference Series: Earth and Environmental Science*. Institute of Physics Publishing. Available at: https://doi.org/10.1088/1755-1315/268/1/012156.

Barchi, G., Pierro, M. and Moser, D. (2019a) 'Predictive energy control strategy for peak switch and shifting using BESS and PV generation applied to the retail sector', *Electronics (Switzerland)*, 8(5). Available at: https://doi.org/10.3390/electronics8050526.

Barchi, G., Pierro, M. and Moser, D. (2019b) 'Predictive energy control strategy for peak switch and shifting using BESS and PV generation applied to the retail sector', *Electronics (Switzerland)*, 8(5). Available at: https://doi.org/10.3390/electronics8050526.

Benetti, G. *et al.* (2016) 'Electric load management approaches for peak load reduction: A systematic literature review and state of the art', *Sustainable Cities and Society*. Elsevier Ltd, pp. 124–141. Available at: https://doi.org/10.1016/j.scs.2015.05.002.

Bereczki, B., Hartmann, B. and Kertész, S. (2019) 'Industrial Application of Battery Energy Storage Systems: Peak shaving', in *2019 7th International Youth Conference on Energy (IYCE)*. Bled, Slovenia: IEEE, pp. 1–5. Available at: https://doi.org/10.1109/IYCE45807.2019.8991594.

Bogdanova, O., Viskuba, K. and Zemīte, L. (2023a) 'A Review of Barriers and Enables in Demand Response Performance Chain', *Energies*. Multidisciplinary

Digital Publishing Institute (MDPI). Available at: https://doi.org/10.3390/en16186699.

Bogdanova, O., Viskuba, K. and Zemīte, L. (2023b) 'A Review of Barriers and Enables in Demand Response Performance Chain', *Energies*. Multidisciplinary Digital Publishing Institute (MDPI). Available at: https://doi.org/10.3390/en16186699.

Borenstein, S. (2016) 'The economics of fixed cost recovery by utilities', *Electricity Journal*, 29(7), pp. 5–12. Available at: https://doi.org/10.1016/j.tej.2016.07.013.

Chakraborty, M.R. *et al.* (2022) 'A Comparative Review on Energy Storage Systems and Their Application in Deregulated Systems', *Batteries*. MDPI. Available at: https://doi.org/10.3390/batteries8090124.

Chatzigeorgiou, N.G. *et al.* (2024) 'A review on battery energy storage systems: Applications, developments, and research trends of hybrid installations in the end-user sector', *Journal of Energy Storage*. Elsevier Ltd. Available at: https://doi.org/10.1016/j.est.2024.111192.

Chua Kein Huat (2016) *Innovative Control Algorithms and Socioeconomic Benefits of Energy Storage System for Peak Reduction*. Universiti Tunku Abdul Rahman (UTAR).

Chua, Kein Huat, Lim, Y.S. and Morris, S. (2017) 'A novel fuzzy control algorithm for reducing the peak demands using energy storage system', *Energy*, 122, pp. 265–273. Available at: https://doi.org/10.1016/j.energy.2017.01.063.

Chua, K. H., Lim, Y.S. and Morris, S. (2017a) 'Peak reduction for commercial buildings using energy storage', in *IOP Conference Series: Earth and Environmental Science*. Institute of Physics Publishing. Available at: https://doi.org/10.1088/1755-1315/93/1/012008.

Chua, K. H., Lim, Y.S. and Morris, S. (2017b) 'Peak reduction for commercial buildings using energy storage', in *IOP Conference Series: Earth and Environmental Science*. Institute of Physics Publishing. Available at: https://doi.org/10.1088/1755-1315/93/1/012008.

Cordeiro, J.R. *et al.* (2021) 'Neural architecture search for 1d cnns. Different approaches tests and measurements', *Sensors*, 21(23). Available at: https://doi.org/10.3390/s21237990.

Danish, S.M.S. *et al.* (2020) 'A coherent strategy for peak load shaving using energy storage systems', *Journal of Energy Storage*, 32. Available at: https://doi.org/10.1016/j.est.2020.101823.

Darwazeh, D. *et al.* (2022) 'Review of peak load management strategies in commercial buildings', *Sustainable Cities and Society*, 77. Available at: https://doi.org/10.1016/j.scs.2021.103493.

Das, C.K. *et al.* (2018) 'Overview of energy storage systems in distribution networks: Placement, sizing, operation, and power quality', *Renewable and Sustainable Energy Reviews*. Elsevier Ltd, pp. 1205–1230. Available at: https://doi.org/10.1016/j.rser.2018.03.068.

Diewvilai, R. and Audomvongseree, K. (2024) 'Enhancing Generation Expansion Planning With Integration of Variable Renewable Energy and Full-Year Hourly Multiple Load Levels Balance Constraints', *IEEE Access*, 12, pp. 41143–41167. Available at: https://doi.org/10.1109/ACCESS.2024.3377660.

Dieziger, D. (2000) *Saving Money by Understanding Demand Charges on Your Electric Bill*. US Department of Agriculture, Forest Service, Technology & Development Program.

Ebrahimi, A. and Hamzeiyan, A. (2023) 'An ultimate peak load shaving control algorithm for optimal use of energy storage systems', *Journal of Energy Storage*, 73. Available at: https://doi.org/10.1016/j.est.2023.109055.

Efkarpidis, N.A. *et al.* (2023) 'Peak shaving in distribution networks using stationary energy storage systems: A Swiss case study', *Sustainable Energy, Grids and Networks*, 34. Available at: https://doi.org/10.1016/j.segan.2023.101018.

Engels, J. *et al.* (2020) 'Optimal Combination of Frequency Control and Peak Shaving with Battery Storage Systems', *IEEE Transactions on Smart Grid*, 11(4), pp. 3270–3279. Available at: https://doi.org/10.1109/TSG.2019.2963098.

GAO (2024a) *Electricity: Information on Peak Demand Power Plants*. Available at: https://www.gao.gov/assets/gao-24-106145.pdf (Accessed: 22 April 2025).

GAO (2024b) *Electricity: Information on Peak Demand Power Plants*. Available at: https://www.gao.gov/assets/gao-24-106145.pdf (Accessed: 22 April 2025).

Ghafoori, M., Abdallah, M. and Kim, S. (2023) 'Electricity peak shaving for commercial buildings using machine learning and vehicle to building (V2B) system', *Applied Energy*, 340. Available at: https://doi.org/10.1016/j.apenergy.2023.121052.

Di Gianfrancesco, A. (2017a) 'The fossil fuel power plants technology', in *Materials for Ultra-Supercritical and Advanced Ultra-Supercritical Power Plants*. Elsevier Inc., pp. 1–49. Available at: https://doi.org/10.1016/B978-0-08-100552-1.00001-4.

Di Gianfrancesco, A. (2017b) 'The fossil fuel power plants technology', *Materials for Ultra-Supercritical and Advanced Ultra-Supercritical Power Plants*, pp. 1–49. Available at: https://doi.org/10.1016/B978-0-08-100552-1.00001-4.

El Gohary, F., Stikvoort, B. and Bartusch, C. (2023) 'Evaluating demand charges as instruments for managing peak-demand', *Renewable and Sustainable Energy Reviews*, 188. Available at: https://doi.org/10.1016/j.rser.2023.113876.

Hannan, M.A. *et al.* (2021) 'Battery energy-storage system: A review of technologies, optimization objectives, constraints, approaches, and outstanding issues', *Journal of Energy Storage*, 42. Available at: https://doi.org/10.1016/j.est.2021.103023.

Hau, L.C. and Lim, Y.S. (2022) 'Proposed method for evaluating controllers of battery-based storage system in maximum demand reductions', *Journal of Energy Storage*, 46. Available at: https://doi.org/10.1016/j.est.2021.103850.

Hau, L.C., Lim, Y.S. and Chua, K.H. (2017a) 'Active Control Strategy of Energy Storage System for Reducing Maximum Demand Charges under Limited Storage Capacity', *Journal of Energy Engineering*, 143(4). Available at: https://doi.org/10.1061/(asce)ey.1943-7897.0000440.

Hau, L.C., Lim, Y.S. and Chua, K.H. (2017b) 'Active Control Strategy of Energy Storage System for Reducing Maximum Demand Charges under Limited Storage Capacity', *Journal of Energy Engineering*, 143(4). Available at: https://doi.org/10.1061/(asce)ey.1943-7897.0000440.

Hau Lee Cheun (2017) *Active Controller in Energy Storage System for Peak Demand Reduction with Limited Capacity*. Universiti Tunku Abdul Rahman (UTAR).

Hoa, P.X., Xuan, V.N. and Thu, N.T.P. (2024) 'Factors affecting carbon dioxide emissions for sustainable development goals – New insights into six asian developed countries', *Heliyon*, 10(21). Available at: https://doi.org/10.1016/j.heliyon.2024.e39943.

Hossain Bhuiyan, M.M. and Siddique, Z. (2025) 'Hydrogen as an alternative fuel: A comprehensive review of challenges and opportunities in production, storage, and transportation', *International Journal of Hydrogen Energy*. Elsevier Ltd, pp. 1026–1044. Available at: https://doi.org/10.1016/j.ijhydene.2025.01.033.

Hu, Y. *et al.* (2013) 'Peak and off-peak operations of the air separation unit in oxy-coal combustion power generation systems', *Applied Energy*, 112, pp. 747–754. Available at: https://doi.org/10.1016/j.apenergy.2012.12.001.

Huang, C., Li, K. and Zhang, N. (2025) 'Strategic joint bidding and pricing of load aggregators in day-ahead demand response market', *Applied Energy*, 377. Available at: https://doi.org/10.1016/j.apenergy.2024.124552.

Ige, A.O. and Sibiya, M. (2024) 'State-of-the-art in 1D Convolutional Neural Networks: A Survey', *IEEE Access* [Preprint]. Available at: https://doi.org/10.1109/ACCESS.2024.3433513.

Iqbal, S. *et al.* (2021a) 'A comprehensive review on residential demand side management strategies in smart grid environment', *Sustainability (Switzerland)*, 13(13). Available at: https://doi.org/10.3390/su13137170.

Iqbal, S. *et al.* (2021b) 'A comprehensive review on residential demand side management strategies in smart grid environment', *Sustainability (Switzerland)*, 13(13). Available at: https://doi.org/10.3390/su13137170.

IRENA (2019) *Innovation landscape brief: Flexibility in conventional power plants*. Abu Dhabi. Available at: https://www.irena.org/-/media/Files/IRENA/Agency/Publication/2019/Sep/IRENA_Flexibility_in_CPPs_2019.pdf?la=en&hash=AF60106EA083E492638D8FA9ADF7FD099259F5A1 (Accessed: 22 April 2025).

Jordehi, A.R. (2019) 'Optimisation of demand response in electric power systems, a review', *Renewable and Sustainable Energy Reviews*. Elsevier Ltd, pp. 308–319. Available at: https://doi.org/10.1016/j.rser.2018.12.054.

Kalkhambkar, V., Kumar, R. and Bhakar, R. (2016) 'Energy loss minimization through peak shaving using energy storage', *Perspectives in Science*, 8, pp. 162–165. Available at: https://doi.org/10.1016/j.pisc.2016.04.022.

Kanakadhurga, D. and Prabaharan, N. (2022) 'Demand side management in microgrid: A critical review of key issues and recent trends', *Renewable and Sustainable Energy Reviews*. Elsevier Ltd. Available at: https://doi.org/10.1016/j.rser.2021.111915.

Kandari, R., Neeraj, N. and Micallef, A. (2023) 'Review on Recent Strategies for Integrating Energy Storage Systems in Microgrids', *Energies*. MDPI. Available at: https://doi.org/10.3390/en16010317.

Kim, J. *et al.* (2017) 'Robust operation of energy storage system with uncertain load profiles', *Energies*, 10(4). Available at: https://doi.org/10.3390/en10040416.

Kim, K. *et al.* (2025) 'Real-Time AI-Based Power Demand Forecasting for Peak Shaving and Consumption Reduction Using Vehicle-to-Grid and Reused Energy Storage Systems: A Case Study at a Business Center on Jeju Island', *Applied Sciences (Switzerland)*, 15(6). Available at: https://doi.org/10.3390/app15063050.

Kwon, K. *et al.* (2024) 'Integrated Battery and Hydrogen Energy Storage for Enhanced Grid Power Savings and Green Hydrogen Utilization', *Applied Sciences (Switzerland)*, 14(17). Available at: https://doi.org/10.3390/app14177631.

Lange, C. *et al.* (2020) 'Dimensioning battery energy storage systems for peak shaving based on a real-time control algorithm', *Applied Energy*, 280. Available at: https://doi.org/10.1016/j.apenergy.2020.115993.

Latif, S.N.A. *et al.* (2021) 'The trend and status of energy resources and greenhouse gas emissions in the Malaysia power generation mix', *Energies*, 14(8). Available at: https://doi.org/10.3390/en14082200.

Lee, J.Y. *et al.* (2023) 'Energy storage systems: A review of its progress and outlook, potential benefits, barriers and solutions within the Malaysian distribution network', *Journal of Energy Storage*. Elsevier Ltd. Available at: https://doi.org/10.1016/j.est.2023.108360.

Leonard, M.D., Michaelides, E.E. and Michaelides, D.N. (2018) 'Substitution of coal power plants with renewable energy sources – Shift of the power demand and energy storage', *Energy Conversion and Management*, 164, pp. 27–35. Available at: https://doi.org/10.1016/j.enconman.2018.02.083.

Li, X. and Palazzolo, A. (2022) 'A review of flywheel energy storage systems: state of the art and opportunities', *Journal of Energy Storage*. Elsevier Ltd. Available at: https://doi.org/10.1016/j.est.2021.103576.

Martinez-Bolanos, J.R. *et al.* (2020) 'Economic feasibility of battery energy storage systems for replacing peak power plants for commercial consumers under energy time of use tariffs', *Journal of Energy Storage*, 29. Available at: https://doi.org/10.1016/j.est.2020.101373.

Mary, N. and Dessaint, L.A. (2025) 'Robust model predictive control of battery energy storage with neural network forecasting for peak shaving in university campus', *Journal of Building Engineering*, 107. Available at: https://doi.org/10.1016/j.jobe.2025.112445.

Mishra, A. *et al.* (2012) 'SmartCharge: Cutting the electricity bill in smart homes with energy storage', in *2012 Third International Conference on Future Systems: Where Energy, Computing and Communication Meet (e-Energy)*. Madrid: ACM Digital Library, pp. 1–10. Available at: https://doi.org/10.1145/2208828.2208857.

Mquqwana, M.A. and Krishnamurthy, S. (2024) 'Particle Swarm Optimization for an Optimal Hybrid Renewable Energy Microgrid System under Uncertainty', *Energies*, 17(2). Available at: https://doi.org/10.3390/en17020422.

Al Mubarak, F., Rezaee, R. and Wood, D.A. (2024) 'Economic, Societal, and Environmental Impacts of Available Energy Sources: A Review', *Eng*, 5(3), pp. 1232–1265. Available at: https://doi.org/10.3390/eng5030067.

Naseri, F. *et al.* (2022) 'Supercapacitor management system: A comprehensive review of modeling, estimation, balancing, and protection techniques', *Renewable and Sustainable Energy Reviews*. Elsevier Ltd. Available at: https://doi.org/10.1016/j.rser.2021.111913.

Nebey, A.H. (2024a) 'Recent advancement in demand side energy management system for optimal energy utilization', *Energy Reports*. Elsevier Ltd, pp. 5422–5435. Available at: https://doi.org/10.1016/j.egyr.2024.05.028.

Nebey, A.H. (2024b) 'Recent advancement in demand side energy management system for optimal energy utilization', *Energy Reports*. Elsevier Ltd, pp. 5422–5435. Available at: https://doi.org/10.1016/j.egyr.2024.05.028.

Ng, R.W. *et al.* (2022a) 'A novel dynamic two-stage controller of battery energy storage system for maximum demand reductions', *Energy*, 248. Available at: https://doi.org/10.1016/j.energy.2022.123550.

Ng, R.W. *et al.* (2022b) 'A novel dynamic two-stage controller of battery energy storage system for maximum demand reductions', *Energy*, 248. Available at: https://doi.org/10.1016/j.energy.2022.123550.

Nikolaos, P.C., Marios, F. and Dimitris, K. (2023) 'A Review of Pumped Hydro Storage Systems', *Energies*. MDPI. Available at: https://doi.org/10.3390/en16114516.

Nolan, S. and O'Malley, M. (2015) 'Challenges and barriers to demand response deployment and evaluation', *Applied Energy*. Elsevier Ltd, pp. 1–10. Available at: https://doi.org/10.1016/j.apenergy.2015.04.083.

Oudalov, A., Cherkaoui, R. and Beguin, A. (2008) 'Sizing and Optimal Operation of Battery Energy Storage System for Peak Shaving Application', in *2007 IEEE Lausanne Power Tech*. Lausanne, Switzerland: IEEE, pp. 621–625. Available at: https://doi.org/10.1109/PCT.2007.4538388.

Panda, S. *et al.* (2022a) 'Residential Demand Side Management model, optimization and future perspective: A review', *Energy Reports*. Elsevier Ltd, pp. 3727–3766. Available at: https://doi.org/10.1016/j.egyr.2022.02.300.

Panda, S. *et al.* (2022b) 'Residential Demand Side Management model, optimization and future perspective: A review', *Energy Reports*. Elsevier Ltd, pp. 3727–3766. Available at: https://doi.org/10.1016/j.egyr.2022.02.300.

Paterakis, N.G., Erdinç, O. and Catalão, J.P.S. (2017) 'An overview of Demand Response: Key-elements and international experience', *Renewable and Sustainable Energy Reviews*. Elsevier Ltd, pp. 871–891. Available at: https://doi.org/10.1016/j.rser.2016.11.167.

Perera, F. (2018) 'Pollution from fossil-fuel combustion is the leading environmental threat to global pediatric health and equity: Solutions exist', *International Journal of Environmental Research and Public Health*. MDPI. Available at: https://doi.org/10.3390/ijerph15010016.

Pholboon, S., Sumner, M. and Kounnos, P. (2016a) 'Community Power Flow Control for Peak Demand Reduction and Energy Cost Savings', in *2016 IEEE PES Innovative Smart Grid Technologies Conference Europe (ISGT-Europe)*. Ljubljana, Slovenia: IEEE, pp. 1–5. Available at: https://doi.org/10.1109/ISGTEurope.2016.7856276.

Pholboon, S., Sumner, M. and Kounnos, P. (2016b) 'Community Power Flow Control for Peak Demand Reduction and Energy Cost Savings', in *2016 IEEE PES Innovative Smart Grid Technologies Conference Europe (ISGT-Europe)*.

Ljubljana, Slovenia: IEEE, pp. 1–5. Available at: https://doi.org/10.1109/ISGTEurope.2016.7856276.

Prakash, K. *et al.* (2022) 'A review of battery energy storage systems for ancillary services in distribution grids: Current status, challenges and future directions', *Frontiers in Energy Research*. Frontiers Media S.A. Available at: https://doi.org/10.3389/fenrg.2022.971704.

Purwono *et al.* (2022) 'Understanding of Convolutional Neural Network (CNN): A Review', *International Journal of Robotics and Control Systems*, 2(4), pp. 739–748. Available at: https://doi.org/10.31763/ijrcs.v2i4.888.

Rafayal, S., Alnaggar, A. and Cevik, M. (2024) 'Optimizing electricity peak shaving through stochastic programming and probabilistic time series forecasting', *Journal of Building Engineering*, 88. Available at: https://doi.org/10.1016/j.jobe.2024.109163.

Reihani, E. *et al.* (2016) 'Load peak shaving and power smoothing of a distribution grid with high renewable energy penetration', *Renewable Energy*, 86, pp. 1372–1379. Available at: https://doi.org/10.1016/j.renene.2015.09.050.

Rowe, M. *et al.* (2014) 'A peak reduction scheduling algorithm for storage devices on the low voltage network', *IEEE Transactions on Smart Grid*, 5(4), pp. 2115–2124. Available at: https://doi.org/10.1109/TSG.2014.2323115.

Sahoo, S. and Timmann, P. (2023) 'Energy Storage Technologies for Modern Power Systems: A Detailed Analysis of Functionalities, Potentials, and Impacts', *IEEE Access*, 11, pp. 49689–49729. Available at: https://doi.org/10.1109/ACCESS.2023.3274504.

Saif-Ul-Allah, M.W. *et al.* (2022) 'Computationally Inexpensive 1D-CNN for the Prediction of Noisy Data of NOx Emissions From 500 MW Coal-Fired Power Plant', *Frontiers in Energy Research*, 10. Available at: https://doi.org/10.3389/fenrg.2022.945769.

Saldarini, A. *et al.* (2023) 'Battery Electric Storage Systems: Advances, Challenges, and Market Trends', *Energies*. Multidisciplinary Digital Publishing Institute (MDPI). Available at: https://doi.org/10.3390/en16227566.

De Salis, R.T. *et al.* (2014) 'Energy storage control for peak shaving in a single building', in *IEEE Power and Energy Society General Meeting*. IEEE Computer Society. Available at: https://doi.org/10.1109/PESGM.2014.6938948.

Shabalov, M. *et al.* (2021) 'The influence of technological changes in energy efficiency on the infrastructure deterioration in the energy sector', *Energy Reports*, 7, pp. 2664–2680. Available at: https://doi.org/doi.org/10.1016/j.egyr.2021.05.001.

Shin, M., So, S. and Kim, K. (2016) 'A Control Approach of Battery Energy Storage Systems to Reduce kW Demand', in *2016 The 3rd International Conference on Industrial Engineering and Applications (ICIEA 2016)*. Available at: https://doi.org/10.1051/matecconf/20166810001.

Siano, P. (2014) 'Demand response and smart grids - A survey', *Renewable and Sustainable Energy Reviews*. Elsevier Ltd, pp. 461–478. Available at: https://doi.org/10.1016/j.rser.2013.10.022.

Silva, B.N., Khan, M. and Han, K. (2020) 'Futuristic sustainable energy management in smart environments: A review of peak load shaving and demand response strategies, challenges, and opportunities', *Sustainability (Switzerland)*. MDPI. Available at: https://doi.org/10.3390/su12145561.

Strbac, G. (2008) 'Demand side management: Benefits and challenges', *Energy Policy*, 36(12), pp. 4419–4426. Available at: https://doi.org/10.1016/j.enpol.2008.09.030.

Su, L. *et al.* (2023) 'A Systematic Review for Transformer-based Long-term Series Forecasting'. Available at: https://doi.org/10.1007/s10462-024-11044-2.

Suruhanjaya Tenaga Malaysia (2020) 'Report on Peninsular Malaysia Generation Development Plan 2019 (2020-2030)', pp. 2–3. Available at: https://www.st.gov.my/contents/files/download/169/REPORT_ON_PENINSULAR_MALAYSIA_GENERATION_DEVELOPMENT_PLAN_2019_(2020_%E2%80%93_2030).pdf (Accessed: 10 April 2025).

Syed M. Hur Rizvi (2022) 'Time Series Deep learning for Robust Steady-State Load Parameter Estimation using 1D-CNN', *Arabian Journal for Science and Engineering*, 47, pp. 2731–2744.

Taylor, Z. *et al.* (2019) 'Customer-Side SCADA-Assisted Large Battery Operation Optimization for Distribution Feeder Peak Load Shaving', *IEEE Transactions on Smart Grid*, 10(1), pp. 992–1004. Available at: https://doi.org/10.1109/TSG.2017.2757007.

Tenaga Nasional Berhad (no date) *Maximum Demand*. Available at: https://www.tnb.com.my/commercial-industrial/maximum-demand (Accessed: 22 April 2025).

Tenaga Nasional Berhad (TNB) (no date) *Pricing & Tariffs*. Available at: https://www.tnb.com.my/commercial-industrial/pricing-tariffs1 (Accessed: 28 April 2025).

Wallberg, A. *et al.* (2024) 'Negative correlation peak shaving control in a parking garage in Uppsala, Sweden', *Applied Energy*, 375. Available at: https://doi.org/10.1016/j.apenergy.2024.124082.

Wang, X., Liu, X. and Bai, Y. (2024) 'Prediction of the temperature of diesel engine oil in railroad locomotives using compressed information-based data fusion method with attention-enhanced CNN-LSTM', *Applied Energy*, 367. Available at: https://doi.org/10.1016/j.apenergy.2024.123357.

Wibawa, A.P. *et al.* (2022) 'Time-series analysis with smoothed Convolutional Neural Network', *Journal of Big Data*, 9(1). Available at: https://doi.org/10.1186/s40537-022-00599-y.

Williams, B. *et al.* (2023) 'Demand Side Management in Industrial, Commercial, and Residential Sectors: A Review of Constraints and Considerations', *Energies*. Multidisciplinary Digital Publishing Institute (MDPI). Available at: https://doi.org/10.3390/en16135155.

XC Miow *et al.* (2025) 'Novel active load tracing controller for battery-based energy storage system for reducing sudden demand surges: A real case study in a factory', *Journal of Energy Storage*, 111.

Yang, H. *et al.* (2023) 'Operation scheduling strategy of battery energy storage system with the integration of differenced power constraint factor', *Journal of Energy Storage*, 74. Available at: https://doi.org/10.1016/j.est.2023.109348.

Yun, X. *et al.* (2016) 'A Comparison Between Two MPC Algorithms for Demand Charge Reduction in a Real-World Microgrid System', in *2016 IEEE 43rd Photovoltaic Specialists Conference (PVSC)*. IEEE, pp. 1875–1880. Available at: https://doi.org/10.1109/PVSC.2016.7749947.

Yunusov, T. *et al.* (2017) 'Evaluating the effectiveness of storage control in reducing peak demand on lowvoltage feeders', in *CIRED - Open Access Proceedings Journal*. Institution of Engineering and Technology, pp. 1745–1749. Available at: https://doi.org/10.1049/oap-cired.2017.0626.

Zhang, Y. and Augenbroe, G. (2018a) 'Optimal demand charge reduction for commercial buildings through a combination of efficiency and flexibility measures', *Applied Energy*, 221, pp. 180–194. Available at: https://doi.org/10.1016/j.apenergy.2018.03.150.

Zhang, Y. and Augenbroe, G. (2018b) 'Optimal demand charge reduction for commercial buildings through a combination of efficiency and flexibility measures', *Applied Energy*, 221, pp. 180–194. Available at: https://doi.org/10.1016/j.apenergy.2018.03.150.

Zhao, X. *et al.* (2024) 'A review of convolutional neural networks in computer vision', *Artificial Intelligence Review*, 57(4). Available at: https://doi.org/10.1007/s10462-024-10721-6.

Zheng, M., Meinrenken, C.J. and Lackner, K.S. (2015) 'Smart households: Dispatch strategies and economic analysis of distributed energy storage for residential peak shaving', *Applied Energy*, 147, pp. 246–257. Available at: https://doi.org/10.1016/j.apenergy.2015.02.039.